From the holdings of the Department of Special Collections , Princeton University Library, Princeton, NJ

These documents are either in the public domain, or can only be used for educational and research purposes (Fair use) as per U.S. Copyright law (text below). By accessing this file, all users agree that their use falls in the public domain or within fair use as defined by the copyrightlaw. We do not charge any permission or usage fees for the publication of images of material inour collections, including those provided by Princeton University Library, via our website, catalog, or directly from staff.For more information regarding copyright, credit, and citation please review the information onthe Copyright, Credit and Citation Guidelines page of our website.
https://library.princeton.edu/special-collections/policies/copyright-credit-and-citation-guidelines. If you have any questions, including how to order higher-quality images from the collection, contact Special Collections Public Services via our Ask Us! Form. https://library.princeton.edu/special-collections/ask-us

---

Doctoral Dissertations, 2011-2026 Psychology

2019

The Role of Acetylcholine and Dopamine in Working Memory

Choi, Jung Yoon

Princeton, NJ : Princeton University

---

http://arks.princeton.edu/ark:/88435/dsp01d791sk04k

U.S. Copyright law: The copyright law of the United States (Title 17, §108, United States Code) governs the making of photocopies or other reproductions of copyrighted material. Under certain conditions specified in the law, libraries and archives are authorized to furnish a photocopy or other reproduction. One of these specified conditions is that the photocopy or reproduction is not to be used for any purpose other than private study, scholarship, or research. If a user makes a request for, or later uses, a photocopy or reproduction for purposes in excess of fair use that user may be liable for copyright infringement. This institution reserves the right to refuse to accept a copying order if, in its judgment, fulfillment of the order would involve a violation of copyright law. https://www.copyright.gov/title17/title17.pdf

THE ROLE OF ACETYLCHOLINE AND DOPAMINE IN WORKING MEMORY

Jung Yoon Choi

A DISSERTATION
PRESENTED TO THE FACULTY
OF PRINCETON UNIVERSITY
IN CANDIDACY FOR THE DEGREE
OF DOCTOR OF PHILOSOPHY

RECOMMENDED FOR ACCEPTANCE BY
THE DEPARTMENT OF PSYCHOLOGY AND
THE PRINCETON NEUROSCIENCE INSTITUTE

Primary Advisor: Ilana B. Witten
Secondary Advisor: Elizabeth Gould

June 2019

© Copyright by Jung Yoon Choi, 2019, All rights reserved.

Abstract

Working memory, the ability to remember a stimulus for a brief period of time and to use that memory flexibly to guide ongoing behavior, is a ubiquitous function essential to our cognition. In this thesis, I investigate the temporally-precise role of two major neuromodulatory systems - midbrain dopaminergic (DA) system and basal forebrain cholinergic (ChAT) system- in spatial working memory.

In the first study, the role of ChAT system in working memory is examined. Using delayed non-match to position task (DNMTP) as a behavioral assay to probe rodent spatial working memory, I first quantitatively demonstrate that animals' locomotion explains more variance in medial septum (MS) ChAT neurons than task events while task events explains more variance in nucleus basalis (NB) ChAT neurons than locomotion, establishing two distinct roles of these ChAT brain regions in subserving DNMTP task. Furthermore, I show that NB ChAT neurons respond to lever press action and reward, and this task event encoding is spatially organized along the medio-lateral axis of the NB. Lastly, I report that these ChAT neurons in the NB are surprisingly integrated within the Basal Ganglia in a topographical fashion, providing an anatomical substrate to the functional heterogeneity in the NB ChAT neurons.

In the second study, the role of DA system in working memory is investigated using the same working memory task. I first quantitatively show that task events such as lever presentation cue and reward, are encoded with phasic elevated activity, similarly between DA neurons in the substantia nigra pars compacta (SNc) and ventral tegmental area (VTA). In contrast, SNc and VTA DA neurons are relatively depressed during the delay period. Next, I present a series of causal, optogenetic experiments to test a set of predictions outlined by the "gating" theory and "inverted-U-shape" hypothesis of DA in working memory. We demonstrate that bi-directional manipulation of VTA DA neurons during the sample and delay period impairs the cognitive component of the task supporting the "inverted-U-shape" hypothesis, while SNc DA neurons may be more involved in the motor execution of the task. This is the first evidence providing dissociable causal roles of VTA and SNc DA neurons in working memory.

Acknowledgements

First and foremost, I would like to express my deepest gratitude to my adviser Ilana Witten. When I first met her as an undergraduate student in her very first class as a professor, I immediately knew that I found my role model. After 6 years of being her graduate student, I cannot believe how I could make such visionary and correct decision when I was just a senior in college. I have witnessed first-hand that Ilana is a brilliant scientist, dedicated teacher, and biggest supporter in life. As a graduate adviser, Ilana provided careful guidance as well as intellectual freedom. But she was more than just a graduate adviser. She was a life mentor. Through all the ups and downs of my life, which were inevitably correlated with the experimental results, I found Ilana to be immensely supportive and cheerful. I am so fortunate and grateful to have her in my life. Thank you so much for having the patience, empathy, and trust in me when I do not deserve them. You inspire me in so many ways.

Next, I would like to thank the members of the Witten Lab for creating such warm and fun lab environment. I take pride in having to work with such brilliant, genuine, and caring people. I would like to highlight my truly amazing research assistants. All the work here would not have been possible without these incredible combo: Heejae Jang and Sharon Ornelas. I would like to thank my officemate, Julia Cox, for providing continued encouragement and enthusiasm for my project when I lost interest in my own project. Also I thank Lili Cai for being such a good listener even in the hallway when I needed to vent out. Thank you, Malu Murugan for giving me such great advice even when I ask the most trivial questions such as which brand of kibble I should try for my puppy. Thank you, Nathan Parker, for being the most fun person to work with as well as to drink beer together in conferences. Thank you, Courtney Cameron for sharing the rat-specific expertise, when everyone else is studying mice. This never ends because I am so indebted to everyone; Ben Engelhard, for providing critical and insightful comments in lab meetings, Scott Bolkan, for providing technical advice on electrophysiology and your face emoji in the Slack channel, Alex Pan, for being in lab on the weekends. Thank you, Weston Fleming and Anna Zhukoskaya, for your friendship. I was fortunate to have Jennifer Au as my superstar undergraduate student. I thank former members of the lab as well as my collaborator - Joost Wiskerke, Joel Finkielstein, Hessam Akhlaghpour,

Daniel Fürth. I also would like to thank my committee members - Asif Ghazanfar, Elizabeth Gould, Tim Buschman, Annegret Falkner, and Jordan Taylor - for insightful comments and guidance throughout my PhD.

Last but not least, I would like to express my infinite love and gratitude to my family - my parents, brother and sister, parents-in-law, soy and husband Jaeho. I dedicate this thesis to my family, especially my husband Jaeho. Towards the end of my PhD and your medical school, we faced our first major obstacle as a couple. Although the uncertainties ahead of us were stressful, we finally made it together! I am grateful that you remained flexible with my ever-changing crazy future plans ranging from quitting my PhD to being a science teacher in Europe. Your flexibility alleviated the pressure on my shoulder and allowed me to have resilience during my PhD when experiments failed. I am so excited for our future together in Baltimore.

This work was undertaken in collaboration with Daniel Fürth, Heejae Jang, Sharon Ornelas, Jennifer Au, Ilana B. Witten. Most of this work has been previously presented as poster abstracts at the following conferences:

"The Spatiotemporal Dynamics of Acetylcholine and Dopamine in Working Memory." Gordon Research Conference, 2017

"Spatial Segregation of Movement and Reward Encoding across the Basal Forebrain Cholinergic System." Society for Neuroscience, 2018

Table of Contents

Abstract……iii
Acknowledgements……iv
Chapter 1: Introduction……1
1.1 Working Memory……1
1.2 Dopamine and Working memory……9
1.3 Acetylcholine and Working Memory……12
1.4 Overview of Thesis Work……16

Chapter 2: The basal forebrain cholinergic system has spatially organized activity and topographic integration within the basal ganglia ……19
2.1 Abstract……19
2.2 Introduction……19
2.3 Results……22
2.3.1 Rats performed a spatial working memory task……22
2.3.2 Task events explain more variance in NB ChAT neurons whereas locomotion explains more variance in MS ChAT neurons……24
2.3.3 NB ChAT neurons show elevated activity to lever press action and reward……28
2.3.4 NB ChAT neurons' response is organized along the medio-lateral axis of the NB……30
2.3.5 Monosynaptic retrograde tracing reveals that the striatum is the strongest projector and the subthalamic nucleus is the densest projector to NB ChAT neurons……33
2.3.6 DMS projects to medial NB ChAT neurons whereas DLS projects to lateral NB Chat neuron respectively……36
2.4 Discussion……38
2.4.1 Dissociative encoding in NB vs MS ChAT neurons……38
2.4.2 Relevance to previously reported functions of NB ChAT neurons……38
2.4.3 M-L Gradient in NB ChAT neurons……39
2.4.4 Topographical integration with the basal ganglia……40
2.5 Methods……42
2.5.1 Rats……42
2.5.2 Delayed non-match to Sample Task……42
2.5.3 Surgery……43
2.5.4 Fiber photometry……43
2.5.5 GCaMP Signal Processing……44
2.5.6 Encoding model……46
2.5.7 Immunohistochemistry……47
2.5.8 Fiber Tip Location……48

2.5.9 WholeBrain Registration and Segmentation…… 49

Chapter 3: The midbrain DA system reveals dissociable and causal contribution to memory and motor execution in a spatial working memory task…… 51

3.1 Abstract…… 51

3.2 Introduction……...52

3.3 Results…….. 55

3.3.1 Rats performed a spatial working memory task…….. 55

3.3.2 Task events explain more variance in DA activity in VTA and SNc compared to locomotion or delay period…….... 57

3.3.3 DA neurons in SNc and VTA similarly show phasic response to lever presentation and reward but low activity during the delay period……...59

3.3.4. Optogenetic inhibition of VTA DA neurons impairs working memory while the same manipulation of SNc DA neurons impairs motor execution of the task..... 61

3.3.5 Optogenetic inhibition of DA neurons in VTA during the sample and delay period impairs WM performance……..66

3.3.6 Optogenetic activation of DA neurons in VTA during the delay period impairs WM performance…… 69

3.4 Discussion……... 71

3.4.1 Similar neural correlate of DNMTP in VTA vs SNc DA neurons……...71

3.4.2 Dissociable role of VTA and SNc DA neurons in WM…… 71

3.4.3 Bidirectional optogenetic manipulation of VTA DA during the delay period impairs WM performance. …… 72

3.4.4 Rewarding/motivational effect of DA stimulation…… 73

3.5 Methods……74

3.5.1 Rats……..74

3.5.2 Delayed non-match to Sample Task and Guided Delayed Response Task…….. 74

3.5.3 Surgery……...75

3.5.4 Fiber photometry…….. 76

3.5.5 GCaMP signal processing…….. 76

3.5.6 Encoding model…… 78

3.5.7 Immunohistochemistry…… 79

3.5.8 Optogenetic experiment…….. 80

Chapter 4: Conclusion…… 82

4.1 Summary of thesis work…… 82

4.1.1 Major findings…… 83

4.1.2 Neural correlates of midbrain DA system and basal forebrain ChAT system in working memory…….. 83

4.1.3 Causal manipulation of midbrain DA system and basal forebrain ChAT system in working memory……84

4.2 Ongoing and Future Direction…….. 86

4.3 Conclusions…….. 88

Chapter 1: Introduction

1.1 Working Memory

"... the brain's working memory function, i.e, the ability to to bring to mind events in the absence direct stimulation, may be its inherently most flexible mechanism and its evolutionarily most significant achievement. At the most elementary level, our basic conceptual ability to appreciate that an object exists when out of view depends on the capacity to keep events in mind beyond the direct experience of those events."

-Goldman-Rakic, 1995

Working memory, the ability to remember a stimulus for a brief period of time and to flexibly use that memory to guide ongoing behavior, is ubiquitous and essential to our life (Baddeley 1986). Working memory deficits accompany multiple debilitating psychiatric diseases ranging from Alzheimer's disease, Parkinson's disease, to Schizophrenia. Yet, our understanding of working memory is rudimentary and there is no cure, let alone an effective treatment, to working memory deficits. In search of effective treatment, neuromodulators have been and continue to be at the spotlight. Why?

From a clinical point of view, cholinergic neurons in the nucleus basalis of meynert is the first site of degeneration in Alzheimer's disease. Accordingly, four out of five FDA approved medications for cognitive deficits, though ineffective, are cholinesterase inhibitors, which increases the extracellular cholinergic tone in the brain. In the case of Parkinson's disease, which often accompanies working memory deficits, the degeneration of dopaminergic neurons in the Substantia Nigra pars compacta is the hallmark of the disease. Taken together, clinical evidence suggests that dysfunction of neuromodulators is at the heart of pathogenesis.

From a biophysical perspective, neuromodulation is interesting because it can influence the state of neuronal network to alter its response to subsequent stimulation, given the relatively long time-scale that neuromodulators can influence neural networks. Specifically in relation to working memory, neuromodulation may be capable of influencing the state of neural networks to facilitate updating of working memory representation or directly modulate the stability of working memory representation.

The most famous neurophysiological correlate of working memory is persistent activity during the delay period; neurons fire persistently in spite of the fact that the trigger stimulus is no longer present, just like working memory keeps the stimulus in mind even when out of sight (Funahashi, Bruce, and Goldman-Rakic 1989; Fuster and Alexander 1971; Goldman-Rakic 1995; Romo et al. 1999). This delay period persistent activity was first discovered in the prefrontal cortex (Fuster and Alexander 1971; Funahashi, Bruce, and Goldman-Rakic 1989; Kubota and Niki 1971) and subsequently found to be widespread throughout the cortex, including higher order association, sensory, and motor cortices (Dotson et al. 2018; Haller et al. 2018; Fuster 1990). A lot of pioneering work used a version of the oculomotor delayed response task in monkeys (Fuster and Alexander 1971; Funahashi, Bruce, and Goldman-Rakic 1989; Kubota and Niki 1971). In this task, a monkey initiates a trial by fixating on a central point followed by a brief presentation of a spatial cue in one of eight possible directions (i.e. 0º, 45º, 90º, etc) relative to the central fixation point. After the delay period, the monkey must make a saccade to the correct location of the cue to show the spatial memory was maintained during the delay period. Recording single unit activity in dlPFC during the task, Goldman-Rakic and colleagues found “cue” cells that fire during cue presentation, “delay” cells that persistently fired for the duration of delay period, and “response” cells that fired at or around saccadic response event (Funahashi, Bruce, and Goldman-Rakic 1989). Interestingly, the tonically active delay cells were directionally tuned such that they fired to the preferred direction but were suppressed for all other

non-preferred directions. This directional tuning suggested that the delay period activity encodes the stimulus identity and therefore was interpreted as “a reflection of information that is on-line” (Goldman-Rakic 1995) .

The finding of persistent delay period activity by Goldman-Rakic and colleagues has culminated in the classic model of PFC microcircuitry (Goldman-Rakic 1995), which was inspired by the orientation column system of primary visual cortex (Gilbert 1993). In this classic model, spatial working memory fields are organized modularly in cortical columns, in which local pyramidal neurons with similar direction tuning are recurrently connected in layer III forming a cluster (Kritzer and Goldman-Rakic 1995). Among these pyramidal neurons exist inhibitory interneurons (possibly basket cells) that connects two pyramidal cells with opposite direction tuning to form a reciprocal excitatory-inhibitory unit. These interneurons suppress interconnected opposite direction pyramidal cell (i.e. 270º) when the other pyramidal cell (i.e. 90º) is active. Together, this reciprocity of the excitatory-inhibitory unit creates local recurrent connectivity. Furthermore, it explains the suppression of non-preferred direction that accompanies the persistent excitation to the best-preferred direction during the delay period in a PFC pyramidal neuron. In formulating this PFC microcircuit to explain persistent delay activity, a lingering question in the back of Goldman-Rakic’s mind was the stability of working memory representation; she questioned, “Is it possible for neurons to remain activated for longer than a few seconds?”(Goldman-Rakic 1995). Only a handful of neurons show cell-autonomous persistent firing, perhaps because it is metabolically costly. Instead, most cortical neurons fire sparsely and decay within 10-20ms (Shafi et al. 2007). Therefore, delay period persistent activity can then only be an emergent property of collective neural network rather than a single neuron phenomenon.

One proposed mechanism of neural network underlying persistent activity is attractor states. Attractor state refers to self-sustaining stable neural activity pattern that is evolved and

reinforced by the synaptic connectivity in the network. In discrete attractor models, such as the Hopfield network, a population of binary neurons (1: superthreshold, spike, 0: suprathreshold, no spike) with simple recurrent connections can learn and evolve, through the updating of synaptic weights, towards the direction that lowers the energy state of the system (Hopfield 1982; Amit and Brunel 1997). Eventually, the network finally settles at the local minimum energy state, where the memory content is found. This minimum energy state is the delay period persistent activity of a recurrent neural network. It is possible to have a discrete number of attractor states, just as it should be possible to remember multiple items in mind, such as “apple” and “orange”. In case of multiple attractor states, the final attractor state is determined by the initial state of the network, which can be nudged by external inputs such as neuromodulators. In multiple discrete attractor model, the boundary between attractor states is the separatrix.

An example where working memory was successfully explained by discrete attractor model comes from the work of Kopec and colleagues (Kopec et al. 2015). They optogenetically inhibited the frontal orienting fields (FOF; rat homolog of primate’s frontal eye fields) and superior colliculus of rats at different times during the delay period of a memory-guided orienting task. Although their earlier work showed monotonically increasing neural encoding of FOF (Erlich, Bialek, and Brody 2011), the effect of inhibition monotonically decreased over the course of the delay period (Kopec et al. 2015). To explain these seemingly contradictory findings, they constructed a discrete attractor model with two attractor states: “go Left” and “go Right”. The intuition was that the delay period will start at the separatrix so the perturbation at around the separatrix (i.e. perturbation early in the delay period) will more easily cause the crossing of the system between the attractor states as a result of inhibition. However, as the system evolves towards the one of two attractor states, away from the separatrix, and further into the delay period, the harder it is to perturb the system. Not only the discrete attractor model recapitulated their data, but furthermore, they were able to provide additional data which confirmed two predictions generated from the model. Their first prediction was that simultaneous inactivation of

both SC and FOF should result in greater bias than sum of silencing each region alone. The second prediction was that the easier trials should be less perturbable than harder trials because easier trials have greater difference in the excitatory input between the two attractors, causing more rapid settlement into the final attractor state. Together, their experimental results and analysis neatly describe the discrete attractor model of upcoming choice during the delay period (Kopec et al. 2015).

A major drawback of the discrete attractor network is the “discretized” memory representation; in this model, only finite number of items can be remembered. However, some memory representation is intrinsically continuous rather than discrete. Take for example, the oculomotor spatial working memory task described above (Funahashi, Bruce, and Goldman-Rakic 1989). The saccade endpoint can fall anywhere along the circle around the center fixation point, resulting in continuous spatial representation between -180º~180º. This motivated the development of “continuous” attractor models. One of such continuous attractor models, the bump attractor model (Compte et al. 2000), was built to reproduce the oculomotor working memory task (Funahashi, Bruce, and Goldman-Rakic 1989). In the bump attractor model, neurons with similar preferred tuning curve excite each other, and likewise, neurons with dissimilar tuning curve inhibit each other, similar to the excitatory-inhibitory unit described by Goldman-Rakic (Goldman-Rakic 1995; Compte et al. 2000). The spatial location of the cue is encoded by the activity of neurons with similar tuning curve, which creates a bump of activity at around that preferred location. Importantly, the bump of activity randomly fluctuates as the delay period progresses, accumulating encoding error from collective neuronal variability.

As a result of bump drifting throughout the delay, bump attractor model of working memory makes unique predictions relating neural activity to behavioral inaccuracies. First, the location of the bump at the end of delay period should predict the direction of upcoming saccade response bias - whether the bias will be clockwise or counterclockwise. Second, the firing rate of

neurons around the bump should predict the magnitude of behavioral bias. Third, neurons around the bump should exhibit larger neuronal variability in incorrect trials than correct trials. Lastly, a pair of neurons on the same side of bump (same-tuning pair) should show positively-correlated firing rate, while a pair of neurons on the opposite side of bump (different-tuning pair) should be negatively correlated. All these predictions were confirmed experimentally from the electrophysiology recording of monkey PFC performing the oculomotor spatial working memory task (Wimmer et al. 2014). In a series of analyses, they convincingly showed that the neural network activity at the end of delay period was sufficient to reconstruct not only the upcoming choice, but also the direction and magnitude of behavioral choice bias in inaccurate trials. Furthermore, the location of the presented cue modulated the neural network variability as well as neuron pairs' activity during the delay period. Taken together, the predictive relationship between the delay period PFC activity and the precision of recalled spatial location on a trial-by-trial basis strongly supports the bump attractor dynamics serving working memory representation (Wimmer et al. 2014). Nonetheless, every rose has its thorn: all recurrent network based on feedback suffer from a fine-tuning problem. Small deviation to the network connectivity or feedback strength abruptly destroy the persistence.

A recent variation of attractor models that circumvent the fine-tuning problem is synaptic-attractor model (SAM) proposed by the Miller group (Miller, Lundqvist, and Bastos 2018). Based on the observation that most cortical neurons exhibit coordinated bursts of spiking in gamma during the delay period, SAM defines attractor state as one gamma burst with a limited lifetime (Bastos et al. 2018; Lundqvist et al. 2016, 2018; Shafi et al. 2007). These gamma bursts not only appear during encoding and decoding of a stimulus but also occur irregularly spanning the delay period. Happening in between the bursts is the spiking-induced temporary change in synaptic weights that strengthen working memory representation. The introduction of synaptic "impression" left in the network provides three advantages. First, synaptic weights are robust to perturbations of neural activity. Second, these shorter bouts of attractor states permit

simultaneous encoding of multiple memory items by multiplexing these gamma bursts in time. Lastly, shorter bouts of persistent activity is metabolically energy-saving than persistent activity throughout the delay period. The second-half of the SAM details the push-pull relationship between the gamma and beta. The role of beta is hypothesized to inhibit gamma thereby exerting executive control over the working memory represented by gamma. Therefore, inhibition of alpha results in excitation of gamma that promotes encoding of sensory stimulus, whereas the activation of alpha results in inhibition of gamma that promotes clearing out of the working memory storage. The extensive and comprehensive theory of working memory representation in SAM is very well supported experimentally. For example, the link between spiking and transient synaptic augmentation uniquely found in PFC has been convincingly shown in the work of Wang, Goldman and colleagues (Wang et al. 2006). Brief attentional perturbation to delay period activity failed to disrupt working memory performance, further bolstering the involvement of synaptic short-term plasticity in maintaining working memory (Watanabe and Funahashi 2014; Spaak et al. 2017). Additionally, a series of work by Lundqvist and colleagues successfully captured important hypotheses in the SAM including gamma burst increase with working memory load, information encoding and decoding from gamma bursts, and antagonistic relationship between beta and gamma (Lundqvist et al. 2016, 2018; Bastos et al. 2018).

Persistent activity can also be achieved without attractor states at all. Another proposed mechanism of neural network underlying persistent activity is a combination of time-varying neural activities whose projection falls onto a time-invariant working stable coding line. In fact, a wealth of studies report rather variable, time-varying delay period activity in PFC neurons, in addition to constantly firing neurons (Barak, Tsodyks, and Romo 2010; Brody et al. 2003; Shafi et al. 2007; Baeg et al. 2003). In a simple example, combination of neurons with ramping firing rate and those with diminishing firing rate can result in constant, stable decoding throughout the delay period. Such model is conceptualized by Druckmann and Chklovskii and named as FEVER network (Druckmann and Chklovskii 2012). The term FEVER comes from Feature Vector

Representation and is inspired by redundant representation of a stimulus in time-varying neuronal activity. The key principle is that a stable stimulus representation as a whole in the network is achieved by linear sum of each neuron's feature vector weighted by its activity. The connectivity of the network ensures that each neuron's feature vector again is expressed as the sum of postsynaptic neurons' feature vector weighted by its synaptic connection. Therefore, individual neuron's time-varying activity is compensated by other laterally-connected neurons' time-varying activity that redundantly encode the stimulus. FEVER network has been observed in large-scale single unit recordings of lateral PFC of monkeys performing oculomotor delayed response task as well as vibrotactile delayed discrimination task (Murray et al. 2017). Murray et al.,uncovered the mnemonic subspace (i.e. stable coding line in FEVER network) among the time-varying population activity of PFC neurons using principal component analysis. This mnemonic subspace emerged from PCA on time-averaged delay activity therefore time-insensitive by definition, but surprisingly, this mnemonic subspace was stable throughout time in delay period (Murray et al. 2017).

An alternative proposal using time-varying neural firing without a recurrent network is feedforward chain. Inspired by the synfire chain of Abeles (Abeles 1982), feedforward chain relays working memory representation by sequentially exciting the chain of the network states, propagating from one layer to the next (Ganguli and Latham 2009; Goldman 2009). Given the intrinsic decay time constant of τ, and number of neurons in a chain N, the working memory representation can last for the duration of Nτ. Simply, the longer the memory maintenance duration, the longer the chain (N increases). A feedforward chain can also incorporate recurrently-connected units that are sequentially activated in a feedforward manner. Therefore, Goldman argues that seemingly recurrent network might be inherently feedforward connection (Goldman 2009). Most straightforward experimental example of feedforward chain is the sequential activity that tiles the duration of delay period reported by multiple groups (Harvey, Coen, and Tank 2012; MacDonald et al. 2011; Pastalkova et al. 2008; Akhlaghpour et al. 2016;

Seidemann et al. 1996; Baeg et al. 2003). However, it should be noted that sequential activity can be achieved through other mechanisms such as bump attractor model (Ben-Yishai, Bar-Or, and Sompolinsky 1995) or feedforward connectivity without the chain.

Above, various biophysical models of working memory representation have been briefly introduced. While the details of the network mechanism behind stable working memory representation are still debated, virtually all agree on the powerful effect of neuromodulation on the network state, dynamics and synaptic connectivity that underlie working memory representation.

1.2 Dopamine and Working memory

In 1979, a landmark study by Brozoski et al. discovered the critical role of dopamine in working memory (Brozoski et al. 1979). The selective depletion of dopamine in money PFC using 6-OHDA resulted in significant deficit in working memory performance, with the effect size equivalent to complete ablation of the PFC. Similar depletion of other neuromodulators such as serotonin and norepinephrine spared the performance, underscoring the role of dopamine in mediating the cognitive deficit. Furthermore, administration of DA receptor agonists (i.e. L-dopa and apomorphine) to these same monkeys reversed the the impairment. This work precipitated the interest in dopamine system in working memory.

Subsequent works revealed that specifically DA stimulation of D1 receptors mediate the effect (Sawaguchi and Goldman-Rakic 1991; Vijayraghavan et al. 2007). Moreover, it has been repeatedly observed across multiple species that the correlation of D1R antagonist and its impact on spatial working memory impairment portrays an inverted-U shape, whereby too much or too little dopamine impairs the performance (Zahrt et al. 1997; Lidow, Koh, and Arnsten 2003; Cai and Arnsten 1997; Gibbs and D'Esposito 2005; Callicott et al. 1999; Vijayraghavan et al. 2007; Williams and Goldman-Rakic 1995; A. F. Arnsten et al. 1994). For example, Arnsten and

colleagues noticed that injection of D1 agonist had contrasting effect on young monkeys versus aged monkeys with presumed dopamine depletion (A. F. Arnsten et al. 1994). Injection of D1 agonist significantly impaired working memory performance in young monkeys but not in aged monkeys. Conversely, D1 partial agonist improved the performance in aged monkeys but not in young monkeys. Later, Arnsten and Goldman-Rakic further revealed that similar baseline-effect of D1 agonist can manifest within a single subject (A. F. Arnsten and Goldman-Rakic 1998). In this study, they induced working memory deficit in monkeys by presenting loud noise stress during a spatial working memory performance. Then they showed this stress-induced deficit could be ameliorated by pretreatment with D1 receptor antagonist. More recently, the effect of D1R stimulation on PFC delay cells have been more directly investigated by recording in the PFC of monkey performing oculomotor spatial working memory task while applying varying doses of D1R agonist through iontophoresis (Vijayraghavan et al. 2007). In this work, low doses of D1R agonist sharpened the direction tuning of PFC delay cell by selectively decreasing the response to non-preferred direction. In contrast, high doses of D1R agonist reduced all PFC delay cell firing and impaired working memory performance. This inverted U-shape of D1R effect on working memory was also captured in the computational simulation of PFC recurrent network during delayed match-to-sample task (Brunel and Wang 2001). Brunel and Wang implemented D1 modulation in the network by assuming that the NMDA conductances on pyramidal cells and those on interneurons are separately modulated by varying levels of D1 activation. They found that the increase in PFC DA tone boosts recurrent persistent firing up to a certain level because NMDA conductances in pyramidal cells are more affected than those in interneurons. But with higher DA tone, NMDA conductances in pyramidal cells saturate and the network become dominated by NMDA conductances in the interneurons, resulting in the decrease in delay persistent activity (Brunel and Wang 2001). Together, inverted U-shape hypothesis of D1R effect in working memory has accumulated ample, converging evidences over the past thirty years and gained much popularity (A. F. T. Arnsten, Wang, and Paspalas 2012; Cools and D'Esposito 2011).

Another computational approach to understand the *flexibility* of working memory evolved into a “gating” hypothesis of DA in working memory (Braver and Cohen 2000). The motivation was that simple working memory attractor system is built for *stable* working memory representation, therefore lacks the flexibility required to update new stimuli or context. This problem can be overcome by introducing a gating mechanism separate from the attractor system in the PFC, and the authors point out that DA is well-positioned to perform such gating role. Physiologically, dopamine afferents in the PFC, together with the spine of pyramidal neurons and the axons of sensory inputs, are thought to form a synaptic triad complex that enable fast and direct DA modulation of the local spinal responses to excitatory sensory input (Goldman-Rakic 1995; Goldman-Rakic et al. 1989).

In the “gating” theory, phasic DA in PFC is hypothesized to update relevant memory to be maintained while filtering out irrelevant distractors (Braver and Cohen 2000). In the simulation, DA gating signal was graded such that more phasic DA at the time of task-relevant stimuli promoted updating of the stimuli into working memory while the failure to update the stimuli due to reduced phasic DA resulted in perseveration (old context is failed to be replaced). Likewise, more phasic DA at the time of irrelevant stimuli resulted in interference of currently maintained context. Interestingly, tonic activity of the gating signal during the delay period had inhibitory effect on memory maintenance; reduced tonic activity during the delay was beneficial to memory maintenance because it decreased the probability of overwriting the current context. A derivative model of the “gating” theory posits that dopamine exerts gating function in PFC via basal ganglia, since the nigrostriatal DA has much faster kinetics suitable for phasic updating, than mesocortical DA (typically longer than 5 sec to go back to baseline) (Seamans and Yang 2004; O’Reilly and Frank 2006; Garris et al. 1993).

Lastly, the “inverted-U” hypothesis and “gating” hypothesis are not necessarily mutually exclusive. The “inverted-U” shape hypothesis emphasizes the role of tonic DA level in PFC during

the maintenance period of working memory. The “gating” hypothesis underscores the role of phasic DA in PFC (or in striatum) during the encoding period of working memory. It is possible for DA to assume both updating and maintenance roles by employing separate anatomical connections (nigrostriatal DA vs mesocortical DA), exploiting different temporal window (earlier update period vs later maintenance period) or recruiting different postsynaptic mechanisms (D1R vs D2R or DA/glutamate co-release).

1.3 Acetylcholine and Working Memory

The cholinergic hypothesis of Alzheimer’s disease blossomed about 40 years ago, when neuropathological studies reported the reduced cholinergic marker in the post-mortem brains correlated with the number of senile plaques and degree of cognitive impairment (Bowen et al. 1982; Perry et al. 1978; Francis et al. 1985). The correlational link was further corroborated by a series of first-generation lesion studies. In these studies, non-specific excitotoxins (i.e ibotenic acid, quisqualic acid) were injected into basal forebrain cholinergic nuclei and reported deficit in spatial memory test such as Morris water maze (Connor, Langlais, and Thal 1991; Mandel et al. 1989; Salamone et al. 1987; Mandel and Thal 1988), and radial maze (Hodges, Thrasher, and Gray 1989; Turner et al. 1992; Lerer and Warner 1986). However, interpretability of these earlier lesion studies was seriously questioned since these nonspecific excitotoxins led to pallaidal cell loss, thereby disrupting cortico-striato-pallidal loops (Robbins et al. 1989; Everitt and Robbins 1997; Dunnett, Everitt, and Robbins 1991; Fibiger 1991). Instead of non-specific excitotoxins, the cholinergic neuron-selective neurotoxin, IgG-saporin, was introduced in 1991 (Wiley, Oeltmann, and Lappi 1991), which led the cholinergic hypothesis in learning and memory to be revisited.

Disappointingly, direct infusion of IgG-saporin into cortically-projecting nucleus basalis resulted in little to no impairment in spatial learning and memory (M. G. Baxter et al. 1995; Torres et al. 1994; Leanza et al. 1995; Mark G. Baxter and Bucci 2013). Instead, cholinergic neurons in the nucleus basalis have also been implicated in attention and vigilance, and this link stood the

test of time. Infusion of not only the excitotoxins but also IgG-saporin into the nucleus basalis resulted in significant impairment in attention tasks such as multiple-choice reaction time task (J. McGaughy, Kaiser, and Sarter 1996; Chiba et al. 1995; Robbins et al. 1989; J. McGaughy et al. 2000). For example, McGaughy et al. examined the effect of cholinergic lesion on a sustained attention task in rats (J. McGaughy, Kaiser, and Sarter 1996). In the task, the behavioral task was to press the left lever upon cue presentation (hit in signal trial) or press the right lever upon the absence of such cue (correct rejection in nonsignal trial). Any deviation from the rule – pressing the right lever upon cue presentation (miss in signal trial) or pressing the left lever when there was no cue (false alarm in nonsignal trial) was followed by inter-trial-interval. Upon comparison of the rats before and after 192 IgG-saporin injection, cholinergic deafferentation impaired the detection of signal, but spared accuracy during nonsignal trials. This distinct impairment only in signal trials but not in nonsignal trials demonstrates that the lesioning did not interrupt the mnemonic processing or the general adherence to the response rule; the deficit was specific to encoding of stimuli in attention-demanding tasks. This conclusion was further bolstered as the same manipulation did not cause impairment in tasks that do not explicitly tax attentional processing, such as the Morris water maze, radial arm maze, or T-maze alternation (Frick, Kim, and Baxter 2004; Vuckovich 2004; Galani et al. 2002).

More direct link between cortically-projecting cholinergic neurons and cue detection was established using novel techniques such as amperometry or optogenetics. Using amperometry technique, which electrochemically detects synaptic ACh release at a sub-second resolution, Parikh and his colleagues recorded cholinergic transients from the prefrontal cortex of rats performing a cued appetitive response task. The task consists of 90+30 sec ITI followed by 1sec cue that predicts reward after a few seconds. Based on the rat's behavior following the cue presentation, they classified cues into detected cues (disengagement from ongoing behavior and monitoring of food port) and missed cues (absence of cue-evoked shift in behavior). The study demonstrated that a phasic ACh transient in the mPFC is observed for detected cues but not for

the missed cues, reward port approach or reward retrieval (Parikh et al. 2007). Additionally, optogenetic activation of cholinergic neurons to generate “fake” cholinergic transient in noncued trials increased the number of invalid claims for cues (Gritton et al. 2016).

In contrast to cortically-projecting cholinergic neurons in the nucleus basalis, hippocampus-projecting cholinergic neurons in the medial septum have been implicated in spatial working memory. Infusion of excitotoxin as well as IgG-saporin into the medial septum significantly impaired performance in a delayed non-match to sample (DNMS) task (McAlonan et al. 1995; Torres et al. 1994). Torres et al., injected IgG-saporin into the medial septum as well as nucleus basalis in rats performing DNMS task. However, only the medial septum lesion led to deficit in DNMS task. Interestingly, the spatial working memory impairment caused by the septo-hippocampal cholinergic pathway was specific to novel stimuli (Jill McGaughy et al. 2005). Lesion of the cholinergic innervation of the entorhinal cortex specifically impaired DNMTP task for novel stimuli but spared DNMS task for familiar odor. Similarly, parahippocampal lesion in monkeys did not impair their performance in delayed-match to sample (DMS) with familiar stimuli but impaired in DMS as well as DNMS with novel stimuli (Eacott, Gaffan, and Murray 1994; Otto and Eichenbaum 1992; Gaffan and Murray 1992).

The selective involvement of septo-hippocampal cholinergic pathway in working memory for novel stimuli precipitated the hypothesis of working memory for novel information (Hasselmo and Stern 2006). In this view, working memory for novel stimuli requires a separate mechanism whose recurrent activity does *not* depend on pre-wired excitatory connectivity of the network. Most models of working memory persistent activity posits such pre-wired excitatory connectivity in PFC, but this specific connectivity can only exist after hebbian synaptic modification of glutamatergic synapses (i.e. after previous exposure to the stimuli, thereby making the stimuli familiar). The mechanism free of pre-wired recurrent connectivity is proposed to be self-generating persistent activity of neurons in layer II of the entorhinal cortex, as shown in slice

preparation (Shalinsky et al. 2002; Klink and Alonso 1997b). A series of work done by Alonso and colleagues demonstrated that the self-sustained spiking was critically dependent on the muscarinic acetylcholine receptor and the presence of acetylcholine. With acetylcholine, a depolarizing intracellular current injection generated self-sustained spiking in the layer II neurons in the entorhinal cortex, beyond the injection duration. Without acetylcholine, the same current caused the neuron to fire until the end of injection and stop spiking beyond the injection duration.

In summary, cortically-projecting cholinergic neurons in the nucleus basalis is hypothesized to be involved in attention and cue-detection whereas hippocampus-projecting cholinergic neurons in the medial septum may be important for working memory representation of novel stimuli.

1.4 Overview of Thesis Work

Working memory, the ability to remember a stimulus for a brief period of time and to use that memory flexibly to guide ongoing behavior, is a ubiquitous function essential to our cognition. While the details of the network mechanism behind stable working memory representation are still debated, virtually all agree that neuromodulation has a powerful effect on the network state, dynamics and synaptic connectivity that underlie working memory representation. In this thesis, I present my research focusing on the temporally-precise role of two major neuromodulatory systems -midbrain dopaminergic (DA) system and basal forebrain cholinergic (ChAT) system- in spatial working memory.

In Chapter 2, I focused on the role of basal forebrain ChAT system in working memory. Using fiber photometry to record time-varying bulk calcium activity of ChAT neurons in rats performing delayed non-match to position (DNMTP) task, I compared how hippocampus-projecting ChAT neurons in the medial septum (MS) and cortex-projecting ChAT neurons in the nucleus basalis (NB) contribute to spatial working memory, respectively. I quantitatively demonstrated that locomotion explains more variance in MS ChAT neuronal activity compared to task events, whereas task events explain more variance in NB ChAT neuronal activity than locomotion. Furthermore, I discovered functional heterogeneity within the NB ChAT neurons: NB ChAT responses to lever press action and reward were graded and spatially organized along the medio-lateral axis of the NB. Monosynaptic retrograde rabies tracing demonstrated that medial versus lateral NB ChAT neurons receive topographic input from the striatum; dorsomedial striatum preferentially projected to medial NB ChAT neurons while dorsolateral striatum projected to lateral NB ChAT neurons. Together, these findings provide the first evidence of functional heterogeneity within the basal forebrain ChAT system and pinpoint its topographic integration to the basal ganglia as a potential anatomical substrate for this heterogeneity.

In Chapter 3, I investigated the role of midbrain DA system in working memory. Using the same fiber photometry technique, I observed that DA neurons in the ventral tegmental area (VTA) and substantia nigra pars compacta (SNc) showed similar phasic responses to lever presentation and reward during the sample, choice, and outcome period of DNMTP task. Notably, both VTA and SNc DA neurons were low in activity during the delay period. To test if the observed DA activity was causal to working memory performance, I optogenetically inhibited VTA and SNc DA neurons while the rats were performing memory-guided (DNMTP) versus sensory-guided delayed response tasks. Optogenetic inhibition of VTA DA neurons impaired performance in memory-guided DNMTP task only, whereas the same manipulation of SNc DA neurons impaired performance in both memory-guided DNMTP and sensory-guided tasks with increased choice lever press latency (slowing of lever press). Similar optogenetic manipulation of ChAT system during DNMTP task did not impair performance, highlighting that DA system is specifically necessary for working memory performance. Together, I propose a dissociable role of VTA versus SNc DA neurons in spatial working memory: VTA DA activity is causally involved in cognitive working memory performance, while SNc DA activity is causally involved in the motor execution of the task.

Next, I further probed if VTA and SNc DA neurons contribute to spatial working memory performance *in a temporally-specific manner*. To this end, I optogenetically inhibited the DA neurons during a specific epoch (sample, delay, choice period) within a trial. Surprisingly, inhibition of VTA DA activity specifically during the sample and delay period causally impaired working memory performance, even though I previously observed low delay-period DA activity. Inhibition of SNc DA activity during the delay and choice period impaired the performance, once again suggesting the role of SNc DA neurons in later motor execution of the task. To test if the effect of VTA DA neurons in working memory is bidirectional, I optogenetically activated the VTA DA neurons during the delay period and found the impairment of working memory performance

analogous to the inhibition experiment result. In summary, VTA DA activity earlier in the trial (sample and delay) seems to be causally involved in maintaining the working memory representation, whereas SNc DA activity later in the trial (delay and choice period) may be necessary for motor execution of the task. Furthermore, bidirectional manipulation of VTA DA neurons during the delay period impair working memory performance, supporting the inverted U dose-response hypothesis of DA.

In Chapter 4, I provide summary of my thesis work and finally close by discussing the remaining future questions to be addressed. Extensive and comparative calcium recordings and optogenetic manipulations of two neuromodulatory systems in spatial working memory provided in this thesis mainly address the question regarding “when” these two neuromodulators are active and if the observed activity is required for working memory performance. In addition, this work opens up a new avenue for addressing “how” working memory representation in the prefrontal cortex (PFC) is modulated by these neuromodulators. Ongoing work and future directions include projection-specific optogenetic manipulation (VTA DA to PFC vs VTA DA to striatum) as well as electrophysiological recording, which allows simultaneous DA manipulation while recording from downstream PFC or striatal neurons.

Chapter 2: The basal forebrain cholinergic system has spatially organized activity and topographic integration within the basal ganglia

2.1 Abstract

Ascending cholinergic transmission from the basal forebrain (BF) has been implicated in numerous aspects of behavior and cognition, including learning, memory, attention and reward. However, due to the sparse and distributed nature of these cholinergic neurons, it remains unclear how cholinergic neurons correlate with behavior, and whether they respond in a homogeneous or heterogeneous fashion. Using fiber photometry, we recorded from cholinergic neurons in the medial septum (MS) and nucleus basalis (NB) in rats performing a spatial working memory task. In the MS, a substantial fraction of the variability in cholinergic activity is explained by locomotion, while task events provided little additional explanation of neural activity. In contrast, NB cholinergic activity is poorly explained by locomotion, while task events accounted for a substantial fraction of response variability. Further, within the NB, responses to task events are spatially organized along the medio-lateral axis: medial and not lateral NB ChAT neurons respond to the lever press, while both regions respond to reward, but on different timescales. Monosynaptic rabies tracing reveals that NB ChAT neurons are topographically integrated within the basal ganglia, such that medial NB ChAT neurons receive inputs from dorsomedial striatum and lateral NB ChAT neurons receive inputs from the dorsolateral striatum. Together, these findings provide the first evidence of heterogeneity across the BF cholinergic system, as well as a potential anatomical substrate for this heterogeneity.

2.2 Introduction

Cholinergic neurons of the basal forebrain (BF) have been a source of intense interest for many decades. These neurons, which comprise ~6% of BF neurons (Gritti et al. 2006)) provide the major ascending cholinergic modulation to the cortex and hippocampus (Rye et al. 1984), and

are thought to regulate a wide range of cognitive functions, including attention, arousal, learning and memory (Everitt and Robbins 1997; Hasselmo and Sarter 2011; Richardson and DeLong 1990; Sarter and Parikh 2005). Higher cholinergic tone is associated with high arousal state such as wakefulness (Hassani et al. 2009; Teles-Grilo Ruivo et al. 2017) and high vigilance state that promotes sensory detection and discrimination through cortical desynchronization (Parikh et al. 2007; Pinto et al. 2013; Froemke et al. 2013; Eggermann et al. 2014). On a shorter timescale, phasic cholinergic transients are observed in rewarding location (Teles-Grilo Ruivo et al. 2017) and mediate cue detection (Parikh et al. 2007; Gritton et al. 2016). In addition, BF cholinergic neurons rapidly signal reinforcement cue such as reward or punishment (Hangya et al. 2015; Lovett-Barron et al. 2014; Harrison et al. 2016), and movement (Harrison et al. 2016). Despite the wealth of reported functions in BF cholinergic neurons, we lack systematic and comprehensive understanding of how to reconcile these findings together.

A long-standing debate in the field has been whether BF nuclei provide a homogeneous cholinergic signal throughout the brain, or if they provide spatially heterogeneous signals organized by anatomical connectivity. This gap in knowledge exists because cholinergic neurons within the BF are sparsely distributed across a large area spanning multiple brain nuclei (e.g medial septum, MS; Horizontal Diagonal Band of Broca, HDB, nucleus basalis, NB) (Gritti et al. 2006)). (M.-M. Mesulam and Geula 1988; Laszlo Zaborszky et al. 2008),(M. M. Mesulam, Mufson, Levey, et al. 1983) (M. M. Mesulam, Mufson, Wainer, et al. 1983; Laszlo Zaborszky et al., n.d.; Laszlo Zaborszky, van den Pol, and Gyengesi 2012; Saper 1984).

In fact, to our knowledge, only a few studies have directly compared cholinergic activity across different BF subregions in the same behavioral paradigm. One study recorded from optically-identified cholinergic neurons in HDB and NB, and concluded that they both responded indistinguishably to primary reinforcers: water reward and airpuff-punishment. (Hangya et al. 2015). Another study electrochemically measured the release of acetylcholine from the

hippocampus and the prefrontal cortex during the sleep-wake cycle and a T-maze memory task (Teles-Grilo Ruivo et al. 2017). Again, they concluded that cholinergic release in the hippocampus and prefrontal cortex were highly coordinated with each other. And this coordinated acetylcholine release was correlated with reward location in a T-maze and arousal states. On the other hand, Parikh and colleagues reported that the cholinergic transient is associated with cue detection only in the mPFC but not in the motor cortex (Parikh et al. 2007). Nonetheless, the lack of cholinergic transient to cue detection in the motor cortex merely serves as a negative control and does not necessarily support the heterogeneity of functions between different BF cholinergic nuclei.

Given the diversity of functions that have been ascribed to BF cholinergic neurons, we sought to examine their activity in a behavioral task that is sufficiently complex to dissociate cue, action, outcome and locomotion. To this end, we recorded from cholinergic neurons in the BF using fiber photometry during a spatial working memory task in freely moving rats. This allowed us to systematically quantify neural correlates of several aspects of behavior that may be relevant to BF cholinergic neurons, as well as compare these correlates across two BF cholinergic nuclei (MS and NB). We found that locomotion explained more variance in MS cholinergic activity while task events explained more variance in NB cholinergic activity. In addition, we identified functional heterogeneity within the NB itself: NB responses to the lever press action and reward were graded and spatially organized along the mediolateral axis of the NB. Monosynaptic rabies tracing revealed that these NB ChAT neurons receive topographic inputs from the striatum. Together, these findings provide the first evidence of functional heterogeneity within the BF cholinergic system and provide its topographic integration to the basal ganglia as a potential anatomical substrate for the heterogeneity.

2.3 Results

To examine the patterns of activity in the basal forebrain cholinergic neurons, we trained ChAT::Cre rats on a spatial delayed non-match to position task (DNMTP, Figure 1A) and used fiber photometry to record from cholinergic neurons in the MS and NB.

2.3.1 Rats performed a spatial working memory task

In the DNMTP task (Figure 1A), rats are presented with a sample lever in one of two possible locations on the front wall of the chamber (sample presentation). Upon pressing the lever (sample press), the lever retracts and the nosepoke on the back wall of the chamber is illuminated. The rat then initiates the delay period by entering the nose poke (delay start). After a delay of either 1, 5, or 10 s (randomly interleaved), if the rat re-enters the nose poke, both levers will be presented on the front wall (choice presentation). To obtain a water reward, the rat must press the lever that does not match the initial sample lever (choice press). Trained rats performed well above chance on the choice press and displayed a delay-dependent decline in performance (Figure 1B; Mean $\pm$ SEM, MS, 1sec: 94.4$\pm$ 1.6, 5ec: 89.3 $\pm$ 2.4, 10sec: 76.7 $\pm$ 4.44; NB, 1sec: 93.0 $\pm$ 1.1, 5sec: 86.4 $\pm$ 2.5, 10sec: 79.4 $\pm$ 2.7)

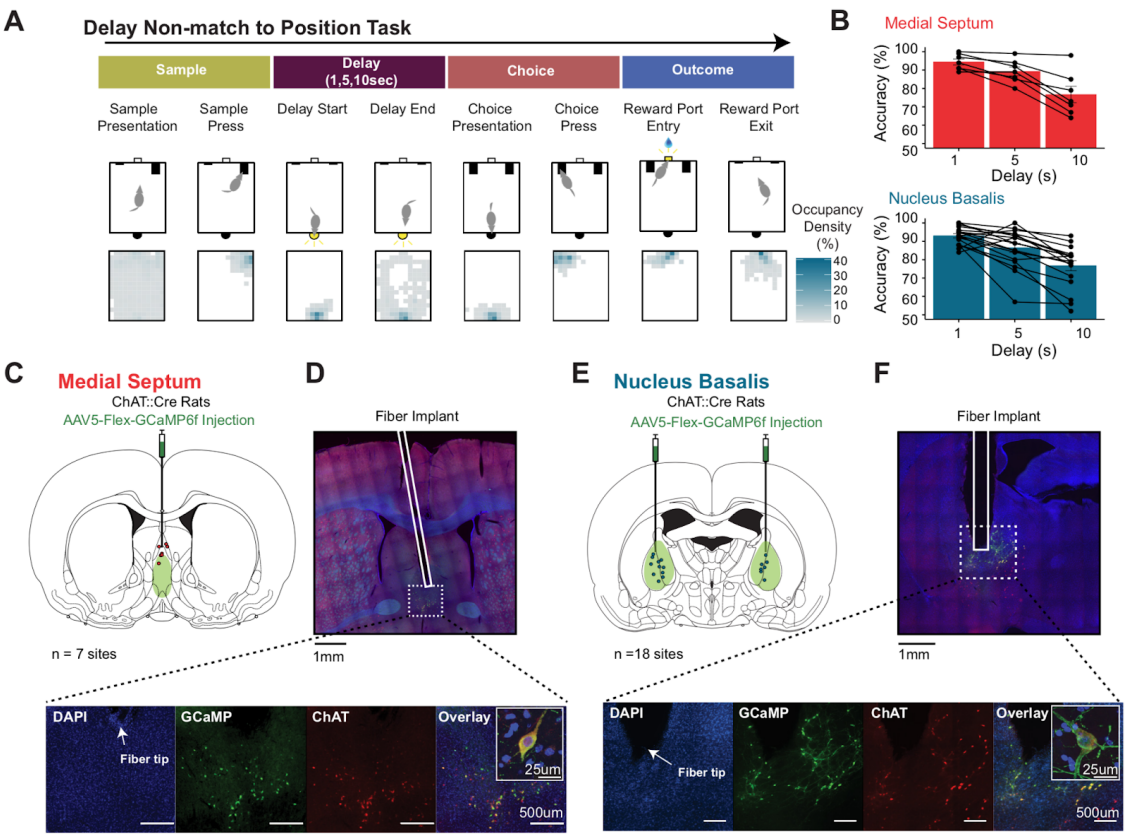


Figure 1 Cholinergic neurons in the NB and MS were monitored during a DNMTP task. (A) Schematic of Delay non-match to position task (DNMTP task). It is a rodent working memory task, in which a rat is required to remember the position of the sample lever presented for a delay period and then to choose a non-match (opposite) lever to get a reward. In the schematic (top) of a single type of trials (correct, right sample lever trials), and different task events are illustrated as the time progresses from left to right. Below is average occupancy density map indicating the position of rats in the operant chamber 0~0.2sec around corresponding event illustrated above. (B) Average performance accuracy plot for all rats in the medial septum group (top, n=7) and the nucleus basalis group (bottom, n=18 sites). Note that the trained rats perform the DNMTP task above chance level (50%), and show delay-dependent impairment in memory. (Mean + SEM, MS, 1sec: 94.4+ 1.6, 5ec: 89.3 + 2.4, 10sec: 76.7 + 4.44; NB, 1sec: 93.0 + 1.1, 5sec: 86.4 + 2.5, 10sec: 79.4 + 2.7) (C) ChAT::Cre rats (n=7) were trained and Cre-dependent GCaMP was

injected into medial septum (green area). Fiber tip locations were confirmed from histology (red dots) (D) Example MS histology image used to confirm the fiber tip location (top, white: fiber track, scale bar: 1mm) and cholinergic neuron-specific expression of GCaMP (bottom zoom-in image, scale bar: 500μm; overlay inset, scale bar: 25μm). (E) and (F), same as (C) and (D) but in nucleus basalis.

To record from ChAT neurons in MS and NB of freely-moving rats performing DNMTP, we employed fiber photometry. Cre-dependent GCaMP6f virus was injected into the medial septum (MS) or nucleus basalis (NB) of the ChAT::Cre rats, and an optical fiber was implanted above the injection site (Figure 1C-F). The combination of ChAT::Cre transgenic rats and cre-dependent virus injection resulted in cell-type specific expression of GCaMP expression in the cholinergic neurons (Figure 1D and 1F). Using GCaMP activity of cholinergic neurons as a proxy for their neuronal activity, we monitored MS and NB cholinergic neurons' activity while the animal was freely-moving and performing the working memory task.

2.3.2 Task events explain more variance in NB ChAT neurons whereas locomotion explains more variance in MS ChAT neurons

We first quantified the extent that "events" in the behavioral task (e.g. lever presentation, lever press, reward delivery), in comparison to the animal's movement in the chamber, relate to ChAT activity in the MS and NB (Figure 2A). Isolating the contribution of task event from the animal's locomotion was particularly important to examine rigorously in the case of an operant task, given that an animal's speed will correlate with task events, and therefore neural correlates of task events may be better explained as neural correlates of movement (eg. speed may be lower during delay or reward period, or higher before the delay period, when the animal traverses the chamber). Thus, before examining in detail the neural correlates of behavioral events, we

wanted to determine if the animals' movement in the chamber provided a better explanation of neural activity than the task events.

To examine the relative contribution of task events versus the animal's movement in explaining GCaMP activity, we built generalized additive linear models in which GCaMP signal was predicted based on 1) delay period only, 2) speed only, 3) task events only and 4) combined task events and speed predictors (Figure 2B). Delay period predictor was a binary predictor which indicated whether the animal was in the delay period (denoted as 1) or in any other period such as sample or reward period (denoted as 0). Since DNMTP is a working memory task, and cholinergic tone during the delay period has been shown to enhance persistent activity in the many brain regions (Hasselmo 2006; Klink and Alonso 1997a; Fransén et al. 2006; Haj-Dahmane and Andrade 1998; Fransén, Alonso, and Hasselmo 2002; Hasselmo and Stern 2006), we wanted to capture if the cholinergic activity is mediated by the delay period. To flexibly model the relationship between GCaMP and speed, a first, second, and third degree polynomial of the animal's speed was used as locomotion predictors. Task event predictors were generated by convolving event times (binary variable) with a spline basis set (degrees of freedom = 10). The duration of the basis set was 3 sec around all types of task events, except reward port entry event was allowed to have a longer 10 sec kernel to capture the entirety of sustained reward response.

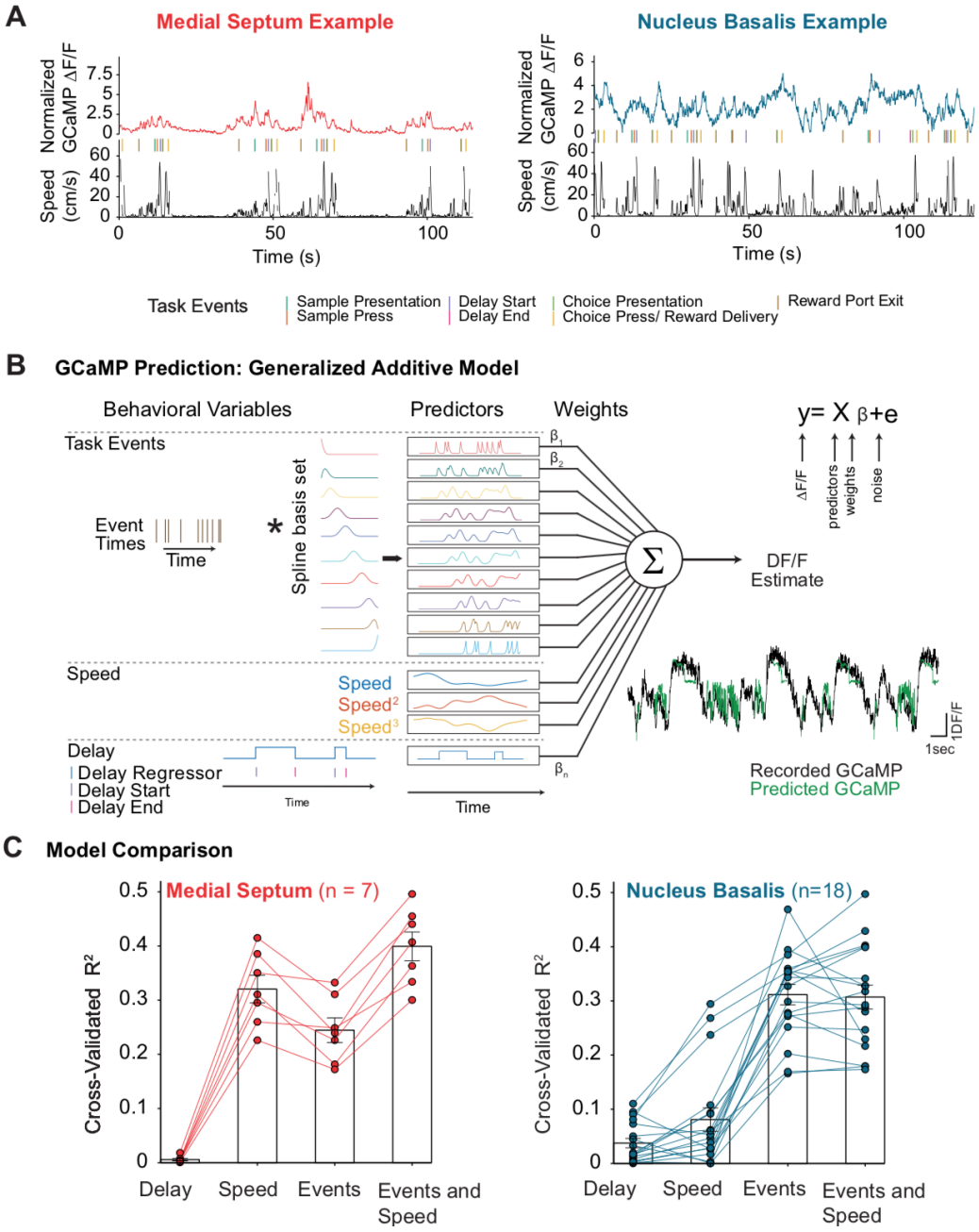


Figure 2 Task events explain relatively more variance in NB ChAT activity, while speed explains more in MS ChAT activity

(A) Example data showing simultaneous acquisition of time-varying GCaMP activity(top), timestamps for different types of task events(middle), and animals speed in the chamber(bottom). (B) Schematic of encoding model in which GCaMP was predicted as a weighted linear sum of predictors. Task event predictors were created by convolving task event time stamps with a spline

basis set of 10 degrees of freedom. Speed predictors include first, second, and third-degree polynomial of the animal's speed. Delay predictor was a binary predictor in which 1 denotes within delay period and 0 denotes all other period. Combination of these predictors were summed linearly with weights to predict GCaMP estimate(green trace) that correlates with recorded GCaMP(black trace)

(C) Four encoding models(x-axis) were generated and compared using cross-validated R^2 (y-axis). Four sets of predictors used for four models include 1) delay only model 2) speed only model 3) task events only model 4) task events plus speed model. In the medial septum group (left, n=7 sites), predicted GCaMP from the speed-only model explained the recorded GCaMP better than that from the task events model. Opposite was true in the nucleus basalis group (right, n=18 sites), that the predicted GCaMP from the task-events model was better correlated with recorded GCaMP than that from the speed-only model. (Mean $\pm$ SEM, MS, Delay: 0.005 $\pm$ 0.002, Speed: 0.32 $\pm$ 0.03, Events: 0.24 $\pm$ 0.02, Events + Speed: 0.40 $\pm$ 0.02; NB, Delay: 0.04 $\pm$ 0.009, Speed: 0.08 $\pm$ 0.02, Events: 0.31 $\pm$ 0.02, Events + Speed: 0.30 $\pm$ 0.02)

Comparing the predictive power of four different encoding models on cross-validated data revealed that MS cholinergic activity was better explained by the speed predictors than by the task events, whereas NB cholinergic activity was poorly explained by speed and much better explained by the task events (Mean $\pm$ SEM, MS, Delay: 0.005 $\pm$ 0.002, Speed: 0.32 $\pm$ 0.03, Events: 0.24 $\pm$ 0.02, Events + Speed: 0.40 $\pm$ 0.02; NB, Delay: 0.04 $\pm$ 0.009, Speed: 0.08 $\pm$ 0.02, Events: 0.31 $\pm$ 0.02, Events + Speed: 0.30 $\pm$ 0.02). Being in the delay period barely explained the GCaMP activity of the cholinergic neurons, to our surprise. More complex, combinatorial model (speed + task event model) did not significantly improve R^2 compared to the simpler models, despite the loss of degrees of freedom. Together, we found that task events explain more variance in NB ChAT activity, whereas locomotion explains more variance in MS ChAT activity. In summary, two different cholinergic nuclei -NB and MS- in the BF are functionally heterogeneous when the animal is performing a spatial working memory task.

2.3.3 NB ChAT neurons show elevated activity to lever press action and reward

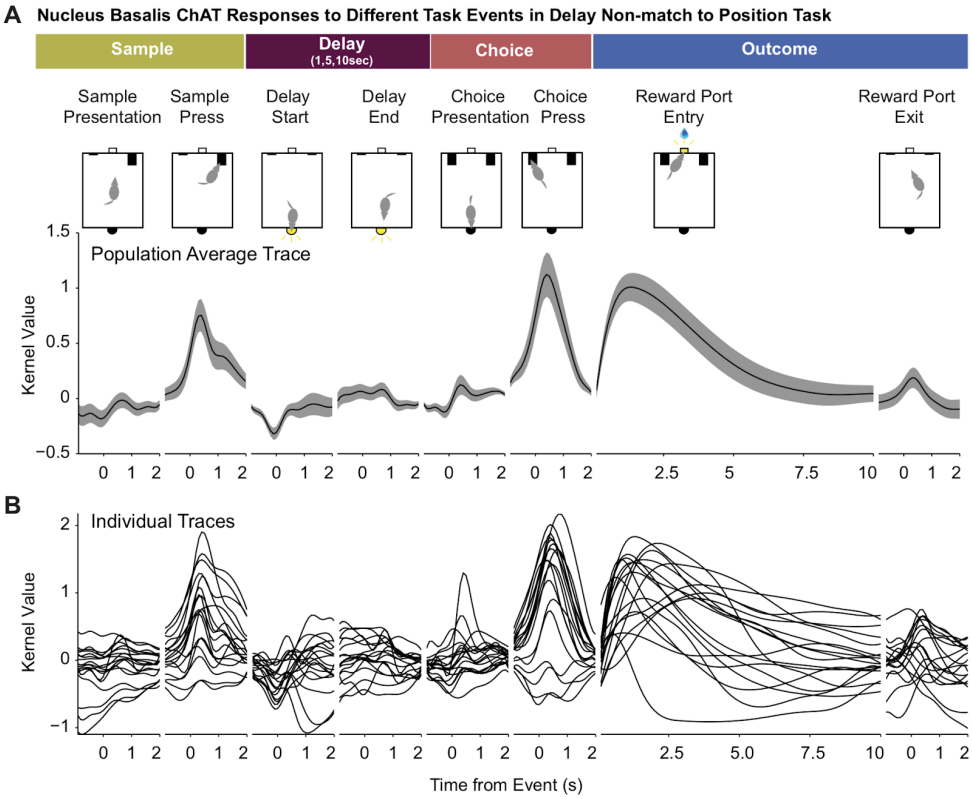


Figure 3 Elevated activity in NB ChAT neurons is associated with lever press action and reward

(A) Kernels for each type of task events (top schematic), created from task-only model, are plotted as population average (black line) and standard error across sites (grey shaded region).

(B) Kernels created from each type of task events are plotted for each individual recording site, showing variability in the traces (n=18 sites).

To determine which task events are encoded by NB cholinergic activity, we plotted the task event kernels for each type of task events generated from the task-only model (Figure 3A). When plotted population average, we observed elevated NB cholinergic activity for the lever

press action (sample lever press, choice lever press), and reward (reward port entry), but not to the lever presentation cue.

However, when individual recordings were plotted, NB cholinergic responses were highly variable across the recording sites (Figure 3B). For example, some NB recordings did not exhibit any lever press response while others showed a clear phasic peak around the lever press action. The absence of lever press response was not due to low signal-to-ratio, because the same trace showed a huge reward response at the end of trial. In addition, the time course of reward responses (phasic vs. sustained reward responses) was also variable across recording sites. Puzzled by such variability, we turned to histology and asked if the spatial location of the recording site within the NB could account for some of this variability.

2.3.4 NB ChAT neurons' response is organized along the medio-lateral axis of the NB

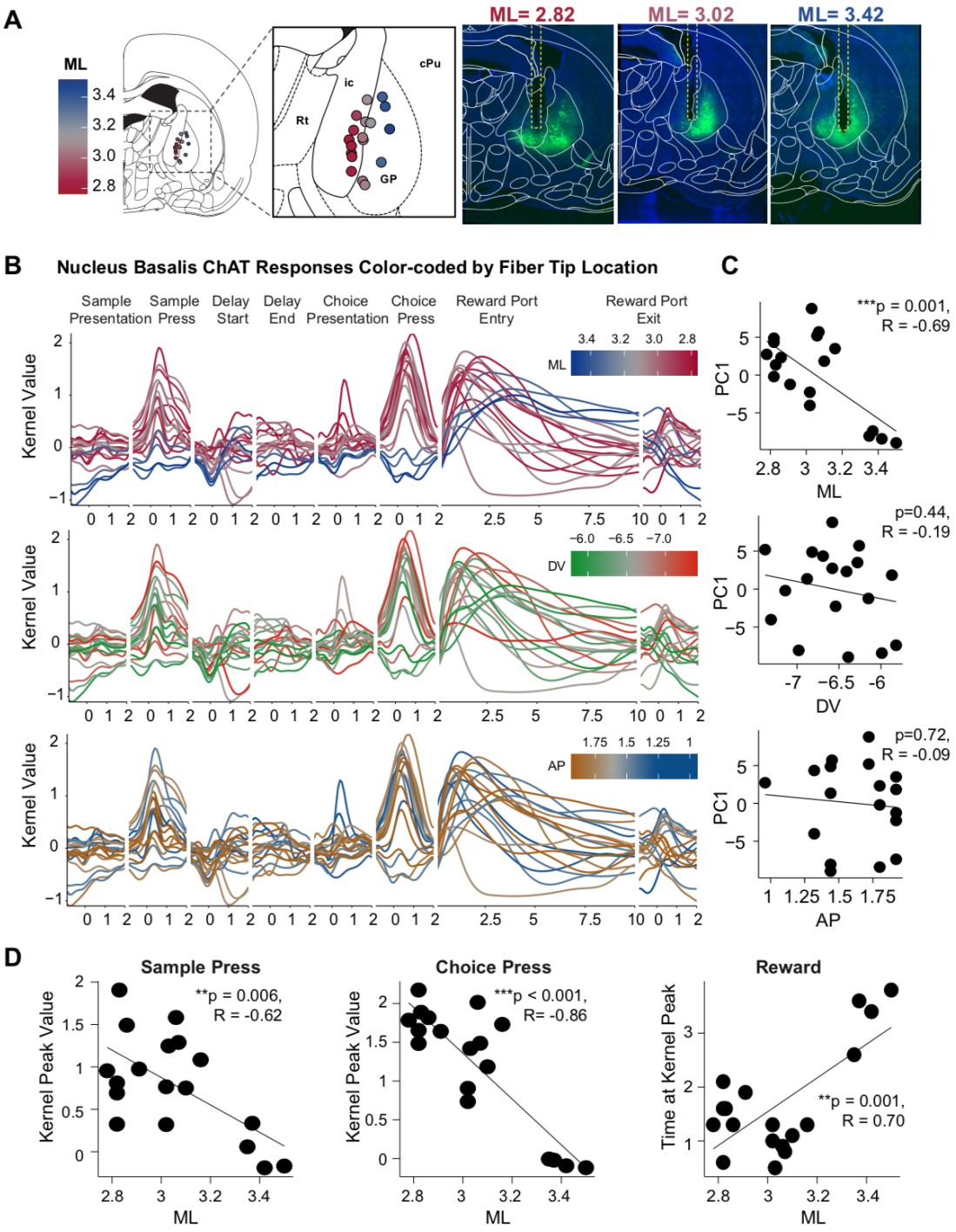


Figure 4 NB ChAT neurons' response variability is best explained by the medio-lateral position of the recording fiber tip within the NB

(A) Recording Fiber Tip Locations Overlaid on the Atlas. Recording fiber tip location is reconstructed from histology and overlaid onto the atlas (left). Each dot is a recording fiber tip, color-coded by its medio-lateral position. Three example images (right) showing fiber tips with ML position variability (left to right, medial–center--lateral location within the NB). Yellow dotted line is reconstructed fiber location from histology, and white is the atlas outline overlaid on the histology image.

(B) Nucleus basalis ChAT Responses color-coded by Fiber Tip Location. Individual kernels for each type of task events (same as Figure 3B) is color-coded by fiber tip location along the Medio-Lateral axis (top) Dorso-Lateral axis (middle) and Anterior-Posterior axis (bottom).

(C) The first principal component (y-axis) from the principal component analysis of the kernel traces (Figure 4B) is correlated with the fiber tip location along the ML (top), DV (middle), AP (bottom) axes (x-axis). Fiber tip location along the ML axis significantly explained the first principal component (Linear Regression of PC1 explained by ML, DV and AP of the fiber tip location, $p = 0.003$**)

(D). ML position of recording fiber tip (x-axis) correlates with the peak value of sample lever press (left panel), the peak value of choice lever press (middle panel) and the time at reward kernel peak (right panel). Lever press action response is stronger in medially-located NB ChAT recordings (sample press, $R= -0.62$, $p = 0.006$**, choice press, $R = -0.86$, $p < 0.001$ ***). Reward response peaks faster in the medially-located NB ChAT recordings ($R=0.70$, $p =0.001$**).

We hypothesized that the functional response properties were anatomically organized within the NB. To answer the question, we carefully re-constructed fiber tracks from the histological sections of post-mortem brains and the recording site was estimated based on the location of fiber tip coordinate.(Figure 4A, see Methods). A/P was determined by the section with the deepest fiber track, and both M/L and D/V were derived by equating the ratio of measured distances (i.e. ratio of measured distance between midline-fiber tip and distance between midline-outer edge of tissue) and that of atlas distances to account for tissue shrinkage during the

fixation step. Note that simply measuring a distance from the midline, or taking a local landmark (GP-striatum border) to measure the relative distance to the fiber tips showed a significant correlation with the ratiometric M/L position. (Pearson's correlation test, ratiometric ML vs Midline - fiber tip distance: R = 0.88 p<0.001***, ratiometric ML vs GP-striatum border distance: R = 0.79, p<0.001***)

Interestingly, we found that NB ChAT responses were significantly correlated with the M/L position of the recording sites but not with the D/V or A/P position. (Figure 4B). To capture the variability in the NB ChAT responses, we performed a principal component analysis on all event kernels and correlated the first PC with M/L, D/V and A/P positions of the recording sites. Only the M/L position of the recording site was significantly correlated with the first PC (Figure 4C, Pearson's correlation test, PC1 vs M/L: R = -0.69, p = 0.001***, PC1 vs D/V: R = -0.19, p = 0.44, PC1 vs A/P: R = -0.09, p = 0.72). In addition, the first PC was significantly predicted by the M/L position but not by the D/V or A/P positions of the recording sites (Linear Regression, M/L: p= 0.003**, D/V: p=0.79, A/P: p=0.73)

How does the M/L gradient of NB ChAT responses correlate with elevated event kernels for lever press action and reward? Correlating the M/L position of recording sites with lever press and reward kernels, we found that medial NB ChAT neurons responded more *strongly* to lever press actions and *transiently* to reward delivery compared to lateral NB ChAT neurons (Figure 4D, Pearson's correlation, sample kernel peak vs ML: R =-0.62, p=0.006**, choice kernel peak vs ML, R=-0.86, p < 0.001***, time to reward kernel peak vs ML: R=0.70, p=0.001**). Together, these results suggest an anatomical organization of cholinergic neurons' functional responses across the M/L axis of the NB.

2.3.5 Monosynaptic retrograde tracing reveals that the striatum is the strongest projector and the subthalamic nucleus is the densest projector to NB ChAT neurons

Next, we addressed if the functional M/L gradient of the NB could be parsimoniously explained by their input connectivity. To characterize input brain regions to medial versus lateral NB ChAT neurons, we first injected a cre-dependent helper virus (AAV5-CMV-DIO-TVA66T-HA -P2A-N2cΔG) into the NB in six ChAT::Cre animals. Then we divided them into two groups - 3 rats in each medial NB ChAT group and lateral NB ChAT group-- and injected a very small volume of rabies virus (50~200nl of RabV-CVS-N2cΔG-mcherry, (Reardon et al. 2016; Wickersham et al. 2007) into either medial or lateral NB coordinates, which were 0.7mm apart from each other medio-laterally (medial NB A/P: -1.5mm, M/L: 2.8mm, D/V: -7.2mm; lateral NB A/P:-1.5mm, M/L: 3.5mm, D/V: -7.2mm). Since the expression of the monosynaptic retrograde tracer was restricted to the helper virus, which was further restricted to the cholinergic neurons, this viral strategy allowed labeling of all input cells to the cholinergic neurons in the NB (Figure 5A). In addition, small injections of the rabies virus into either the medial versus lateral NB locations allowed us to compare the input cells to the medial vs lateral NB ChAT neurons. In total, coronal brain sections from 6 rats' entire brains (approximate AP range from +4~-9mm) in 100μm spacing were collected and analyzed using the *Wholebrain* package(Fürth et al. 2018).

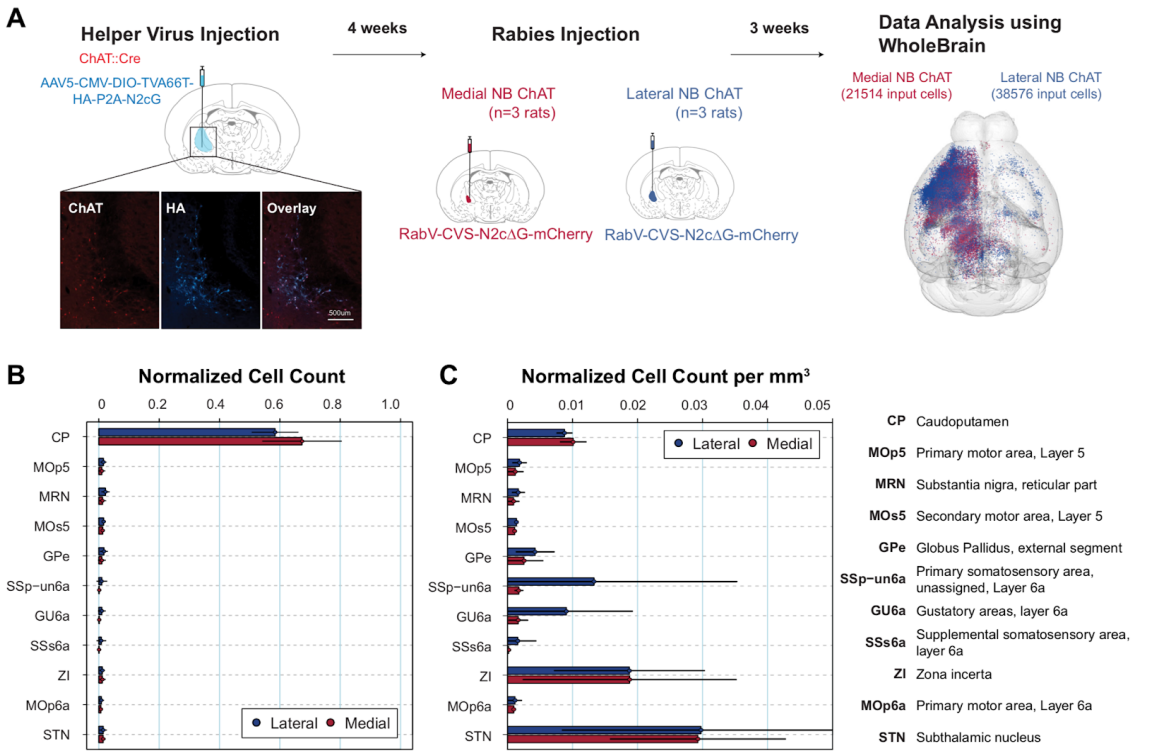


Figure 5 Monosynaptic rabies tracing reveals that the striatum is the strongest, projector and the subthalamic nucleus is the densest projector to NB ChAT neurons (A) Schematic of Monosynaptic Retrograde Tracing Experiment. ChAT::Cre rats are injected with Cre-dependent helper virus to express TVA specifically in the cholinergic neurons (Red: ChAT staining, Blue: HA tag in helper virus, Overlay: helper virus expression in the cholinergic neurons). After 4 weeks, rabies virus was injected either in the medial or lateral NB. Since the expression of the helper virus to the rabies virus was restricted to the cholinergic neurons, it allowed monosynaptic retrograde tracing from medial or lateral NB ChAT neurons. After 3 weeks of virus expression, animals are sacrificed and histology sections were registered and segmented using the Wholebrain package (Fürth et al., 2018).

(B) The majority of input to NB ChAT neurons comes from the striatum. X-axis: regional cell count normalized by the total input cells, Y-axis: input brain regions that have >100 cells. Blue dot and error bar: Mean ± SEM for lateral NB ChAT group (n=3), Red dot and error bar: Mean ± SEM for medial NB ChAT group (n=3)

(C) The Densest input area to NB ChAT neurons is the subthalamic nucleus. X-axis: regional cell count normalized by the total input cells and by the size of the structure, Y-axis: input brain regions that have >100 cells. Blue dot and error bar: Mean $\pm$ SEM for lateral NB ChAT group (n=3), Red dot and error bar: Mean $\pm$ SEM for medial NB ChAT group (n=3)

We found that NB ChAT neurons received a strong input from the striatum and dense input from the subthalamic nucleus, which are two major nodes in the basal ganglia. The striatum was the strongest projector to the NB ChAT neurons for both groups, comprising 63 + 4% of total input cells to NB ChAT neurons (Figure 5B, Mean + SEM: medial NB: 67 + 6%, lateral NB: 58 + 4%).

In addition, when the normalized cell count was again controlled for how big the brain structure is in mm^3, we found that the subthalamic nucleus was the densest projector to the NB ChAT neurons for both groups (Figure 5C, Mean + SEM: medial NB: 3.0 + 1%/mm^3, lateral NB: 3.0 + 0.6%/mm^3). Although it was interesting to find a strong connection between these NB ChAT neurons and the basal ganglia system, we did not find any noticeable difference between the groups of interest (i.e. medial NB ChAT vs lateral NB ChAT groups) in the input region.

2.3.6 DMS projects to medial NB ChAT neurons whereas DLS projects to lateral NB Chat neuron respectively

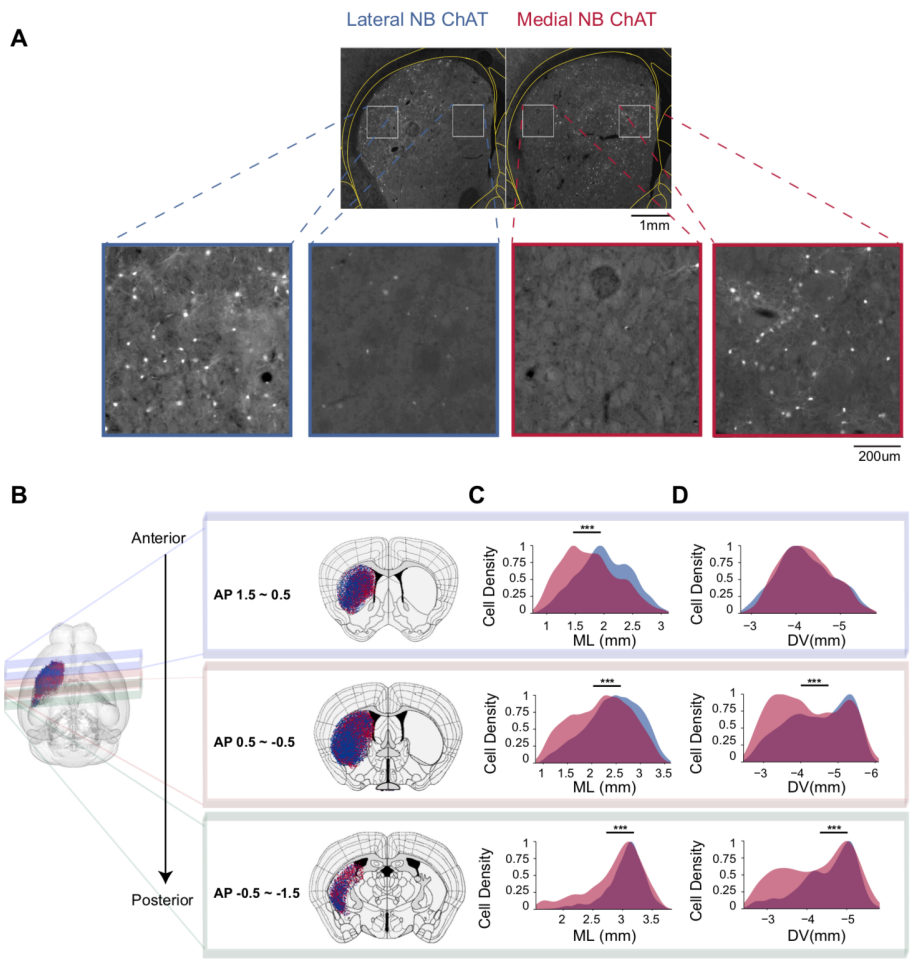


Figure 6 Striatal projection to NB ChAT neurons is topographic (A) Example image of input cells in the striatum (Blue insets: DMS and DLS of a rat in lateral ChAT NB injection group, Red insets: DMS and DLS of a rat in medial ChAT NB injection group, scale bar for the top images: 1mm, scale bar for the insets: 200um)

(B) Striatum input cells to NB ChAT neurons in 3D brain (left) and coronal sections (right) collapsed across different APs (top: AP 1.5~ 0.5, middle: AP 0.5~-0.5, bottom: AP -0.5~-1.5). Red cells: input cells in the medial NB injection group, Blue cells: input cells in the lateral NB

injection group. Note that the registration was done on the mouse brain atlas, thus the coordinates corresponds to that of a mouse brain.

(C) Striatum input cell density (y-axis) across M-L axis (x-axis) shows that medial NB ChAT neurons receive preferential input from the medial striatal cells (red distribution), while lateral NB ChAT neurons receive preferential input from lateral striatal cells (blue distribution; student's t-test on the ML location of striatum cells between medial NB ChAT injection groups and lateral NB ChAT injection groups show significant difference in the mean of their ML distribution across all APs; top: $p<0.001$***, middle: $p<0.001$***, bottom: $p<0.001$***)

(D) Striatum input cell density (y-axis) across D-V axis (x-axis) shows that medial NB ChAT neurons receive preferential input from the dorsal striatal cells (red distribution), while lateral NB ChAT neurons receive preferential input from ventral striatal cells (blue distribution; student's t-test on the DV location of striatum cells between medial NB ChAT injection groups and lateral NB ChAT injection groups show significant difference in the mean of their DV distribution only in the posterior APs; top: $p=0.17$, middle: $p<0.001$***, bottom: $p<0.001$***)

To our surprise, the input connectivity difference between the medial vs. lateral NB ChAT groups emerged when we analyzed the *topography* of input cells in the strongest projector, striatum. Medial NB ChAT group received more input from the DMS (Figure 6A Blue), whereas lateral NB ChAT group received more input from the DLS (Figure 6A Red). This DMS-to-medial NB ChAT and DLS-to-lateral NB ChAT topographic pattern was present throughout the striatum across different APs (Figure 6B~C). In addition, dorso-ventral input topography appeared towards the posterior striatum; medial NB ChAT neurons received more input from the dorsal striatum whereas lateral NB ChAT neurons received preferential input from the ventral striatum (Figure 6D). Together, we found that the striatum input to NB ChAT neurons was topographic, potentially mediating the functional response gradient along the M/L axis of NB.

2.4 Discussion

2.4.1 Dissociative encoding in NB vs MS ChAT neurons

The dissociative encoding in NB versus MS ChAT neurons (Figure1) that we report provides a convincing case for the heterogeneity of functions between different BF cholinergic nuclei. The notion of BF cholinergic system as a diffuse neuromodulatory system that broadcast unitary information redundantly throughout cortex has been long been debated. Recent anatomical findings spearheaded by Zaborszky group illustrate highly topographical nature of BF cholinergic system consisting of cell clusters, cluster-specific dendritic organization and connectivity (Laszlo Zaborszky, van den Pol, and Gyengesi 2012; Laszlo Zaborszky et al., n.d.; L. Zaborszky et al. 2013; Gielow and Zaborszky 2017; Laszlo Zaborszky et al. 2015). In light of this, several recent studies addressed a similar question and compared the cholinergic neuronal activity between NB and HDB (Hangya et al. 2015) or the release of acetylcholine in PFC and hippocampus (Teles-Grilo Ruivo et al. 2017) or in PFC and motor cortex ((Teles-Grilo Ruivo et al. 2017; Parikh et al. 2007). None of these studies reported distinctly heterogeneous functional encoding between the two different BF cholinergic nuclei or between their projection targets, unlike our finding. We attribute this disparity to the complexity of the task; our DNMTP task was sufficiently complex to dissociate locomotion and diverse behavioral events ranging from sensory cue, operant actions, to reward. Lastly, one should note that we did find some weaker task encoding in the MS cholinergic neurons as well as locomotion encoding in the NB cholinergic neurons. Our interpretation does understate this weaker encoding as some degree of confounding between locomotion and task events in a freely-moving operant task is inherently unavoidable and inseparable even with careful quantification and modeling.

2.4.2 Relevance to previously reported functions of NB ChAT neurons

The task encoding in NB ChAT neurons showed elevated response to lever press action and reward (Figure 3). This is in contrast to previously reported function of cholinergic transient

in cue-detection. Acetylcholine release in mPFC is associated with detected cue and its optogenetic manipulation bidirectionally modulates cue detection rate (Parikh et al. 2007; Gritton et al. 2016). In this framework, glutamate transients are hypothesized to be the first one to "notice" the stimuli and update it to the cortical circuit. These signal-evoked glutamatergic transients are present in all signal trial regardless of behavioral signature of "detection", and their amplitude correlate with the cue duration (W. M. Howe et al. 2013). Then the signal-evoked cholinergic transients follows the signal-evoked glutamate transient in mPFC. The cholinergic transients are hypothesized to follow up on the glutamate transient to "detect" and "orient" to the cue by synchronizing signal-bound actions across cortices through evoked high frequency oscillations (W. M. Howe et al. 2013). However in our DNMTP task, NB ChAT neurons did not respond to the cue, which was the lever presentation. Instead, NB ChAT neurons responded to lever press action. Since we find the topographical connection between the basal ganglia and NB ChAT neurons, it is possible that the "action" signal is comes from the basal ganglia. Additionally, NB ChAT response to lever press action suggest that the cholinergic transients is implicated in "behavioral" signature of detection rather than behavioral signature of "detection" as suggested by the cue-detection hypothesis.

NB ChAT response to reward that we report here is in line with previous findings (Hangya et al. 2015; Teles-Grilo Ruivo et al. 2017) Hangya and colleagues recorded from optically tagged cholinergic neurons and found their response to rewarding and punishment cues in auditory detection task (Hangya et al. 2015). A separate group of researchers also found phasic cholinergic transients in "reward-zone" in a T-maze task (Teles-Grilo Ruivo et al. 2017).

2.4.3 M-L Gradient in NB ChAT neurons

We found a spatial organization of cholinergic neurons within the NB, along the medio-lateral axis (Figure 4). This is surprising given that the medio-lateral extent of the structure is only about a mm wide, whereas its dorso-ventral (d-v) or anterior-posterior (a-p) axes are much

longer. In fact, NB ChAT neurons' response to reinforcement surprise was reported to be graded along the dorso-ventral axis of the NB (Hangya et al. 2015). Although we did not find a graded response along the a-p or d-v axes in our data, it does not eliminate the possibility of a-p or d-v gradient in the NB ChAT neurons; since this m-l gradient was a serendipitous finding post-data collection, we did not fully take advantage of the long a-p and d-v axes of the structure. Future experiment can address this concern by systematically sampling recording sites along all three axes of the NB.

Another potential valid concern is the possibility of this m-l gradient emerging from the cholinergic interneurons in the striatum as the striatum is situated laterally to the NB. However, this ChAT::Cre rats do not express cre in the cholinergic interneurons, so we are positive that this m-l gradient is well confined within the NB structure.

2.4.4 Topographical integration with the basal ganglia

We found that NB ChAT neurons are topographically integrated with the basal ganglia. Specifically, the strongest projector to NB ChAT neurons was the striatum and the densest projector was the subthalamic nucleus. In addition, the input from the striatum was topographic such that DMS projected to medial NB ChAT neurons and DLS projected to lateral NB ChAT neurons.

Our finding closely aligns with another monosynaptic retrograde tracing work published by Zaborsky group in 2017 (Gielow and Zaborszky 2017). Of note, Zaborszky group and we used a different viral strategy to label input neurons. Our strategy labeled all inputs to NB ChAT neurons, whereas Zaborszky group used a strategy that labels inputs to NB ChAT neurons that projects to a specific output such as M2, VO, mPFC, and amygdala (input cells to pathway-specific NB ChAT neurons). Regardless, we found that the striatum was the stronger projector, and likewise, they also found striatum to be the strongest projector in all output-specific

groups. Our findings further elaborate on the connection by showing that the densest input to NB ChAT neurons was the subthalamic nucleus. We sought to examine the densest input, given that striatum is a large structure therefore the strongest projector could be different from the densest projector. Moreover, our medio-lateral functional gradient of NB ChAT neurons was manifest by the topographical input from the striatum. Given that two of the major hubs of basal ganglia connects to the NB ChAT neurons, and the connection shows medio-lateral topography, which is the principal organization of the basal ganglia, we propose that NB ChAT neurons potentially might serve as a node in the basal ganglia circuitry.

2.5 Methods

2.5.1 Rats

ChAT::IRES-Cre rats expressing Cre recombinase under the control of choline acetyltransferase were maintained on a Long Evans background. 16 male and 1 female rats weighing > 300g at the start of the training were used for experimentation. Most rats were double-housed, unless they weigh over 500g (single-housed due to space constraint). Rats were maintained on a 12-hour light on – 12-hour light off schedule. All surgical and behavioral procedures were performed during the light off cycle.

All experimental procedures were conducted in accordance with the National Institute of Health guidelines and were approved by the Princeton University Institutional Animal Care and Use Committee.

2.5.2 Delayed non-match to Sample Task

Rats were water-restricted to 80-85% of their *ad-libitum* weight and trained on a delayed non-match to position spatial working memory task in operant chambers (Med-associates). The operant chamber had two retractable levers on the front wall and a nose port on the opposite, back wall. The goal of the task was to remember the position of the sample lever – either right or left – during the delay period, and to show that memory in the choice period by pressing the non-match, opposite lever. At the beginning of each trial, the sample period begins as a sample lever was presented out of the wall, either on the right or the left side, randomly interleaved. Upon pressing the sample lever, the lever retracted back into the wall and the light in the back nose port was illuminated. The delay period begins as the rat goes to the back wall to poke his nose into the illuminated nose port. The delay period lasted for 1, 5 or 10 sec (randomly interleaved) during which rats usually kept constantly poking his nose into the nose port, not knowing when the delay period would end. At the end of delay period, the nose port lighted up again and the rat must then

make the second nose poke for both levers to extend from the front wall and to begin the choice period. Between the two levers, the correct response is to press the lever that does not match the sample lever. Correct response is rewarded with water in the reward receptacle. The rats are given 15 sec to press the sample lever and 5 sec to poke illuminated nose port and press the choice lever. An incorrect lever press or a failure to response within the time limit resulted in 3s time-out. Trials were followed by 5 sec inter-trial interval.

2.5.3 Surgery

ChAT::Cre Rats trained in DNMTP task were deeply anaesthetized in 1-2% isoflurane and placed in a stereotactic setup. Virus was injected with a microsyringe.

For Fiber photometry experiments, 1μl of Cre-dependent GCaMP virus (AAV5-CAG-Flex-GCamP6f or AAV5-CAG-DIO-RatOpt-GCaMP6f) was injected to the nucleus basalis (A/P: -1.5mm, M/L: 2.8~3.0mm, D/V: -7.0mm). 0.75ul of Cre-dependent GCaMP virus (AAV5-CAG-Flex-GCamP6f) was injected into the medial septum (A/P: +0.5mm, M/L: 0mm, D/V: -7.0mm) at a 10º angle. After virus injection, optical fiber (400μm core diameter) was implanted -0.1 mm above the injection site.

For Rabies experiment, 1.5 μl of helper virus (AAV5-CMV-DIO-TVA66T-HA-P2A-N2cΔG) was injected into the nucleus basalis (A/P: -1.5mm, M/L: 0.75 μl into 2.8mm, 0.75 μl into 3.5mm, D/V: -7.2mm). 4 weeks later, 50~200nl of rabies virus (RabV-CVS-N2cΔG-mcherry) was injected into medial nucleus basalis (A/P: -1.5mm, M/L: 2.8mm, D/V: -7.2mm) in three animals, and into lateral nucleus basalis (A/P:-1.5mm, M/L: 3.5mm, D/V: -7.2mm) in other three animals.

2.5.4 Fiber photometry

We recorded the endogenous GCaMP activity of the cholinergic neurons through an implanted fiber while the rats were performing the DNMTP task. Through a single 400μm core fiber, we excited GCaMP with two different wavelengths - 405nm (intensity at fiber tip: 5-10μW,

frequency: 531Hz) and 488nm (intensity at fiber tip: 15-25μW, frequency: 211 Hz) using an LED driver (Thorlabs DC4104). Emission light from GCaMP was collected through the same fiber using a photodetector (Newport, Femtowatt 215) and the analog data was digitized by the TDT system (RZ5D) which served both as a A-D converter and lock-in amplifier (Gunaydin et al. 2014). A small head-mounted LED was used to track animal's position while recording. The position data was simultaneously acquired through the TDT tracker (RV2). The timestamps for task events were registered by Med-associates system and fed to TDT system through PCI Med associates interface card (DIG-704PCI-2).

2.5.5 GCaMP Signal Processing

With 488nm excitation, the fluorescence of GCaMP is calcium-dependent but with 405nm excitation, its fluorescence is calcium-independent. We utilized the calcium-independent signal as a control, isosbestic signal to filter out motion-artifact during the freely moving operant task.

Acquired signals were processed according to the following steps;

First, control 405nm signal ($S_{control}(t)$) was fit to 488nm GCaMP signal ($S_{GCaMP}(t)$) using least-squares regression to calculated fitted control signal ($S_{fitted}(t)$).

$$S_{GCaMP}(t) = \beta_0 + \beta_1 (S_{control}(t)) + \varepsilon$$

where

$$\hat{\beta}_1 = \frac{\sum (S_{control}(t) - \overline{S_{control}}) * (S_{GCaMP}(t) - \overline{S_{GCaMP}})}{\sum (S_{control}(t) - \overline{S_{control}})^2}$$

$$\hat{\beta}_0 = \left(\overline{S_{control}} - \hat{\beta}_1 \overline{S_{GCaMP}} \right)$$

$$S_{fitted}(t) = \hat{\beta}_0 + \hat{\beta}_1 (S_{control}(t))$$

Second, the relative change in fluorescence signal, $\Delta S/S\ (t)$, was calculated using 488nm GCaMP signal ($S_{GCaMP}\ (t)$) and fitted control signal ($S_{fitted}(t)$).

$$\Delta S/S\ (t) = \frac{S_{GCaMP}(t)) - S_{fitted}(t))}{S_{fitted}(t))}$$

Third, smoothed time-dependent baseline of $\Delta S/S\ (t)$, $f_{baseline}(t)$, was calculated to capture low frequency fluctuation. $f_{baseline}(t)$ was equivalent to smoothed moving minimum signal of $\Delta S/S\ (t)$ with 30 sec time window. 30 sec time window was chosen, because it was much longer than a single trial, therefore did not affect GCaMP response to various task events happening within a trial.

$$f_{min}(t) = \{ t \leq x < t + \tau \}$$

$$f_{baseline}(t) = \frac{1}{\tau} \sum_{t=1}^{t+\tau} f_{min}(t) \; where \; \tau = 30sec$$

Lastly, final $\Delta F/F$ was calculated by subtracting $f_{base}(t)$ from $\Delta S/S\ (t)$ and scaling by its standard deviation to facilitate comparison across recording sessions.

$$f_{filtered}(t) = \Delta S/S\ (t) - f_{base}(t)$$

$$\Delta F/F\ (t) = f_{filtered}(t)\ /\ std(f_{filtered})$$

2.5.6 Encoding model

Rats were freely-moving in the chamber while performing the DNMTP task. Therefore, isolating the contribution of task events to resulting GCaMP signal from that of animal's movement was important. To do so, we built generalized additive linear models in which GCaMP signal was predicted by the weighted linear sum of predictors such as different types of task events, animal's speed in the chamber, delay period predictor and the combination of task events and speed.

Task event predictors were generated by convolving binary event times (1 or 0) with a 10 degrees-of-freedom spline basis set, spanning -1~2sec around task events such as sample lever presentation, choice lever press, reward port exit, etc. Note the duration of spline basis set for reward respond (reward port entry) was longer (0~10 sec) to capture the sustained reward response observed. Speed predictor was a continuous variable which included first, second, and third-degree polynomial of the animal's speed to allow flexible modeling of GCaMP. Delay period predictor was a binary variable, in which 1 denoted time within the delay period and 0 denoted all other times besides the delay period. We included this predictor since memory related activity during the delay period is of particular importance to a working memory task.

Together, the model is as follows:

$$g(t) = \beta_0 + \sum_{i=1}^{N_{event}} \sum_{j=1}^{N_{bs}} \beta_{i,j} E_{i,j} + \sum_{k=1}^{N_{poly}} \beta_k S^k + \beta_d D + error$$

Where g(t) is the predicted GCaMP signal, N_{event} is the number of different types of task events (total 8 types of task events), and N_{bs} is the degrees of freedom of a spline basis set used for convolution (10df in all cases). $E_{i,j}$ is the i^{th} type of task events (task event types include sample presentation, sample press, delay start, delay end, choice presentation, choice press, reward port entry, reward port exit) convolved with j^{th} spline basis set. $\beta_{i,j}$ is the weight for

$E_{i,j}$. N_{poly} is the number of polynomials for the speed predictor (up to third-degree polynomials), S^k is the k^{th} degree polynomial of continuous speed predictor, and β_k is the weight for the speed predictors, S^k. Finally D is the binary delay predictor and β_d is the weight for the delay predictor, D. function *lm* in R was used to fit the model.

Four models were generated and their fit to recorded GCaMP was compared using average R^2 of 3-fold cross-validation. Four models include 1) delay predictor only model 2) speed predictor only model 3) task events predictor only model 4) task events plus speed model.

2.5.7 Immunohistochemistry

Rats were deeply anaesthetized using euthasol and transcardially perfused with 1X phosphate-buffered saline and 4% paraformaldehyde in PBS (PFA). Brains were collected and post-fixed in PFA overnight. Then the brains were placed in 30% sucrose in PBS solution for 2-5 days in 4ºC. Frozen brains were cut into 40µm thick coronal sections using a cryostat.

For the fiber photometry experiment, one-third of coronal sections in the MS or NB were directly mounted from the cryostat and cover-slipped with a mounting solution (fluoromount-G with DAPI, Southern Biotech) to get accurate fiber location and to confirm virus expression without any staining. These images were taken using a microscope (Nikon Ti2000E) or whole slide scanner (Hamamatsu Nanozoomer). Other one-third of sections was used to stain for ChAT (to see co-localization with GCaMP), GFP (for enhanced visibility of virus injection) and PV (to see GP-striatum border, which served as a local landmark close to NB). For staining, the primary antibodies were Goat-ChAT (1:100, Millipore AB144P), Mouse-PV (1:250, Millipore MAB1572), Rabbit-GFP (1:250, Life Technologies G10362), and the secondary antibodies were Donkey anti-Goat 647 (1:1000, Jackson ImmunoResearch 705-605-147), Donkey anti-Mouse Cy3

(1:1000, Jackson ImmunoResearch 715-166-151), Donkey anti-Rabbit 488 (1:1000, Jackson ImmunoResearch 711-545-152).

For retrograde monosynaptic tracing experiment, 50μm-thick coronal sections of the entire brain were sectioned and collected. One-third of the whole brain were mounted and cover-slipped with (fluoromount-G with DAPI, Southern Biotech) and imaged using a whole slide scanner (Hamamatsu Nanozoomer). Imaged brain sections covered the entire brain (approximate AP range from +4~-9mm) in 100μm spacing. With the brain of the control animal used to confirm specific labeling of the helper virus in the cholinergic neurons (Figure 5A), coronal sections were stained for ChAT, a marker for cholinergic neurons, and HA, a tag for the helper virus expression. The primary antibodies were Goat-ChAT (1:100, Millipore AB144P), and Rabbit-HA (1:1000, Invitrogen QG217964), and the secondary antibodies were Donkey anti-Goat 488 (1:500, Jackson ImmunoResearch 705-546-147), and Donkey anti-Rabbit 647 (1:1000, Life Technologies A31573)

2.5.8 Fiber Tip Location

Fiber tip location of the recording sites were reconstructed from the histology of coronal brain sections referencing the Paxinos Rat Atlas (Paxinos and Watson, 6th edition). A/P position of the fiber tip was approximated by the section with the deepest fiber tip location.

In that section, M/L position of the fiber tip was determined by measuring the distance from the midline to the fiber tip. Then the distance to the midline to the outermost edge of the section was used to account for the shrinkage in the tissue during fixation steps; the ratio of the measured distances should be equal to the ratio of the same distances in the Paxinos rat atlas such that,

$$\frac{measured\ ML\ distance_{fiber\ tip\ to\ midline}}{measured\ ML\ distance_{outer\ edge\ \ to\ midline}} = \frac{atlas\ ML\ distance_{fiber\ tip\ to\ midline}}{atlas\ ML\ distance_{outer\ edge\ \ to\ midline}}$$

$$atlas\ ML\ distance_{fiber\ tip\ to\ midline} = \frac{measured\ ML\ distance_{fiber\ tip\ to\ midline} * atlas\ ML\ distance_{outer\ edge\ \ to\ midline}}{measured\ ML\ distance_{outer\ edge\ \ to\ midline}}$$

$$M/L\ position\ of\ the\ fiber\ tip\ = \ atlas\ ML\ distance_{fiber\ tip\ to\ midline}$$

Similarly, the D/V position of the fiber tip was derived by measuring the distance from the bottom of the section to the fiber tip, as well as the longest distance of the entire section as the reference distance to take the ratio.

$$\frac{measured\ DV\ \ distance_{fiber\ tip\ to\ top\ edge}}{measured\ DV\ \ distance_{top\ edge\ to\ bottom\ edge}} = \frac{atlas\ DV\ \ distance_{fiber\ tip\ to\ top\ edge}}{atlas\ DV\ \ distance_{top\ edge\ to\ bottom\ edge}}$$

$$atlas\ DV\ distance_{fiber\ tip\ to\ top\ edge} = \frac{measured\ DV\ \ distance_{fibertip\ to\ top\ edge} * atlas\ DV\ \ distance_{top\ \ edge\ \ to\ bottom\ edge}}{measured\ DV\ \ distance_{top\ edge\ to\ bottom\ edge}}$$

$$D/V\ \ position\ of\ the\ fiber\ tip\ = \quad atlas\ DV\ distance_{fiber\ tip\ to\ top\ edge}$$

2.5.9 WholeBrain Registration and Segmentation

Imaged brain sections covering the entire brain (approximate AP range from +4~-9mm) in 100μm spacing were analyzed using a recently published platform, WholeBrain (Fürth et al. 2018). WholeBrain is an interactive framework to easily annotate, analyze and visualize labeled cells in the brain.

For registration, we found the corresponding mouse AP coordinate of all rat brain sections, referencing Openbrainmap (http://openbrainmap.org). Then the sections of the rat brains were registered into the Allen brain atlas using the *registration* function. Note that Figure 6 coordinates are mouse brain coordinates, as the rat brain was registered to the mouse atlas. Registered brain was individually inspected and corresponding points used for registration were fixed manually, when necessary. Similarly, detection of labeled cells were done using *segment* function, with manual clean-up when necessary.

Chapter 3: The midbrain DA system reveals dissociable and causal contribution to memory and motor execution in a spatial working memory task

3.1 Abstract

Dopamine (DA) plays such a critical role in working memory (WM) that DA depletion in Prefrontal cortex (PFC) causes working memory deficit equivalent to the complete ablation of the PFC (Brozoski et al. 1979). Two major theories postulate the role of DA in WM. In the "gating" theory, phasic DA is hypothesized to update relevant memory to be maintained while filtering out irrelevant distractors (Braver and Cohen 2000; Seamans and Yang 2004; O'Reilly and Frank 2006). Notably, in the "gating" theory, tonic activity of the gating signal during the delay period has an inhibitory effect on memory maintenance; reduced tonic activity during the delay decreases the probability of overwriting the current context. Alternatively, "inverted U-shape" hypothesis posits that the relationship between tonic DA during the delay period and working memory performance draws and inverted-U shape such that optimal level of tonic DA during the delay period stabilizes the working memory representation (A. F. T. Arnsten, Wang, and Paspalas 2012; A. F. Arnsten 1997).

To understand the dissociative or complementary contribution of midbrain DA system in the proposed theories, we recorded and manipulated VTA and SNc DA neurons (mesocortical pathway and nigrostriatal pathway) while animals are performing a spatial working memory task, in a millisecond temporal resolution. In the fiberphotometry recording, we found a similar pattern of DA activity between VTA and SNc. Furthermore, we observed phasic DA response to lever presentation during sample encoding and decoding period, but low activity during the delay period. This pattern of activity was consistent with the "gating" theory of DA.

Next, we questioned if the observed activity was causal to WM performance. To this end, we optogenetically inhibited VTA and SNc DA neurons in memory-guided DNMTP task as well as sensory-guided task. Optogenetic inhibition of VTA DA neurons impaired performance in memory-guided DNMTP task only, whereas the same manipulation of SNc DA neurons impaired performance in both memory-guided DNMTP and sensory-guided tasks with increased choice lever press latency (slowing of lever press).This result suggest a dissociable role of VTA versus SNc DA neurons in spatial working memory; VTA DA activity is causally involved in cognitive working memory performance, while SNc DA activity is causally involved in the motor execution of the task.

Finally, we probed if VTA and SNc DA neurons contribute to spatial working memory performance *in a temporally-specific manner*. To this end, we optogenetically inhibited the DA neurons during a specific epoch (sample, delay, choice period) within a trial. We found that VTA DA activity earlier in the trial (sample and delay) is causally involved in working memory stability and moreover, optogenetic activation of VTA DA neurons during the delay period also impaired working memory performance, supporting the inverted U dose-response hypothesis of DA.

3.2 Introduction

In 1979, a landmark study by Brozoski et al. discovered the critical role of dopamine in working memory (Brozoski et al. 1979). The selective depletion of dopamine in money PFC using 6-OHDA resulted in significant deficit in working memory performance, with the effect size equivalent to complete ablation of the PFC.

Two major theories postulate the role of DA in WM. In the “gating” theory, phasic DA is hypothesized to update relevant memory to be maintained while filtering out irrelevant distractors (Braver and Cohen 2000; Seamans and Yang 2004; O’Reilly and Frank 2006). Notably, in the “gating” theory, tonic activity of the gating signal during the delay period has an inhibitory effect on

memory maintenance; reduced tonic activity during the delay decreases the probability of overwriting the current context. Alternatively, “inverted U-shape” hypothesis posits that the relationship between tonic DA during the delay period and working memory performance draws and inverted-U shape such that optimal level of tonic DA during the delay period stabilizes the working memory representation (A. F. T. Arnsten, Wang, and Paspalas 2012; A. F. Arnsten 1997).

The “inverted-U” hypothesis and “gating” hypothesis are not necessarily mutually exclusive. The “inverted-U” shape hypothesis emphasizes the role of tonic DA level in PFC during the maintenance period of working memory. The “gating” hypothesis underscores the role of phasic DA in PFC (or in striatum) during the encoding period of working memory. It is possible for DA to assume both updating and maintenance roles by employing separate anatomical connections (nigrostriatal DA vs mesocortical DA) or exploiting different temporal window (earlier update period vs later maintenance period).

To address these questions, it is necessary to compare DA in two distinct pathways with fast temporal resolution to distinguish their contributions to each period (sample, delay, choice periods) of a trial. Using fiberphotometry and optogenetics with millisecond temporal resolution, we monitored the endogenous pattern of DA activity in VTA and SNc while the rats were performing delayed non-match to position task, and manipulated the observed DA activity during different epochs of the tasks.

We report highly homogenous DA activity between VTA and SNc; in both VTA and SNc, we observed phasic DA response to lever presentation during sample encoding and decoding period, but low activity during the delay period. This pattern of activity was consistent with the “gating” theory of DA. However with the optogenetic manipulation, we show that only the VTA DA neurons contribute to cognitive working memory. Temporally-specific bidirectional optogenetic

manipulation revealed that the low activity during the delay period was indeed crucial to working memory performance, supporting the “inverted U-shape” hypothesis.

3.3 Results

To examine the patterns of activity in dopaminergic neurons in SNc and VTA, we trained TH::Cre rats on a spatial delayed non-match to position task (DNMTP, Figure 1A) and used fiber photometry to record GCaMP activity from the DA neurons.

3.3.1 Rats performed a spatial working memory task

In the DNMTP task (Figure 1A), rats are presented with a sample lever in one of two possible locations on the front wall of the chamber (sample presentation). Upon pressing the lever (sample press), the lever retracts and the nosepoke on the back wall of the chamber is illuminated. The rat then initiates the delay period by entering the nose poke (delay start). After a delay of either 1, 5, or 10 s (randomly interleaved), if the rat re-enters the nose poke, both levers will be presented on the front wall (choice presentation). To obtain a water reward, the rat must press the lever that does not match the initial sample lever (choice press). Trained rats performed well above chance level and displayed a delay-dependent decline in performance accuracy (Figure 1B; Mean ± SEM, SNc, 1sec: 95.6± 1.3, 5ec: 90.4 ± 3.2, 10sec: 87.5 ± 3.6; Figure 1C; Mean ± SEM, VTA, 1sec: 92.0 ± 2.9, 5sec: 91.8 ± 2.2, 10sec: 81.3 ± 3.7).

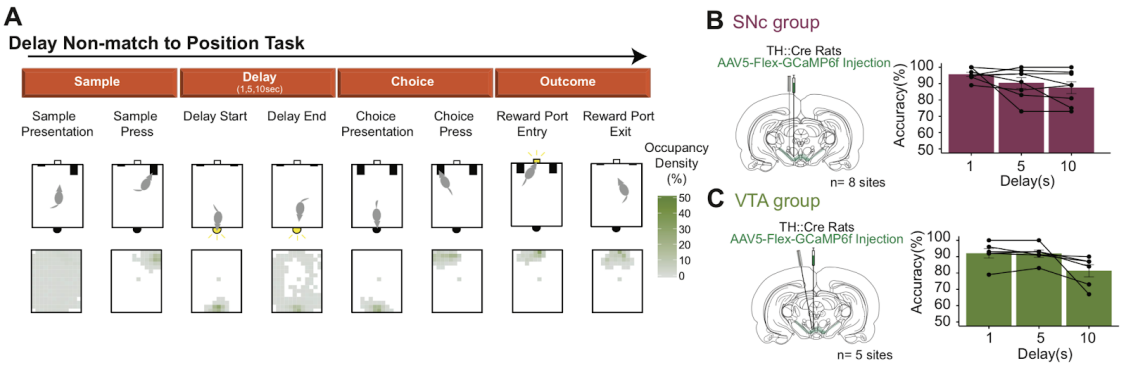


Figure 7 Dopaminergic neurons in the VTA and SNc were monitored during a DNMTP task

(A) Schematic of Delay non-match to position task (DNMTP task). It is a rodent working memory task, in which a rat is required to remember the position of the sample lever presented for a delay

period and then to choose a non-match (opposite) lever to get a reward. In the schematic (top) of a single type of trials (correct, right sample lever trials), and different task events are illustrated as the time progresses from left to right. Below is average occupancy density map indicating the position of rats in the operant chamber 0~0.2sec around corresponding event illustrated above. (B) TH::Cre rats that were trained on the task were injected with a Cre-dependent GCaMP virus into the SNc and implanted with an optical fiber for the fluorescence recording (left, n=8 sites). The trained rats' DNMTP performance accuracy (right) shows that they perform above chance level (50%) and show delay-dependent impairment in memory. (C) Same as (B) but in VTA (n= 5 sites)

To observe the natural pattern of dopaminergic activity during behavior, we employed fiber photometry to record GCaMP6f fluorescence. Cre-dependent GCaMP6f virus was injected into the Substantia Nigra pars compacta (SNc) or Ventral Tegmental Area (VTA) of the TH::Cre rats, and an optical fiber was implanted above the injection site. The use of transgenic animal together with cre-dependent virus injection cell-type specific expression of GCaMP in the dopaminergic neurons. Using GCaMP activity as a proxy for neuronal activity, we were able to monitor the time-varying dopaminergic activity in SNc and VTA, as a function of animal's locomotion and/or task events.

3.3.2 Task events explain more variance in DA activity in VTA and SNc compared to locomotion or delay period

We first quantified the extent that *events* in the behavioral task (e.g. lever presentation, lever press, reward delivery), in comparison to the animal's movement in the chamber, relate to DA activity in the SNc and VTA. Isolating the contribution of task event from the animal's locomotion was particularly important to examine rigorously in the case of an operant task, given that an animal's speed will correlate with task events, and therefore neural correlates of task events may be better explained as neural correlates of movement (eg. speed may be lower during delay or reward period, or higher before the delay period, when the animal traverses the chamber). Particularly, numerous recent studies reported that dopaminergic neurons encode animal's locomotion such as acceleration and speed (Engelhard et al. 2018; M. W. Howe and Dombeck 2016; da Silva et al. 2018). Thus, before examining in detail the neural correlates of behavioral events, we wanted to determine if the animals' movement in the chamber provided a better explanation of neural activity than the task events.

To examine the relative contribution of task events versus the animal's movement in explaining GCaMP activity, we built generalized additive linear models in which GCaMP signal was predicted based on 1) delay period only, 2) speed only, 3) task events only and 4) combined task events and speed predictors (For detail, Methods 3.5.6 Encoding Model). Delay period predictor was a binary predictor which indicated whether the animal was in the delay period (denoted as 1) or in any other period such as sample or reward period (denoted as 0).

Delay period predictor was of particular interest because "gating" theory and "inverted U-shape" theory makes opposite predictions regarding the DA activity during the delay. In the "inverted U-shape" theory, low level of DA tone in the PFC during the delay period decrease the

signal-to-noise ratio of working memory representation (Brunel and Wang 2001; Vijayraghavan et al. 2007; A. F. T. Arnsten, Wang, and Paspalas 2012). On the other hand, “gating” theory suggest that low level of DA during the delay protects the current working memory representation from being overwritten by distractors (Braver and Cohen 2000). Accordingly, we wanted to capture if the DA activity is high or low during the delay period. To flexibly model the relationship between GCaMP and speed, a first, second, and third degree polynomial of the animal’s speed was used as locomotion predictors. Task event predictors were generated by convolving event times (binary variable) with a spline basis set (degrees of freedom = 10). The duration of the basis set was 3 sec around all types of task events, except reward port entry event was allowed to have a longer 10 sec kernel to capture the entirety of sustained reward response.

Comparison of aforementioned four different encoding models using cross-validated R^2 demonstrated that the task events were most predictive of dopaminergic activity in SNc (Figure 8A) and VTA (Figure 8B). Being in the delay period did not explain much GCaMP activity of the dopaminergic neurons, to our surprise. Also, speed predictor barely explained the DA GCaMP activity. More complex, combinatorial model (speed + task event model) did worse than simply having task events as predictors. Together, we found that dopaminergic neurons in both SNc and VTA prominently and similarly encode different types of task events during DNMTP.

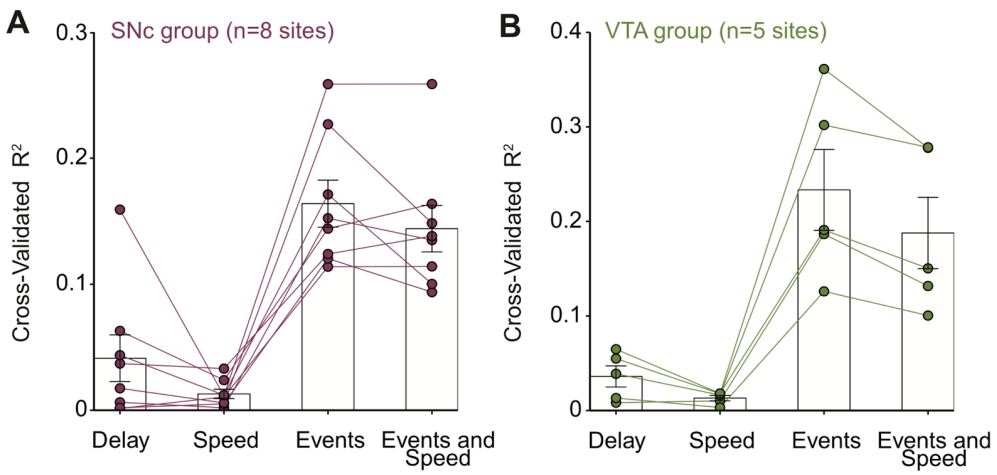


Figure 8 Task events explain the most variance in dopamine activity in both SNc and VTA

(A) Comparison of R^2 (y-axis) for 4 different encoding models (x-axis, For detail, see Methods 3.5.6 Encoding Model) reveals that Task Events model explain the most variance in dopamine GCaMP activity in SNc (Mean ± SEM, Delay: 0.04 ± 0.02, Speed: 0.01 ± 0.004, Events: 0.16 ± 0.02, Events + Speed: 0.14 ± 0.02) (B) same as (A) but in VTA (Mean ± SEM, Delay: 0.04 ± 0.02 , Speed: 0.01 ± 0.004 , Events: 0.23 ± 0.04, Events + Speed: 0.19 ± 0.04)

3.3.3 DA neurons in SNc and VTA similarly show phasic response to lever presentation and reward but low activity during the delay period

Now that we have established the prominent encoding of task events by the dopaminergic neurons in SNc and VTA, we next asked *which* specific task events were represented by these neurons. Plotting the task event kernels for each type of task events generated from the task-only model (Figure 9A), we found that DA neurons in SNc and VTA also similarly exhibited elevated activity to lever presentation cue (sample lever presentation cue as well as choice lever presentation cue) and reward. It is also interesting to note that ChAT neurons in NB responded to lever press action and reward. This finding is in line with the most renowned function of dopamine in reward (Cohen et al. 2012; Mirenowicz and Schultz 1994; Engelhard et

al. 2018; Roesch, Calu, and Schoenbaum 2007) and reward predicting cue (Cohen et al. 2012; Schultz, Dayan, and Montague 1997; Saunders et al. 2018; Engelhard et al. 2018). Intrigued by little activity during the delay period activity, we plotted the normalized GCaMP signal of correct 5sec trials for both SNc and VTA (Figure 9B). As the kernel suggestd, there was little to low activity during the delay period. Together with the phasic peak to lever presentation at the time of encoding as well as low tonic delay period activity, the neural correlates of DA activity in VTA and SNc were consistent with the prediction from the “gating” theory.

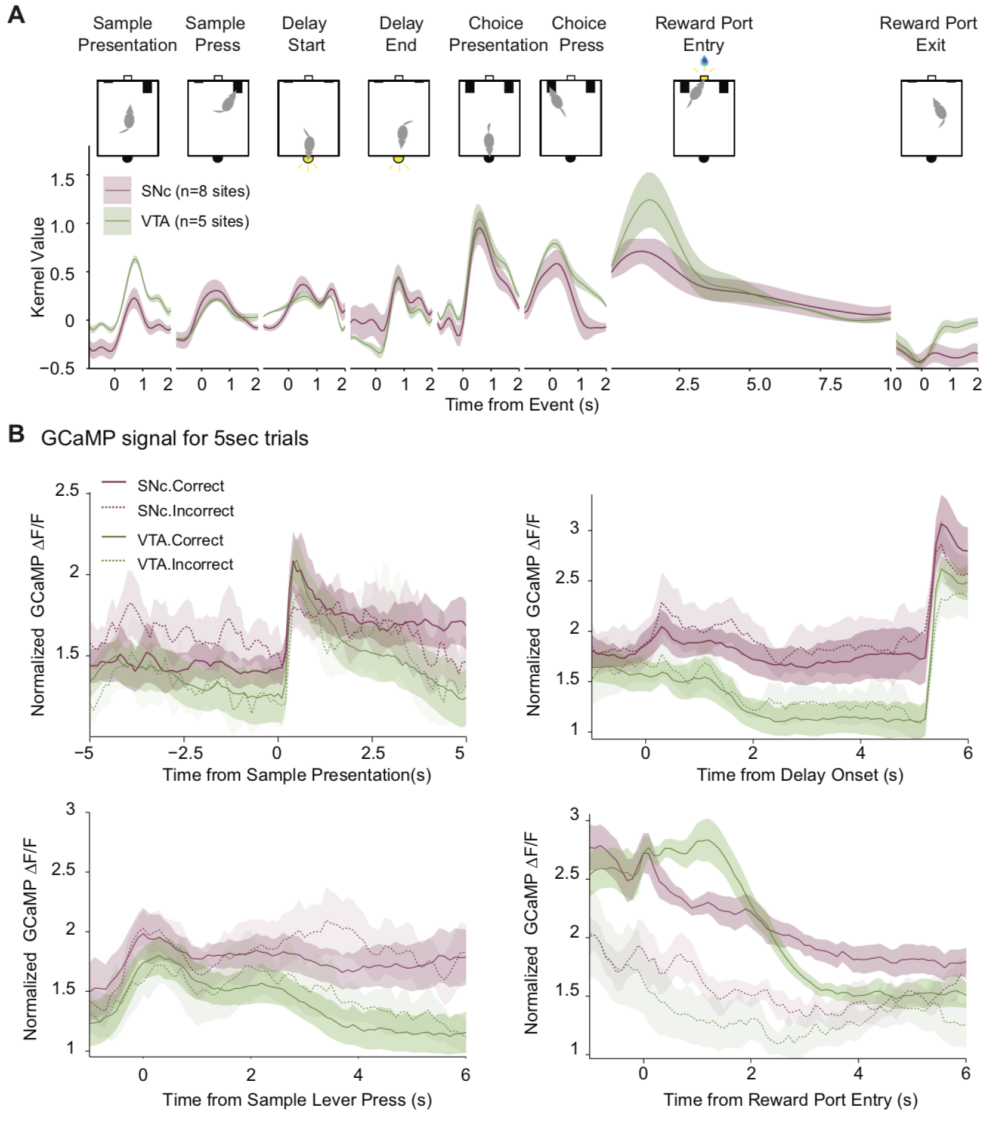


Figure 9 Dopamine neurons in SNc and VTA show similar task encoding during DNMTP (A) Kernels for each type of task events (top schematic), created from Task Events-only model, are plotted as population average (purple line: SNc, n=8, green line: VTA, n=5) and standard error across sites (shaded region; SNc, n=8; VTA, n=5). Both SNc (purple) and VTA (green) show elevated activity to lever presentation cue and reward.

(B) Normalized GCaMP trace (y-axis) for correct 5sec trials time-locked to various task events (x-axis). Again, SNc (purple) and VTA (green) traces are similar to each other, with phasic response to lever presentation and low activity during the delay period.

3.3.4. Optogenetic inhibition of VTA DA neurons impairs working memory while the same manipulation of SNc DA neurons impairs motor execution of the task.

To address if the observed DA activity is causal to DNMTP performance, we optogenetically inhibited the DA neurons in SNc and VTA during the entire trial, combining sample, delay and choice periods (Figure 10A~10B). Continuous light was delivered throughout the trial at 5-6mW intensity. To prevent plasticity, we randomly presented light-on trials in only 20% of all trials, and the rats had light-on condition every other day for 5 sessions.

As a control, we not only had light-off trials, but also applied sensory-guided DNMTP task, in which rats did not have to use their memory (Figure 10C). In the sensory-guided DNMTP task, everything was the same as memory-guided DNMTP task in terms of motor requirement such as lever press or nosepoke. The key difference was that in the sensory-guided task, the rats were *signaled* to which choice lever was the correct one to press with a cue light illuminated directly above the correct lever. Consequently, the rats did not need to use their working memory.

Optogenetic inhibition of DA neurons in VTA significantly impaired rats' performance in DNMTP task (Figure 10D left, Mixed-effect binomial logistic regression, fixed effect of light, $p < 0.001$***) but spared their performance in the control guided task (Figure 10D right, Mixed-effect binomial logistic regression, fixed effect of light, $p = 0.13$). This suggests that the DA neurons in VTA is specifically required for the working memory performance.

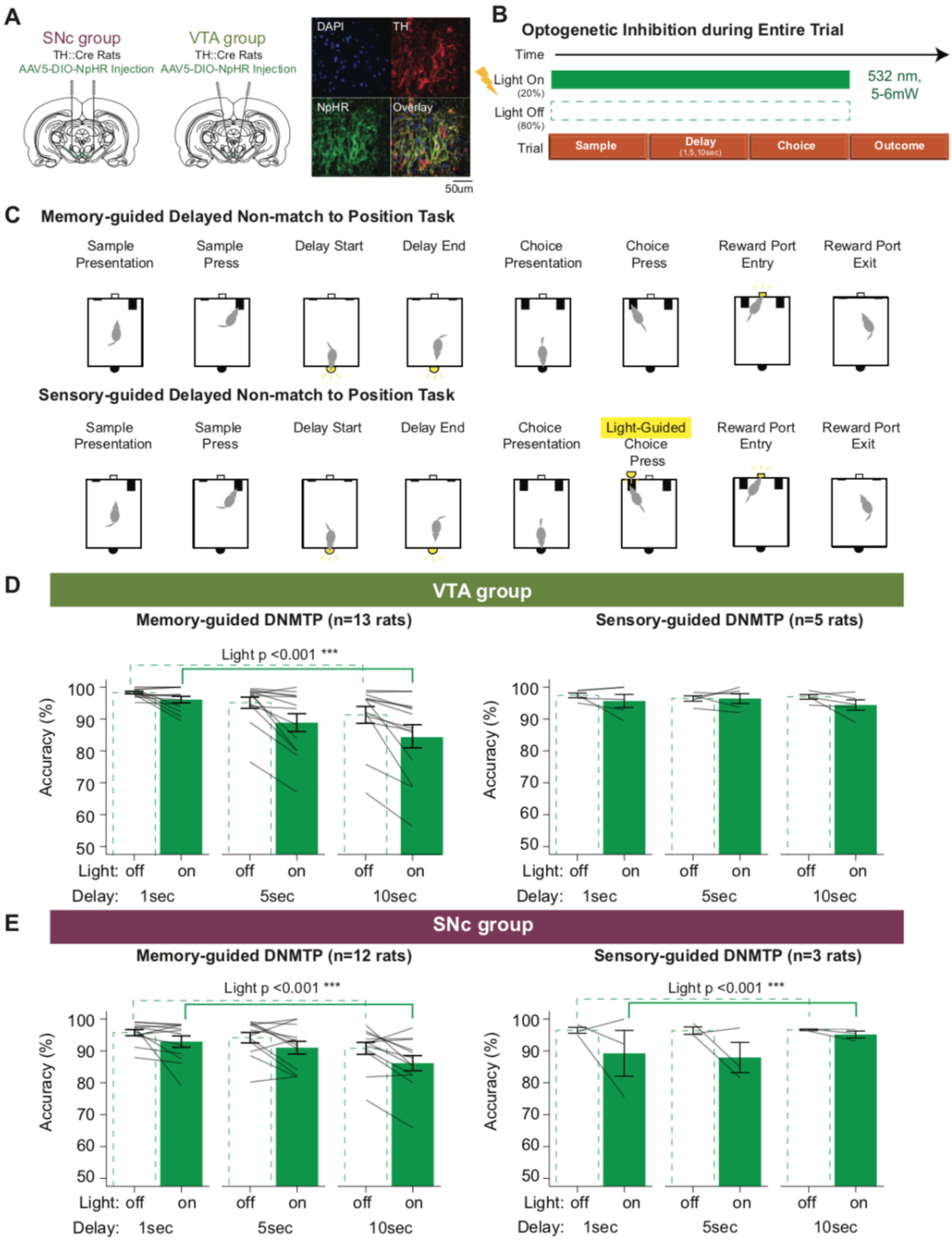


Figure 10 Optogenetic inhibition of DA neurons in VTA and SNc during memory-guided DNMTP and sensory-guided DNMTP (A) Trained TH::cre rats were injected with a Cre-dependent NpHR virus and bilaterally implanted with optical fibers in SNc (left) and VTA

(middle). The use of transgenic rats with cre-dependent virus resulted in dopamine-specific (red) labeling of NpHR (green and overly; right) (B) Schematic of optogenetic inhibition during the entire trial spanning all sample, delay, choice periods. 532nm continuous light was delivered at 5-6mW intensity at the fiber tip in random 20% of trials for 5 sessions (C) Schematic of Memory-guided Delayed non-match to position task (top) as a working memory paradigm and Sensory-guided Delayed non-match to position task (bottom) as a control task that does not involve working memory component. The key difference is that in the sensory-guided delayed response task, the correct choice press position is signaled to the rat with a cue light above the correct choice lever. Of note, the guided cue is randomly-chosen between left and right, independently from the sample lever position, resulting in delay non match to position as well as delay match to position trials. (D) Optogenetic inhibition of VTA DA neurons impairs the task performance in the DNMTP task with working memory component (left, Mixed-effect binomial logistic regression, fixed effect of light, $p < 0.001$***) but not in the control Guided delayed response task (right, Mixed-effect binomial logistic regression, fixed effect of light, $p = 0.13$) (E) Optogenetic inhibition of SNc DA neurons impairs the task performance in the DNMTP task with working memory component (left, Mixed-effect binomial logistic regression, fixed effect of light, $p < 0.001$***) and also in the control Guided delayed response task (right, Mixed-effect binomial logistic regression, fixed effect of light, $p < 0.001$***).

Interestingly, optogenetic inhibition of SNc DA neurons impaired accuracy in *both* DNMTP task and control guided task (Figure 10E, Mixed-effect binomial logistic regression, fixed effect of light, DNMTP: $p < 0.001$***, control Guided task: $p < 0.001$***), suggesting that SNc DA neurons may be necessary to correctly execute the motor action of pressing the choice lever. Previous findings have also implicated SNc DA neurons in movement (M. W. Howe and Dombeck 2016; da Silva et al. 2018) more so than VTA DA neurons.

Accordingly, to test if the performance impairment in SNc DA neurons is indeed related to motor rather than cognitive deficit, we further analyzed the latency data. As hypothesized, we found that the optogenetic inhibition of SNc DA neurons resulted in significant slowing of choice lever pressing action in the control sensory-guided task (Table 1, Mixed-effect linear regression, fixed effect of accuracy x light = 0.005**). This was in contrast to the inhibition of VTA DA neurons which did not show significant difference in choice latency between light-on versus light-off trials.

Together, these results converge onto a dissociable role of VTA versus SNc DA neurons in spatial working memory; VTA DA activity is causally involved in cognitive working memory performance, while SNc DA activity is causally involved in the motor execution of the task.

SNc	Accuracy	Choice Latency	VTA	Accuracy	Choice Latency
Sensory-guided Guided	Impaired (p<0.001***)	Slower (accuracy x light p=0.005**)	Sensory-guided Guided	n.s.	n.s.

Table 1 Summary of entire-trial optogenetic inhibition effect in accuracy and choice latency

Since we observed significant effect of DA manipulation in working memory performance, we questioned if the effect was specific to DA system or the effect can be generalized to other neuromodulators such as acetylcholine. To address this, we optogenetically inhibited cholinergic neurons in the medial septum and nucleus basalis in ChAT::Cre rats performing DNMTP task. We found that the inhibition of basal forebrain cholinergic system did not affect the working memory performance, pointing out that the contribution of DA to working memory is unique.

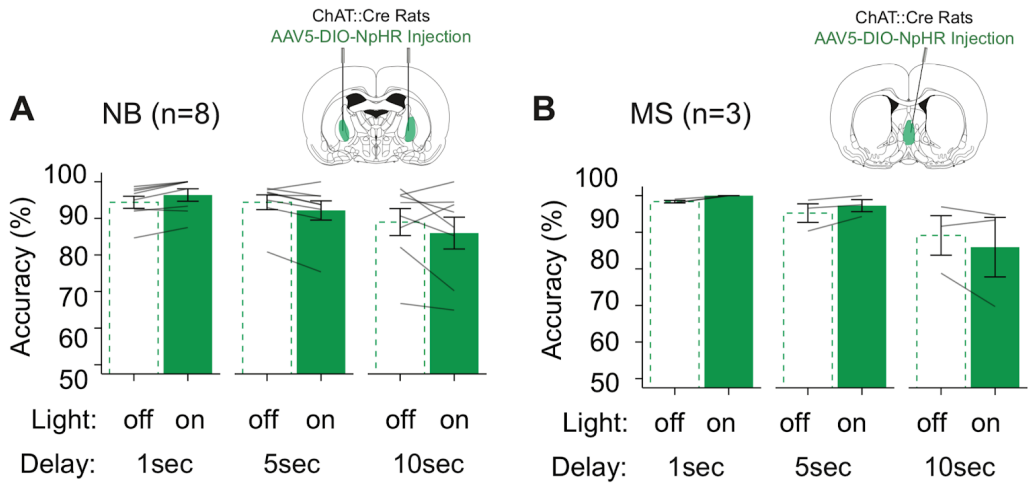


Figure 11 Optogenetic inhibition of basal forebrain cholinergic neurons during memory-guided DNMTP does not impair working memory performance (A) Optogenetic inhibition of nucleus basalis ChAT neurons, Accuracy (y-axis) plotted for each delay condition (1, 5, 10sec) and light condition (on/off) (B) same as (A) but in cholinergic neurons in the medial septum

3.3.5 Optogenetic inhibition of DA neurons in VTA during the sample and delay period impairs WM performance

Many seminal pharmacological studies have implicated dopamine in working memory (Brozoski et al. 1979; Sawaguchi and Goldman-Rakic 1991; Sawaguchi, Matsumura, and Kubota 1990; Simon, Scatton, and Moal 1980), and since then, it has long been theorized to modulate different aspects of working memory. Two major theories relating DA to WM are the “gating” and “inverted-U-shape” hypotheses. “Gating” hypothesis posits that phasic DA is specifically involved in the earlier encoding phase to gate and update task-relevant stimuli into the PFC working memory sketchpad (Braver and Cohen 2000). “inverted-U-shape” hypothesis emphasizes the extrasynaptic DA tone in PFC during the delay period stabilizes working memory representation(Brunel and Wang 2001; Cools and D’Esposito 2011). These two theories are not

necessarily mutually exclusive, but underscore the role of DA in different temporal window. However, the technical challenge associated with specifically manipulating dopaminergic neurons on a precise timescale hindered investigators from directly testing these hypotheses. Therefore, our logical next step was to optogenetically inhibit these DA neurons during sample, delay, and choice periods within a trial (Figure 12A).

Optogenetic inhibition of SNc DA neurons during delay and choice period impaired performance (Figure 12C, Mixed-effect binomial logistic regression, effect of light, delay, p=0.002**, choice, p=0.008**), whereas the same manipulation in VTA DA neurons during sample and delay period impaired performance (Figure 11D, Mixed-effect binomial logistic regression, effect of light, sample, p=0.002**, delay, p<0.001***). The role of VTA DA in encoding and maintenance phase of DNMTP supports both “gating” and “inverted-U-shape” hypotheses. However, it should be noted that the effect size for the sample period inhibition was small, though significant (β=-0.25). Also this sub-trial inhibition effect in the later delay and execution period further buttress the aforementioned interpretation that SNc DA inhibition is more suggestive of motor execution deficit rather than cognitive working memory impairment. Together, these results demonstrate that the role of DA neurons in VTA and SNc are temporally and functionally dissociated from each other; VTA DA neurons modulate working memory during the earlier encoding and maintenance period, while the SNc DA neurons contributes to later motor execution of the task.

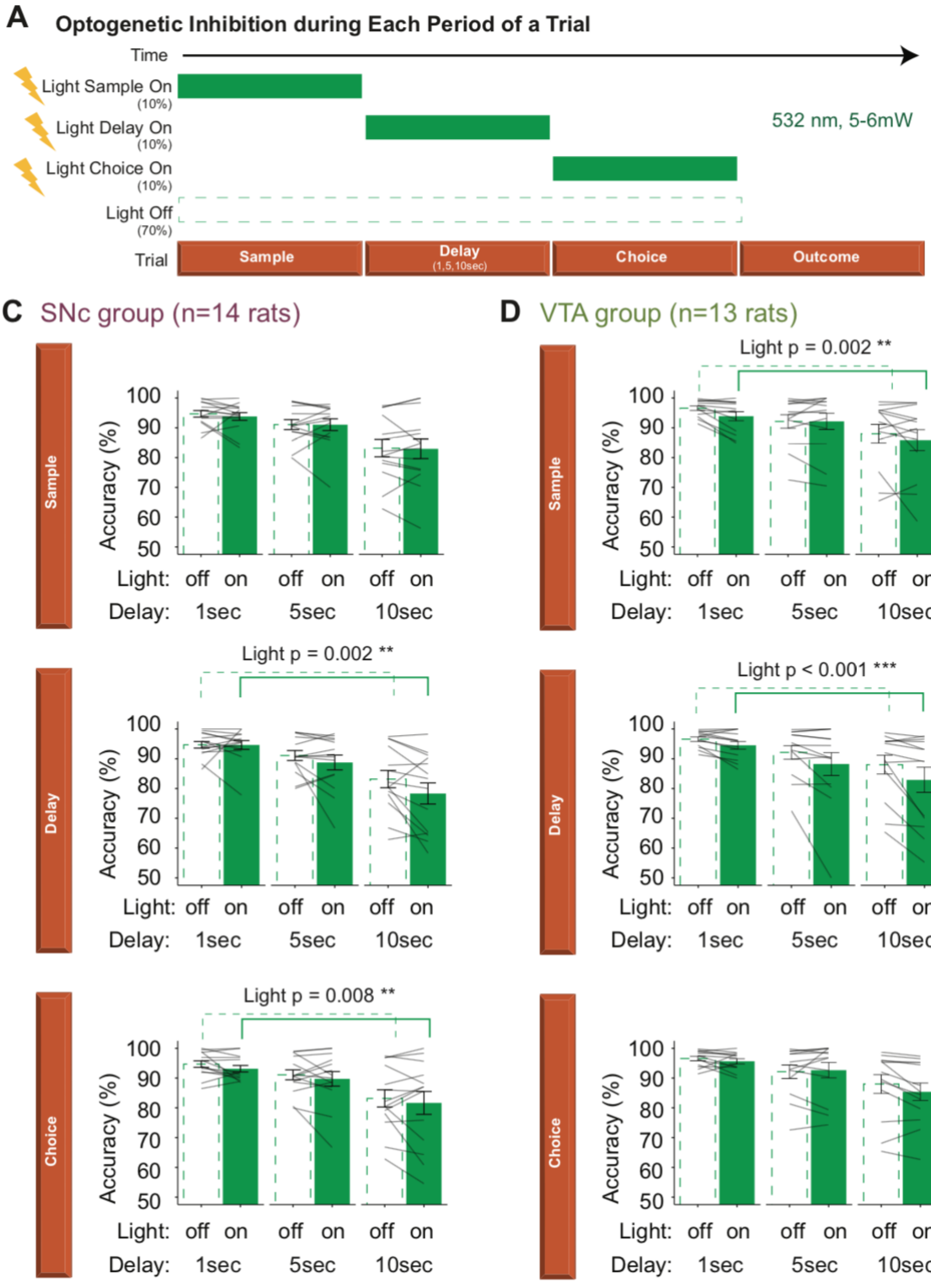

A
Optogenetic Inhibition during Each Period of a Trial
Time
Light Sample On
(10%)
Light Delay On
(10%)
Light Choice On
(10%)
Light Off
(70%)
532 nm, 5-6mW
Trial
Sample
Delay
(1,5,10sec)
Choice
Outcome
C
SNc group (n=14 rats)
D
VTA group (n=13 rats)
Sample
Delay
Choice
Accuracy (%)
100
90
80
70
60
50
Light: off on off on off on
Delay: 1sec 5sec 10sec
Light p = 0.002 **
Light p < 0.001 ***
Light p = 0.008 **

Figure 12 ***Optogenetic inhibition of DA neurons in VTA and SNc during each period within a trial in DNMTP*** (A) Schematic of optogenetic inhibition during each sample (sample lever presentation ~ sample lever press), delay (delay start nosepoke ~ delay end nosepoke light) or choice (choice lever presentation ~ choice lever press) period of a trial. 532nm continuous light was delivered at 5-6mW intensity at the fiber tip in random 30% of trials (10% for sample light-on, 10% for delay light-on, and 10% for choice light-on trials) for 5 sessions (B) Optogenetic inhibition during the delay (middle) and choice (bottom) period results in significant impairment in accuracy in light-on condition compared to light-off condition (Mixed-effect binomial logistic regression, fixed effect of light, Delay: p = 0.002**, Choice: p=0.008**). (C) Optogenetic inhibition during the sample (top) and delay (middle) period results in significant impairment in accuracy in light-on condition compared to light-off condition (Mixed-effect binomial logistic regression, fixed effect of light, Sample: p = 0.002**, Delay: p<0.001***).

3.3.6 Optogenetic activation of DA neurons in VTA during the delay period impairs WM performance

Another key prediction from the “inverted-U-shape” hypothesis is that over-dosing DA in PFC also disrupts working memory (Vijayraghavan et al. 2007; Cools and D’Esposito 2011; A. F. Arnsten 1997). We tested this prediction by optogenetically activating the VTA DA neurons specifically during the delay period (Figure 13A). As predicted, we found that the optogenetic activation of VTA DA neurons resulted in significant impairment of task performance (Figure 13C, Mixed-effect binomial logistic regression, fixed effect of light, p< 0.001***). More surprisingly, a single pulse activation of VTA DA neurons during delay period (Figure 13D, Mixed-effect binomial logistic regression, fixed effect of light, p< 0.001***) still resulted in significant impairment in working memory performance. Together with the inhibition experiment, our data indicate that bi-directional manipulation of VTA DA neurons during the delay period impairs working memory performance, supporting the “inverted-U-shape” hypothesis.

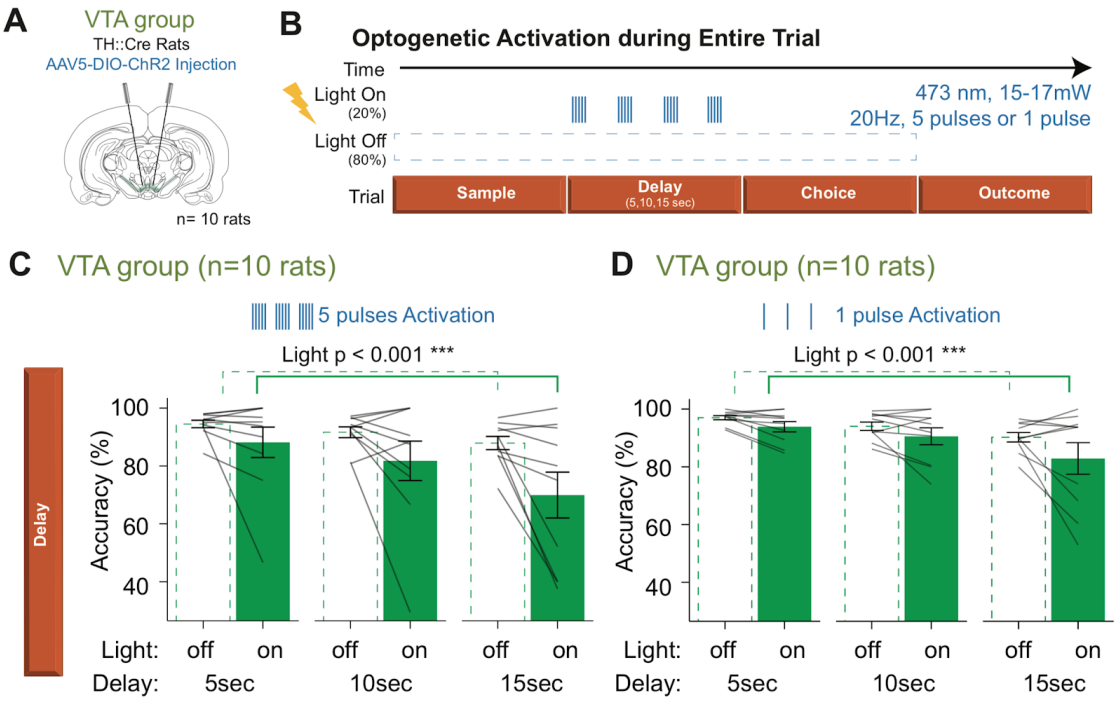


Figure 13 Optogenetic activation of DA neurons in VTA during delay period impairs working memory (A) Trained TH::cre rats (n=10) were injected with a Cre-dependent ChR2 virus and bilaterally implanted with optical fibers in VTA to specifically activate DA neurons in VTA (B) Schematic of optogenetic activation during the delay period of a trial. 477nm pulsed light was delivered at 15-17mW intensity at the fiber tip in random 20% of trials for 5 sessions. (C) 5 pulse Optogenetic activation of DA neurons in VTA significantly impaired accuracy in light-on condition compared to light-off condition (Mixed-effect binomial logistic regression, fixed effect of light: p <0.001***) (D) same as (C) except optogenetic activation parameter was 1 pulse instead of 5 pulses (Mixed-effect binomial logistic regression, fixed effect of light: p <0.001***) .

3.4 Discussion

3.4.1 Similar neural correlate of DNMTP in VTA vs SNc DA neurons

Fiberphotometry recording revealed that task events explained most variance in VTA and SNc DA activity (Figure 8). In addition, they both responded phasically to lever presentation cue and reward but showed depressed activity during the delay period (Figure 9). DA's most well-known function in reinforcement learning is recapitulated in our neural correlates; both reward-predicting cues (lever presentation cue during the sample and choice period) and reward (difference between correct rewarded trials vs incorrect unrewarded trials in the outcome period) were signaled with phasic DA response.

Interestingly, we found DA activity during the delay period was low. Few studies reported silent delay period activity of DA neurons in delayed alternation task (Ljungberg, Apicella, and Schultz 1991) and odor-outcome association task (Cohen et al. 2012). We point out that this is consistent with the "gating" theory, which predicts that low delay period activity of the gating signal stabilizes working memory representation by preventing distractors or newer context to overwrite the currently-held memory item (Braver and Cohen 2000).

3.4.2 Dissociable role of VTA and SNc DA neurons in WM

Through the optogenetic inhibition of memory-guided and sensory-guided DNMTP, we report causal and dissociable roles of VTA vs SNc DA neurons in working memory; VTA DA activity is causally involved in cognitive working memory performance, whereas SNc DA activity mediate motor execution of the task (Figure 12). We find these dissociative roles to be consistent with the previous literature. VTA DA neurons primarily projects to PFC and comprise a mesocortical pathway. Given DA level in PFC have been the focus of WM research, most previous lesion and pharmacological studies have focused on this mesocortical pathway to show

WM deficit (Sawaguchi and Goldman-Rakic 1991; Williams and Goldman-Rakic 1995; Seamans and Yang 2004) . Also, it has been recently shown that DA neurons in medial VTA have different responses depending on the accuracy of the trial (Engelhard et al. 2018). On the other hand, SNc DA neurons primarily projects to dorsal striatum, representing the nigrostriatal pathway. The activity of DA neurons in the SNc has been associated with movement (M. W. Howe and Dombeck 2016; da Silva et al. 2018; Barter et al. 2015). The role of VTA DA neurons in the cognitive component of WM and the dissociable role of SNc DA neurons in motor execution together comprise another example of heterogeneity in the midbrain DA system.

3.4.3 Bidirectional optogenetic manipulation of VTA DA during the delay period impairs WM performance

We demonstrate that bi-directional optogenetic manipulation of VTA DA neurons during the delay period impairs WM performance (Figure 11 and 13), supporting the “inverted U-shape” hypothesis. Then, how is it possible that DA levels in PFC during the delay period causally influence WM performance, when we observed low DA neuronal activity from VTA which sends projection to PFC through the mesocortical DA pathway? First, dopamine levels in PFC are long-lasting and slow to decay back to baseline, typically taking longer than 5 sec (Cass and Gerhardt 1995; Seamans and Yang 2004). This possibility would require us to analyze DA activity not within a trial but across multiple trials. Second possible explanation is that DA release in PFC is modulated by local interactions at the presynaptic terminals of DA neurons. Moreover, DA terminals express receptors for other transmitters such as glutamate, opioids and acetylcholine. In this case, our cell-bodies recording would not be able to necessarily capture the varying DA concentration in the PFC terminals.

3.4.4 Rewarding/motivational effect of DA stimulation

An established phenomenon of DA stimulation is that it is rewarding. While acknowledging the rewarding effect of DA stimulation, we propose that the rewarding effect does not complicate our interpretation based on the “accuracy” of the performance. If the stimulation is rewarding, the most obvious outcome is the increase in omission rate. Each action in the task is given only 5 seconds of time window (15 seconds to initiate a trial by pressing the sample lever) within which the rats can respond. If the stimulation was rewarding enough to interfere with the task performance, rats would try to lengthen the stimulation duration as much as possible by not progressing to the next period of a trial. And this would result in omission. Although we found that rats were less likely to initiate a trial when the DA stimulation was on, we did not find any systematic change in omission rate once they initiated the trial.

3.5 Methods

3.5.1 Rats

TH::IRES-Cre rats expressing Cre recombinase under the control of tyrosine hydroxylase were maintained on a Long Evans background. Male rats weighing > 300g at the start of the training were used for experimentation. Most rats were double-housed, unless they weigh over 500g (single-housed due to space constraint). Rats were maintained on a 12-hour light on – 12-hour light off schedule. All surgical and behavioral procedures were performed during the light off cycle.

All experimental procedures were conducted in accordance with the National Institute of Health guidelines and were approved by the Princeton University Institutional Animal Care and Use Committee.

3.5.2 Delayed non-match to Sample Task and Guided Delayed Response Task

Rats were water-restricted to 80-85% of their *ad-libitum* weight and trained on a delayed non-match to position spatial working memory task in operant chambers (Med-associates). The operant chamber had two retractable levers on the front wall and a nose port on the opposite, back wall. The goal of the task was to remember the position of the sample lever – either right or left – during the delay period, and to show that memory in the choice period by pressing the non-match, opposite lever. At the beginning of each trial, the sample period begins as a sample lever was presented out of the wall, either on the right or the left side, randomly interleaved. Upon pressing the sample lever, the lever retracted back into the wall and the light in the back nose port was illuminated. The delay period begins as the rat goes to the back wall to poke his nose into the illuminated nose port. The delay period lasted for 1, 5 or 10 sec (randomly interleaved) during which rats usually kept constantly poking his nose into the nose port, not knowing when the delay

period would end. At the end of delay period, the nose port lighted up again and the rat must then make the second nose poke for both levers to extend from the front wall and to begin the choice period. Between the two levers, the correct response is to press the lever that does not match the sample lever. Correct response is rewarded with water in the reward receptacle. The rats are given 15 sec to press the sample lever and 5 sec to poke illuminated nose port and press the choice lever. An incorrect lever press or a failure to response within the time limit resulted in 3s time-out. Trials were followed by 5 sec inter-trial interval.

Guided delayed response task served as a control task for DNMTP, as the task does not require working memory component. All task structure was the same as DNMTP with one key difference; the rats were “guided” to the correct choice lever with a cue light directly above the correct response.

3.5.3 Surgery

TH::Cre Rats trained in DNMTP task were deeply anaesthetized in 1-2% isoflurane and placed in a stereotactic setup. Virus was injected with a microsyringe.

For Fiber photometry experiments, 1µl of Cre-dependent GCaMP virus (AAV5-CAG-Flex-GCamP6f or AAV5-CAG-DIO-RatOpt-GCaMP6f) was injected to the SNc (A/P: -5.6mm, M/L: 2.25mm, D/V: -7.7mm) or VTA (A/P: -6.0mm, M/L: 0.8mm, D/V: -8.0mm). After virus injection, optical fiber (400µm core diameter) was implanted -0.1 mm above the injection site.

For Optogenetic experiments, 1µl of Cre-dependent NpHR or ChR2 virus (AAV5-EF1a-DIO-eNpHR3.0-eYFP or AAV5-EF1a-DIO-ChR2-eYFP) was injected bilaterally and the optical fibers (300µm core diameter) were also bilaterally implanted at the injection site.

3.5.4 Fiber photometry

We recorded the endogenous GCaMP activity of the cholinergic neurons through an implanted fiber while the rats were performing the DNMTP task. Through a single 400μm core fiber, we excited GCaMP with two different wavelengths - 405nm (intensity at fiber tip: 5-10μW, frequency: 531Hz) and 488nm (intensity at fiber tip: 15-25μW, frequency: 211 Hz) using an LED driver (Thorlabs DC4104). Emission light from GCaMP was collected through the same fiber using a photodetector (Newport, Femtowatt 215) and the analog data was digitized by the TDT system (RZ5D) which served both as a A-D converter and lock-in amplifier (Gunaydin et al. 2014). A small head-mounted LED was used to track animal's position while recording. The position data was simultaneously acquired through the TDT tracker (RV2). The timestamps for task events were registered by Med-associates system and fed to TDT system through PCI Med associates interface card (DIG-704PCI-2).

3.5.5 GCaMP signal processing

With 488nm excitation, the fluorescence of GCaMP is calcium-dependent but with 405nm excitation, its fluorescence is calcium-independent. We utilized the calcium-independent signal as a control, isosbestic signal to filter out motion-artifact during the freely moving operant task.

Acquired signals were processed according to the following steps;

First, control 405nm signal ($S_{control}(t)$) was fit to 488nm GCaMP signal ($S_{GCaMP}(t)$) using least-squares regression to calculated fitted control signal ($S_{fitted}(t)$).

$$S_{GCaMP}(t) = \beta_0 + \beta_1 (S_{control}(t)) + \varepsilon$$

where

$$\hat{\beta}_1 = \frac{\sum(S_{control}(t) - \overline{S_{control}}) * (S_{GCaMP}(t) - \overline{S_{GCaMP}})}{\sum(S_{control}(t) - \overline{S_{control}})^2}$$

$$\hat{\beta}_0 = \left(\overline{S_{control}} - \hat{\beta}_1 \overline{S_{GCaMP}}\right)$$

$$S_{fitted}(t) = \hat{\beta}_0 + \hat{\beta}_1 (S_{control}(t))$$

Second, the relative change in fluorescence signal, $\Delta S/S\ (t)$, was calculated using 488nm GCaMP signal ($S_{GCaMP}\ (t)$) and fitted control signal ($S_{fitted}(t)$).

$$\Delta S/S\ (t) = \frac{S_{GCaMP}(t)) - S_{fitted}(t))}{S_{fitted}(t))}$$

Third, smoothed time-dependent baseline of $\Delta S/S\ (t)$, $f_{baseline}(t)$, was calculated to capture low frequency fluctuation. $f_{baseline}(t)$ was equivalent to smoothed moving minimum signal of $\Delta S/S\ (t)$ with 30 sec time window. 30 sec time window was chosen, because it was much longer than a single trial, therefore did not affect GCaMP response to various task events happening within a trial.

$$f_{min}(t) = \{\, t \le x\ < t + \tau\}$$

$$f_{baseline}(t) = \frac{1}{\tau} \sum_{t=1}^{t+\tau} f_{min}(t)\ where\ \tau = 30sec$$

Lastly, final $\Delta F/F$ was calculated by subtracting $f_{base}(t)$ from $\Delta S/S\ (t)$ and scaling by its standard deviation to facilitate comparison across recording sessions.

$$f_{filtered}(t) = \Delta S/S\ (t) - f_{base}(t)$$

$$\Delta F/F\ (t) = f_{filtered}(t)\ /\ std(f_{filtered})$$

3.5.6 Encoding model

Rats were freely-moving in the chamber while performing the DNMTP task. Therefore, isolating the contribution of task events to resulting GCaMP signal from that of animal's movement was important. To do so, we built generalized additive linear models in which GCaMP signal was predicted by the weighted linear sum of predictors such as different types of task events, animal's speed in the chamber, delay period predictor and the combination of task events and speed.

Task event predictors were generated by convolving binary event times (1 or 0) with a 10 degrees-of-freedom spline basis set, spanning -1~2sec around task events such as sample lever presentation, choice lever press, reward port exit, etc. Note the duration of spline basis set for reward respond (reward port entry) was longer (0~10 sec) to capture the sustained reward response observed.

Speed predictor was a continuous variable which included first, second, and third-degree polynomial of the animal's speed to allow flexible modeling of GCaMP.

Delay period predictor was a binary variable, in which 1 denoted time within the delay period and 0 denoted all other times besides the delay period. We included this predictor since

memory related activity during the delay period is of particular importance to a working memory task.

Together, the model is as follows:

$$g(t) = \beta_0 + \sum_{i=1}^{N_{event}} \sum_{j=1}^{N_{bs}} \beta_{i,j} E_{i,j} + \sum_{k=1}^{N_{poly}} \beta_k S^k + \beta_d D + error$$

Where g(t) is the predicted GCaMP signal, N_{event} is the number of different types of task events (total 8 types of task events), and N_{bs} is the degrees of freedom of a spline basis set used for convolution (10df in all cases). $E_{i,j}$ is the i^{th} type of task events (task event types include sample presentation, sample press, delay start, delay end, choice presentation, choice press, reward port entry, reward port exit) convolved with j^{th} spline basis set. $\beta_{i,j}$ is the weight for $E_{i,j}$. N_{poly} is the number of polynomials for the speed predictor (up to third-degree polynomials), S^k is the k^{th} degree polynomial of continuous speed predictor, and β_k is the weight for the speed predictors, S^k. Finally D is the binary delay predictor and β_d is the weight for the delay predictor, D. function *lm* in R was used to fit the model.

Four models were generated and their fit to recorded GCaMP was compared using average R^2 of 3-fold cross-validation. Four models include 1) delay predictor only model 2) speed predictor only model 3) task events predictor only model 4) task events plus speed model.

3.5.7 Immunohistochemistry

Rats were deeply anaesthetized using euthasol and transcardially perfused with 1X phosphate-buffered saline and 4% paraformaldehyde in PBS (PFA). Brains were collected and post-fixed in PFA overnight. Then the brains were placed in 30% sucrose in PBS solution for 2-5 days in 4ºC. Frozen brains were cut into 40µm thick coronal sections using a cryostat.

For the fiber photometry experiment, one-third of coronal sections were directly mounted from the cryostat and cover-slipped with a mounting solution (fluoromount-G with DAPI, Southern Biotech) to get accurate fiber location and to confirm virus expression without any staining. These images were taken using a microscope (Nikon Ti2000E) or whole slide scanner (Hamamatsu Nanozoomer). Other one-third of sections was used to stain for TH, to see co-localization with GCaMP. For staining, the primary antibodies were Chicken-TH (1:500, Aves lab TYH), and the secondary antibodies were Donkey anti-Chicken-Cy3 (1:500, Jackson ImmunoResearch 703-165-155)

3.5.8 Optogenetic experiment

For both NpHR and ChR2 experiments, rats bilaterally expressing opsin in DA neurons were back on water-restriction and training regime after post-op recovery. During this period, rats were used to being tethered having ambient green light in the chamber. Approximately 6-7 weeks post injection, re-trained rats were tested on DNMTP task.

For Sub-trial inhibition experiment, rats received green light (532nm continuous light, 5-6mW intensity at the fiber tip) in SNc or VTA in randomly-selected 30% of all trials for 10 sessions, every other day. 30% laser-on trials were further randomly and equally distributed into sample light-on trials (10%), delay light-on trials (10%), and choice light-on trials (10%). In other words, on Day 1, a rat had its first session with 30% light-on and 70% light-off trials, and on Day 2, the rat got 100% light-off trials. On the following Day 3, the rat had its second session again with 30% light-on and 70% light-off trials. Light was introduced every other day to further reduce plasticity. As a result, 10 sessions required 20 days of testing period in total. Only 10 sessions of data where light-on and light-off trials were interleaved were used for data analysis.

Similarly, in the Entire-trial inhibition experiment, rats received green light in SNc or VTA in randomly-selected 20% of all trials for 5 sessions, every other day.

A subset of rats from Entire-trial inhibition experiment were kept, retrained on control Guided Delayed Response Task, to use cue light to guide their choice. As they quickly learned the new rule (in 2 weeks), delay-dependence accuracy impairment dissipated and they reached >95 % accuracy in all delays. Then these re-trained rats received entire-trial inhibition using the same parameter (30% 532nm continuous green light-on trials, 5-6mW, 5 sessions) from the DNMTP Entire-trial inhibition experiment.

For the ChR2 activation experiment, rats received pulsed blue light (477nm pulse light, 20Hz, 5 pulses, 15 -17mW intensity at the fiber tip) in VTA. The blue light was on during the delay period in randomly-selected 20% of all trials for 5 sessions, every other day.

Chapter 4: Conclusion

4.1 Summary of thesis work

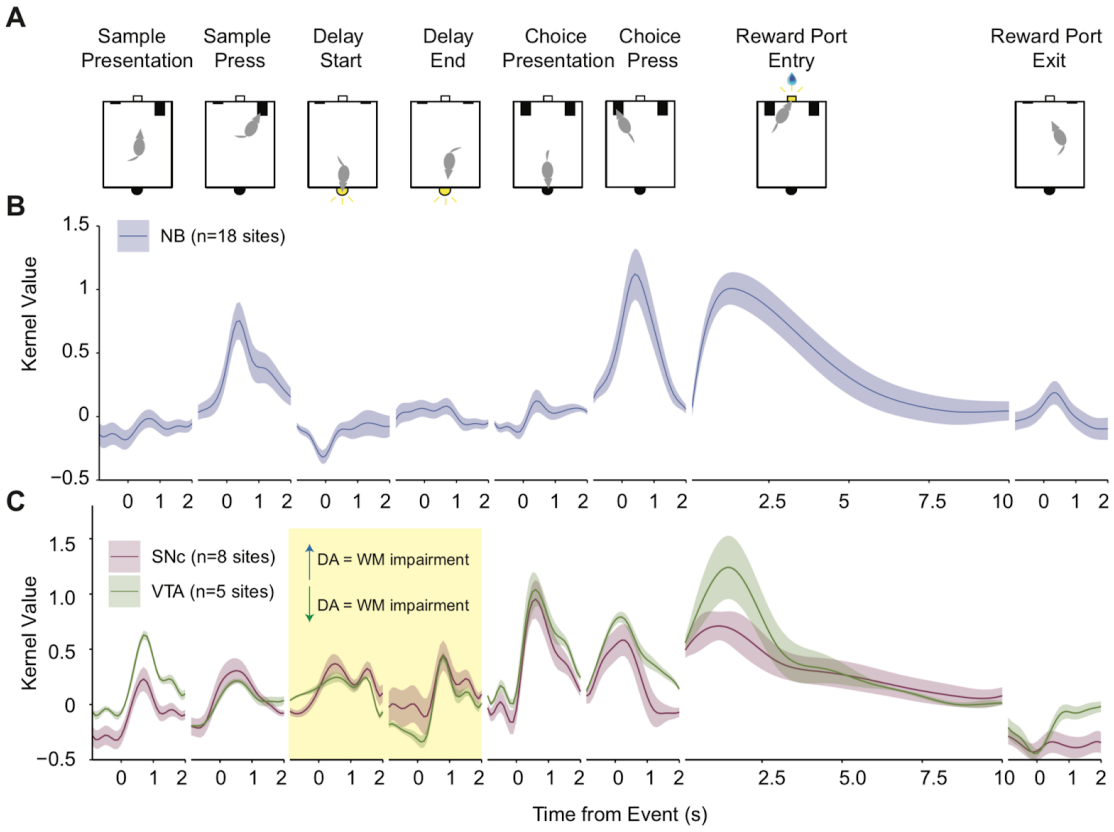


Figure 14 Summary of task events encoded in ChAT neurons in NB and DA neurons in SNc and VTA (A) Schematic of different types of task events in DNMTP Task (B) Lever press action and reward are encoded in ChAT neurons in NB (C) Lever presentation cue and reward are encoded in DA neurons in SNc and VTA. Bidirectional Optogenetic manipulation (Blue upward arrow: optogenetic activation, Green downward arrow: optogenetic inhibition) of VTA DA during delay period (yellow shaded region) supports inverted-U-shape hypothesis of DA.

4.1.1 Major findings

- Task events explain more variance in NB ChAT neurons whereas locomotion explains more variance in MS ChAT neurons
- NB ChAT neurons show elevated activity to lever press action and reward
- NB ChAT neurons' response is organized along the medio-lateral axis of the NB
- Monosynaptic retrograde tracing reveals that the striatum is the strongest projector and the subthalamic nucleus is the densest projector to NB ChAT neurons
- DMS projects to medial NB ChAT neurons whereas DLS projects to lateral NB Chat neuron respectively
- Task events explain more variance in DA activity in VTA and SNc compared to locomotion or delay period
- DA neurons in SNc and VTA similarly show phasic response to lever presentation and reward but low activity during delay period
- Optogenetic inhibition of VTA DA neurons impairs working memory while the same manipulation of SNc DA neurons impairs motor execution of the task.
- Optogenetic inhibition of DA neurons in VTA during sample and delay period impairs WM performance
- Optogenetic activation of DA neurons in VTA during the delay period impairs WM performance

4.1.2 Neural correlates of midbrain DA system and basal forebrain ChAT system in working memory

Using fiber photometry, I recorded and analyzed endogenous activity of DA neurons in SNc (SNc-DA) and VTA (VTA-DA) and ChAT neurons in MS (MS-ChAT) and NB (NB-ChAT) while rats were performing DNMTP task. I found that task events were more predictive of variance in GCaMP activity of SNc-DA, VTA-DA, NB-ChAT neurons compared to locomotion. In contrast, locomotion explained more variance in MS-ChAT activity.

When the encoding of task events were further examined in SNc-DA, VTA-DA, and NB-CHAT neurons, I observed that both SNc-DA and VTA-DA neurons were phasically active at the sample and choice lever presentation cue (i.e. reward-predicting cues) whereas NB-ChAT neurons were phasically active at the sample and choice lever press action. NB-ChAT neurons received a strong and topographic input from the striatum, suggestive of lever press action signal coming from the basal ganglia. All three groups showed phasic response to reward during the outcome period. Also, all three groups showed low activity during the delay period. The neural correlate of VTA-DA and SNc-DA during DNMTP task is consistent with the prediction from "gating" hypothesis of DA in WM.

4.1.3 Causal manipulation of midbrain DA system and basal forebrain ChAT system in working memory

Using optogenetics, I inhibited SNc-DA, VTA-DA, MS-ChAT, and NB-ChAT neurons while rats were performing DNMTP task. Optogenetic inhibition of the dopaminergic system impaired WM performance, while the same manipulation of the cholinergic system did not. Comparison of optogenetic inhibition during the memory-guided DNMTP vs sensory-guided DNMTP revealed that VTA-DA contributes to the cognitive component of WM whereas SNc-DA is involved in the motor execution of the task. More temporally-specific optogenetic inhibition of specific periods (sample, delay, choice periods) of a trial demonstrated that VTA-DA inhibition early in the trial (sample and delay period) disrupts WM whereas SNc-DA inhibition later in the trial (delay and

choice period) impairs performance, consistent with its role in motor execution. Optogenetic activation of VTA-DA during the delay period also impaired WM performance, supporting the “inverted U-shape” hypothesis of DA.

4.2 Ongoing and Future Direction

The work presented in this thesis poses two important questions, especially related to the neuromodulatory effects in the downstream regions. The first critical question is the projection-specificity of the VTA-DA modulation of WM. In other words, does the VTA projection to PFC modulate WM differently than VTA projection to NAc? VTA sends dense projection to both PFC and NAc. To answer this question, I injected Cre-dependent ChR2 into the VTA and implanted optical fibers in the projection (Figure 15 A). If both projections impairs WM, it would be interesting to further investigate if separate projections modulate different period of a trial. Since I observed that inhibition of VTA-DA during both sample and delay period impairs WM, projection-specific manipulation might contribute to only one of the two periods.

Based on the results from the projection-specific optogenetics, I plan to address the next question: how does the downstream activity change as a function of DA manipulation? To better understand the role of DA in WM, we need to be able to observe how working memory representation downstream is affected by the DA activity. This can be achieved by combination of electrophysiology recording in the downstream region while optogenetically manipulating DA projection to the downstream area (Figure 15B). Iontophoresis of D1R agonists in the PFC of behaving monkeys increased the stimulus-selectivity of the delay-firing neurons in PFC (Vijayraghavan et al. 2007). With faster optogenetic, projection-specific manipulation together with the information about the endogenous activity of DA activity during the task, I am equipped with appropriate tool set to unveil the role of DA not only in WM *performance* but also more specifically in WM *representation*.

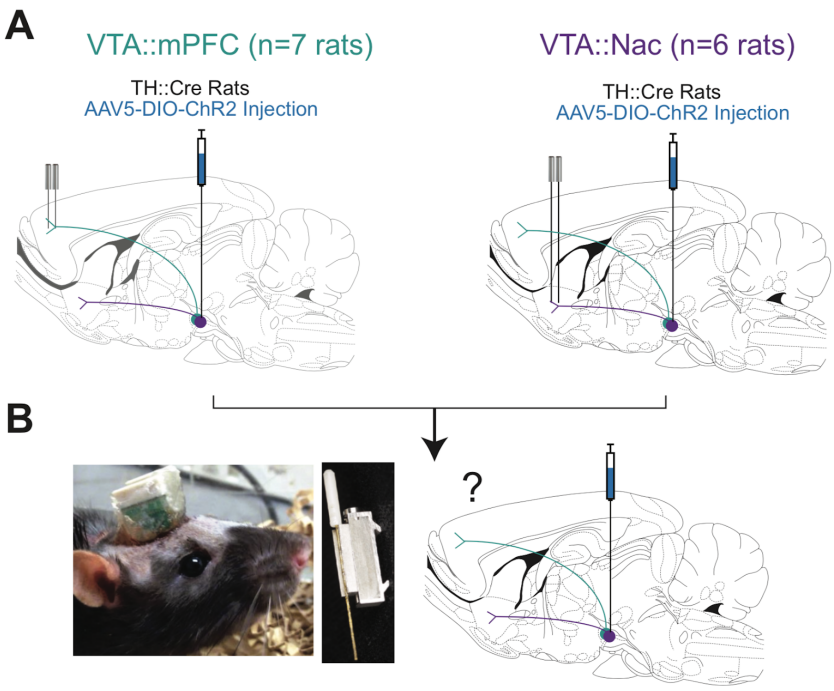


Figure 15 Schematic of ongoing experiment and future directions (A) Trained TH::cre rats were injected with a Cre-dependent ChR2 virus and bilaterally implanted with optical fibers in its two prominent projection targets: mPFC (left, n=7) and Nac (right, n=6). This allows us to specifically activate and dissociate which of the two projections is comparatively more important to working memory impairment . (B) Based on this result from (A), one could do electrophysiology recording of the downstream region combined with projection-specific optogenetics to better clarify the mechanism behind observed WM performance impairment.

4.3 Conclusions

In this thesis, I investigated the temporally-precise role of two major neuromodulatory systems -midbrain DA system and basal forebrain ChAT system- in spatial working memory. Working memory task events such as reward-predicting cue and reward were encoded in the VTA DA and SNc DA neurons, whereas reward-predicting action and reward were encoded in the NB ChAT neurons. The encoding of reward-predicting action and reward in the NB ChAT neurons was organized along the medio-lateral axis, potentially mediated by its topographical input from the striatum. Only the midbrain DA system, but not the basal forebrain ChAT system, was causally involved in the working memory performance. Specifically, I demonstrated that the bidirectional manipulation of VTA DA neurons during the delay period mediate the cognitive component of the working memory task supporting the “inverted-U-shape” hypothesis, while SNc DA neurons are involved in the motor execution of the task. This is the first evidence providing dissociable causal roles of VTA and SNc DA neurons in working memory performance.

References

Abeles, Moshe. 1982. *Local Cortical Circuits*.

Akhlaghpour, Hessameddin, Joost Wiskerke, Jung Yoon Choi, Joshua P. Taliaferro, Jennifer Au, and Ilana B. Witten. 2016. “Dissociated Sequential Activity and Stimulus Encoding in the Dorsomedial Striatum during Spatial Working Memory.” *eLife* 5. https://doi.org/10.7554/elife.19507.

Amit, D. J., and N. Brunel. 1997. “Model of Global Spontaneous Activity and Local Structured Activity during Delay Periods in the Cerebral Cortex.” *Cerebral Cortex* 7 (3): 237–52.

Arnsten, A. F. 1997. “Catecholamine Regulation of the Prefrontal Cortex.” *Journal of Psychopharmacology* 11 (2): 151–62.

Arnsten, A. F., J. X. Cai, B. L. Murphy, and P. S. Goldman-Rakic. 1994. “Dopamine D1 Receptor Mechanisms in the Cognitive Performance of Young Adult and Aged Monkeys.” *Psychopharmacology* 116 (2): 143–51.

Arnsten, A. F., and P. S. Goldman-Rakic. 1998. “Noise Stress Impairs Prefrontal Cortical Cognitive Function in Monkeys: Evidence for a Hyperdopaminergic Mechanism.” *Archives of General Psychiatry* 55 (4): 362–68.

Arnsten, Amy F. T., Min J. Wang, and Constantinos D. Paspalas. 2012. “Neuromodulation of Thought: Flexibilities and Vulnerabilities in Prefrontal Cortical Network Synapses.” *Neuron* 76 (1): 223–39.

Baddeley, Alan D. 1986. *Working Memory*. Oxford University Press.

Baeg, E. H., Y. B. Kim, K. Huh, I. Mook-Jung, H. T. Kim, and M. W. Jung. 2003. “Dynamics of Population Code for Working Memory in the Prefrontal Cortex.” *Neuron* 40 (1): 177–88.

Barak, Omri, Misha Tsodyks, and Ranulfo Romo. 2010. “Neuronal Population Coding of Parametric Working Memory.” *The Journal of Neuroscience: The Official Journal of the Society for Neuroscience* 30 (28): 9424–30.

Barter, Joseph W., Suellen Li, Dongye Lu, Ryan A. Bartholomew, Mark A. Rossi, Charles T. Shoemaker, Daniel Salas-Meza, Erin Gaidis, and Henry H. Yin. 2015. “Beyond Reward Prediction Errors: The Role of Dopamine in Movement Kinematics.” *Frontiers in Integrative Neuroscience* 9 (May): 39.

Bastos, André M., Roman Loonis, Simon Kornblith, Mikael Lundqvist, and Earl K. Miller. 2018. “Laminar Recordings in Frontal Cortex Suggest Distinct Layers for Maintenance and Control of Working Memory.” *Proceedings of the National Academy of Sciences of the United States of America* 115 (5): 1117–22.

Baxter, Mark G., and David J. Bucci. 2013. “Selective Immunotoxic Lesions of Basal Forebrain Cholinergic Neurons: Twenty Years of Research and New Directions.” *Behavioral Neuroscience* 127 (5): 611–18.

Baxter, M. G., D. J. Bucci, L. K. Gorman, R. G. Wiley, and M. Gallagher. 1995. “Selective Immunotoxic Lesions of Basal Forebrain Cholinergic Cells: Effects on Learning and Memory in Rats.” *Behavioral Neuroscience* 109 (4): 714–22.

Ben-Yishai, R., R. L. Bar-Or, and H. Sompolinsky. 1995. “Theory of Orientation Tuning in Visual Cortex.” *Proceedings of the National Academy of Sciences of the United States of America* 92 (9): 3844–48.

Bowen, D. M., J. S. Benton, J. A. Spillane, C. C. T. Smith, and S. J. Allen. 1982. “Choline Acetyltransferase Activity and Histopathology of Frontal Neocortex from Biopsies of Demented Patients.” *Journal of the Neurological Sciences*. https://doi.org/10.1016/0022-510x(82)90026-0.

Braver, Todd S., and Jonathan D. Cohen. 2000. “On the Control of Control: The Role of Dopamine in Regulating Prefrontal Function and Working Memory.” *Control of Cognitive Processes: Attention and Performance XVIII*, 713–37.

Brody, Carlos D., Adrián Hernández, Antonio Zainos, and Ranulfo Romo. 2003. “Timing and Neural Encoding of Somatosensory Parametric Working Memory in Macaque Prefrontal Cortex.” *Cerebral Cortex* 13 (11): 1196–1207.

Brozoski, T. J., R. M. Brown, H. E. Rosvold, and P. S. Goldman. 1979. “Cognitive Deficit Caused by Regional Depletion of Dopamine in Prefrontal Cortex of Rhesus Monkey.” *Science* 205 (4409): 929–32.

Brunel, N., and X. J. Wang. 2001. “Effects of Neuromodulation in a Cortical Network Model of Object Working Memory Dominated by Recurrent Inhibition.” *Journal of Computational Neuroscience* 11 (1): 63–85.

Cai, J. X., and A. F. Arnsten. 1997. “Dose-Dependent Effects of the Dopamine D1 Receptor Agonists A77636 or SKF81297 on Spatial Working Memory in Aged Monkeys.” *The Journal of Pharmacology and Experimental Therapeutics* 283 (1): 183–89.

Callicott, J. H., V. S. Mattay, A. Bertolino, K. Finn, R. Coppola, J. A. Frank, T. E. Goldberg, and D. R. Weinberger. 1999. “Physiological Characteristics of Capacity Constraints in Working Memory as Revealed by Functional MRI.” *Cerebral Cortex* 9 (1): 20–26.

Cass, W. A., and G. A. Gerhardt. 1995. “In Vivo Assessment of Dopamine Uptake in Rat Medial Prefrontal Cortex: Comparison with Dorsal Striatum and Nucleus Accumbens.” *Journal of Neurochemistry* 65 (1): 201–7.

Chiba, A. A., D. J. Bucci, P. C. Holland, and M. Gallagher. 1995. “Basal Forebrain Cholinergic Lesions Disrupt Increments but Not Decrements in Conditioned Stimulus Processing.” *The Journal of Neuroscience: The Official Journal of the Society for Neuroscience* 15 (11): 7315–22.

Cohen, Jeremiah Y., Sebastian Haesler, Linh Vong, Bradford B. Lowell, and Naoshige Uchida. 2012. “Neuron-Type-Specific Signals for Reward and Punishment in the Ventral Tegmental Area.” *Nature* 482 (7383): 85–88.

Compte, A., N. Brunel, P. S. Goldman-Rakic, and X. J. Wang. 2000. “Synaptic Mechanisms and Network Dynamics Underlying Spatial Working Memory in a Cortical Network Model.” *Cerebral Cortex* 10 (9): 910–23.

Connor, D. J., P. J. Langlais, and L. J. Thal. 1991. “Behavioral Impairments after Lesions of the Nucleus Basalis by Ibotenic Acid and Quisqualic Acid.” *Brain Research* 555 (1): 84–90.

Cools, Roshan, and Mark D'Esposito. 2011. "Inverted-U–Shaped Dopamine Actions on Human Working Memory and Cognitive Control." *Biological Psychiatry* 69 (12): e113–25.

Dotson, Nicholas M., Steven J. Hoffman, Baldwin Goodell, and Charles M. Gray. 2018. "Feature-Based Visual Short-Term Memory Is Widely Distributed and Hierarchically Organized." *Neuron* 99 (1): 215–26.e4.

Druckmann, Shaul, and Dmitri B. Chklovskii. 2012. "Neuronal Circuits Underlying Persistent Representations despite Time Varying Activity." *Current Biology: CB* 22 (22): 2095–2103.

Dunnett, S., B. Everitt, and T. Robbins. 1991. "The Basal Forebrain-Cortical Cholinergic System: Interpreting the Functional Consequences of Excitotoxic Lesions." *Trends in Neurosciences*. https://doi.org/10.1016/0166-2236(91)90061-x.

Eacott, M. J., D. Gaffan, and E. A. Murray. 1994. "Preserved Recognition Memory for Small Sets, and Impaired Stimulus Identification for Large Sets, Following Rhinal Cortex Ablations in Monkeys." *The European Journal of Neuroscience* 6 (9): 1466–78.

Eggermann, Emmanuel, Yves Kremer, Sylvain Crochet, and Carl C. H. Petersen. 2014. "Cholinergic Signals in Mouse Barrel Cortex during Active Whisker Sensing." *Cell Reports* 9 (5): 1654–60.

Engelhard, Ben, Joel Finkelstein, Julia Cox, Weston Fleming, Hee Jae Jang, Sharon Ornelas, Sue Ann Koay, et al. 2018. "Specialized and Spatially Organized Coding of Sensory, Motor, and Cognitive Variables in Midbrain Dopamine Neurons." https://doi.org/10.1101/456194.

Erlich, Jeffrey C., Max Bialek, and Carlos D. Brody. 2011. "A Cortical Substrate for Memory-Guided Orienting in the Rat." *Neuron* 72 (2): 330–43.

Everitt, B. J., and T. W. Robbins. 1997. "Central Cholinergic Systems and Cognition." *Annual Review of Psychology* 48: 649–84.

Fibiger, H. C. 1991. "Cholinergic Mechanisms in Learning, Memory and Dementia: A Review of Recent Evidence." *Trends in Neurosciences* 14 (6): 220–23.

Francis, P. T., A. M. Palmer, N. R. Sims, D. M. Bowen, A. N. Davison, M. M. Esiri, D. Neary, J. S. Snowden, and G. K. Wilcock. 1985. "Neurochemical Studies of Early-Onset Alzheimer's

Disease. Possible Influence on Treatment." *The New England Journal of Medicine* 313 (1): 7–11.

Fransén, Erik, Angel A. Alonso, and Michael E. Hasselmo. 2002. "Simulations of the Role of the Muscarinic-Activated Calcium-Sensitive Nonspecific Cation Current INCM in Entorhinal Neuronal Activity during Delayed Matching Tasks." *The Journal of Neuroscience: The Official Journal of the Society for Neuroscience* 22 (3): 1081–97.

Fransén, Erik, Babak Tahvildari, Alexei V. Egorov, Michael E. Hasselmo, and Angel A. Alonso. 2006. "Mechanism of Graded Persistent Cellular Activity of Entorhinal Cortex Layer v Neurons." *Neuron* 49 (5): 735–46.

Frick, Karyn M., Jeansok J. Kim, and Mark G. Baxter. 2004. "Effects of Complete Immunotoxin Lesions of the Cholinergic Basal Forebrain on Fear Conditioning and Spatial Learning." *Hippocampus* 14 (2): 244–54.

Froemke, Robert C., Ioana Carcea, Alison J. Barker, Kexin Yuan, Bryan A. Seybold, Ana Raquel O. Martins, Natalya Zaika, et al. 2013. "Long-Term Modification of Cortical Synapses Improves Sensory Perception." *Nature Neuroscience* 16 (1): 79–88.

Funahashi, S., C. J. Bruce, and P. S. Goldman-Rakic. 1989. "Mnemonic Coding of Visual Space in the Monkey's Dorsolateral Prefrontal Cortex." *Journal of Neurophysiology* 61 (2): 331–49.

Fürth, Daniel, Thomas Vaissière, Ourania Tzortzi, Yang Xuan, Antje Märtin, Iakovos Lazaridis, Giada Spigolon, et al. 2018. "An Interactive Framework for Whole-Brain Maps at Cellular Resolution." *Nature Neuroscience* 21 (1): 139–49.

Fuster, J. M. 1990. "Inferotemporal Units in Selective Visual Attention and Short-Term Memory." *Journal of Neurophysiology* 64 (3): 681–97.

Fuster, J. M., and G. E. Alexander. 1971. "Neuron Activity Related to Short-Term Memory." *Science* 173 (3997): 652–54.

Gaffan, D., and E. A. Murray. 1992. "Monkeys (Macaca Fascicularis) with Rhinal Cortex Ablations Succeed in Object Discrimination Learning despite 24-Hr Intertrial Intervals and Fail at Matching to Sample despite Double Sample Presentations." *Behavioral Neuroscience* 106

(1): 30–38.

Galani, Rodrigue, Olivia Lehmann, Tristan Bolmont, Elizabeth Aloy, Fabrice Bertrand, Christine Lazarus, Hélène Jeltsch, and Jean-Christophe Cassel. 2002. “Selective Immunolesions of CH4 Cholinergic Neurons Do Not Disrupt Spatial Memory in Rats.” *Physiology & Behavior*. https://doi.org/10.1016/s0031-9384(02)00674-1.

Ganguli, Surya, and Peter Latham. 2009. “Feedforward to the Past: The Relation between Neuronal Connectivity, Amplification, and Short-Term Memory.” *Neuron* 61 (4): 499–501.

Garris, P. A., L. B. Collins, S. R. Jones, and R. M. Wightman. 1993. “Evoked Extracellular Dopamine in Vivo in the Medial Prefrontal Cortex.” *Journal of Neurochemistry* 61 (2): 637–47.

Gibbs, Sasha E. B., and Mark D’Esposito. 2005. “A Functional MRI Study of the Effects of Bromocriptine, a Dopamine Receptor Agonist, on Component Processes of Working Memory.” *Psychopharmacology* 180 (4): 644–53.

Gielow, Matthew R., and Laszlo Zaborszky. 2017. “The Input-Output Relationship of the Cholinergic Basal Forebrain.” *Cell Reports* 18 (7): 1817–30.

Gilbert, Charles D. 1993. “Circuitry, Architecture, and Functional Dynamics of Visual Cortex.” *Cerebral Cortex* 3 (5): 373–86.

Goldman, Mark S. 2009. “Memory without Feedback in a Neural Network.” *Neuron* 61 (4): 621–34.

Goldman-Rakic, P. S. 1995. “Cellular Basis of Working Memory.” *Neuron* 14 (3): 477–85.

Goldman-Rakic, P. S., C. Leranth, S. M. Williams, N. Mons, and M. Geffard. 1989. “Dopamine Synaptic Complex with Pyramidal Neurons in Primate Cerebral Cortex.” *Proceedings of the National Academy of Sciences of the United States of America* 86 (22): 9015–19.

Gritti, I., P. Henny, F. Galloni, L. Mainville, M. Mariotti, and B. E. Jones. 2006. “Stereological Estimates of the Basal Forebrain Cell Population in the Rat, Including Neurons Containing Choline Acetyltransferase, Glutamic Acid Decarboxylase or Phosphate-Activated Glutaminase and Colocalizing Vesicular Glutamate Transporters.” *Neuroscience* 143 (4):

1051–64.

Gritton, Howard J., William M. Howe, Caitlin S. Mallory, Vaughn L. Hetrick, Joshua D. Berke, and Martin Sarter. 2016. “Cortical Cholinergic Signaling Controls the Detection of Cues.” *Proceedings of the National Academy of Sciences of the United States of America* 113 (8): E1089–97.

Gunaydin, Lisa A., Logan Grosenick, Joel C. Finkelstein, Isaac V. Kauvar, Lief E. Fenno, Avishek Adhikari, Stephan Lammel, et al. 2014. “Natural Neural Projection Dynamics Underlying Social Behavior.” *Cell* 157 (7): 1535–51.

Haj-Dahmane, S., and R. Andrade. 1998. “Ionic Mechanism of the Slow Afterdepolarization Induced by Muscarinic Receptor Activation in Rat Prefrontal Cortex.” *Journal of Neurophysiology* 80 (3): 1197–1210.

Haller, Matar, John Case, Nathan E. Crone, Edward F. Chang, David King-Stephens, Kenneth D. Laxer, Peter B. Weber, Josef Parvizi, Robert T. Knight, and Avgusta Y. Shestyuk. 2018. “Persistent Neuronal Activity in Human Prefrontal Cortex Links Perception and Action.” *Nature Human Behaviour* 2 (1): 80–91.

Hangya, Balázs, Sachin P. Ranade, Maja Lorenc, and Adam Kepecs. 2015. “Central Cholinergic Neurons Are Rapidly Recruited by Reinforcement Feedback.” *Cell* 162 (5): 1155–68.

Harrison, Thomas C., Lucas Pinto, Julien R. Brock, and Yang Dan. 2016. “Calcium Imaging of Basal Forebrain Activity during Innate and Learned Behaviors.” *Frontiers in Neural Circuits* 10 (May): 36.

Harvey, Christopher D., Philip Coen, and David W. Tank. 2012. “Choice-Specific Sequences in Parietal Cortex during a Virtual-Navigation Decision Task.” *Nature* 484 (7392): 62–68.

Hassani, O. K., M. G. Lee, P. Henny, and B. E. Jones. 2009. “Discharge Profiles of Identified GABAergic in Comparison to Cholinergic and Putative Glutamatergic Basal Forebrain Neurons across the Sleep-Wake Cycle.” *Journal of Neuroscience* 29 (38): 11828–40.

Hasselmo, Michael E. 2006. “The Role of Acetylcholine in Learning and Memory.” *Current Opinion in Neurobiology* 16 (6): 710–15.

Hasselmo, Michael E., and Martin Sarter. 2011. “Modes and Models of Forebrain Cholinergic Neuromodulation of Cognition.” *Neuropsychopharmacology: Official Publication of the American College of Neuropsychopharmacology* 36 (1): 52–73.

Hasselmo, Michael E., and Chantal E. Stern. 2006. “Mechanisms Underlying Working Memory for Novel Information.” *Trends in Cognitive Sciences* 10 (11): 487–93.

Hodges, H., S. Thrasher, and J. A. Gray. 1989. “Improved Radial Maze Performance Induced by the Benzodiazepine Antagonist ZK 93 426 in Lesioned and Alcohol-Treated Rats.” *Behavioural Pharmacology* 1 (1): 45–55.

Hopfield, J. J. 1982. “Neural Networks and Physical Systems with Emergent Collective Computational Abilities.” *Proceedings of the National Academy of Sciences of the United States of America* 79 (8): 2554–58.

Howe, M. W., and D. A. Dombeck. 2016. “Rapid Signalling in Distinct Dopaminergic Axons during Locomotion and Reward.” *Nature* 535 (7613): 505–10.

Howe, William M., Anne S. Berry, Jennifer Francois, Gary Gilmour, Joshua M. Carp, Mark Tricklebank, Cindy Lustig, and Martin Sarter. 2013. “Prefrontal Cholinergic Mechanisms Instigating Shifts from Monitoring for Cues to Cue-Guided Performance: Converging Electrochemical and fMRI Evidence from Rats and Humans.” *The Journal of Neuroscience: The Official Journal of the Society for Neuroscience* 33 (20): 8742–52.

Klink, Ruby, and Angel Alonso. 1997a. “Ionic Mechanisms of Muscarinic Depolarization in Entorhinal Cortex Layer II Neurons.” *Journal of Neurophysiology* 77 (4): 1829–43.

. 1997b. “Muscarinic Modulation of the Oscillatory and Repetitive Firing Properties of Entorhinal Cortex Layer II Neurons.” *Journal of Neurophysiology*. https://doi.org/10.1152/jn.1997.77.4.1813.

Kopec, Charles D., Jeffrey C. Erlich, Bingni W. Brunton, Karl Deisseroth, and Carlos D. Brody. 2015. “Cortical and Subcortical Contributions to Short-Term Memory for Orienting Movements.” *Neuron* 88 (2): 367–77.

Kritzer, M. F., and P. S. Goldman-Rakic. 1995. “Intrinsic Circuit Organization of the Major Layers

and Sublayers of the Dorsolateral Prefrontal Cortex in the Rhesus Monkey." *The Journal of Comparative Neurology* 359 (1): 131–43.

Kubota, K., and H. Niki. 1971. "Prefrontal Cortical Unit Activity and Delayed Alternation Performance in Monkeys." *Journal of Neurophysiology* 34 (3): 337–47.

Leanza, G., O. G. Nilsson, R. G. Wiley, and A. Björklund. 1995. "Selective Lesioning of the Basal Forebrain Cholinergic System by Intraventricular 192 IgG--Saporin: Behavioural, Biochemical and Stereological Studies in the Rat." *The European Journal of Neuroscience* 7 (2): 329–43.

Lerer, B. E., and John Warner. 1986. "Radial Maze Performance Deficits Following Lesions of Rat Basal Forebrain." In *Alzheimer's and Parkinson's Disease: Strategies for Research and Development*, edited by Abraham Fisher, Israel Hanin, and Chaim Lachman, 419–26. Boston, MA: Springer US.

Lidow, Michael S., Phil-Ok Koh, and Amy F. T. Arnsten. 2003. "D1 Dopamine Receptors in the Mouse Prefrontal Cortex: Immunocytochemical and Cognitive Neuropharmacological Analyses." *Synapse* 47 (2): 101–8.

Ljungberg, T., P. Apicella, and W. Schultz. 1991. "Responses of Monkey Midbrain Dopamine Neurons during Delayed Alternation Performance." *Brain Research* 567 (2): 337–41.

Lovett-Barron, Matthew, Patrick Kaifosh, Mazen A. Kheirbek, Nathan Danielson, Jeffrey D. Zaremba, Thomas R. Reardon, Gergely F. Turi, René Hen, Boris V. Zemelman, and Attila Losonczy. 2014. "Dendritic Inhibition in the Hippocampus Supports Fear Learning." *Science* 343 (6173): 857–63.

Lundqvist, Mikael, Pawel Herman, Melissa R. Warden, Scott L. Brincat, and Earl K. Miller. 2018. "Gamma and Beta Bursts during Working Memory Readout Suggest Roles in Its Volitional Control." *Nature Communications* 9 (1). https://doi.org/10.1038/s41467-017-02791-8.

Lundqvist, Mikael, Jonas Rose, Pawel Herman, Scott L. Brincat, Timothy J. Buschman, and Earl K. Miller. 2016. "Gamma and Beta Bursts Underlie Working Memory." *Neuron* 90 (1): 152–64.

MacDonald, Christopher J., Kyle Q. Lepage, Uri T. Eden, and Howard Eichenbaum. 2011. "Hippocampal 'Time Cells' Bridge the Gap in Memory for Discontiguous Events." *Neuron* 71 (4): 737–49.

Mandel, R. J., A. D. Chen, D. J. Connor, and L. J. Thal. 1989. "Continuous Physostigmine Infusion in Rats with Excitotoxic Lesions of the Nucleus Basalis Magnocellularis: Effects on Performance in the Water Maze Task and Cortical Cholinergic Markers." *The Journal of Pharmacology and Experimental Therapeutics* 251 (2): 612–19.

Mandel, R. J., and L. J. Thal. 1988. "Physostigmine Improves Water Maze Performance Following Nucleus Basalis Magnocellularis Lesions in Rats." *Psychopharmacology* 96 (3): 421–25.

McAlonan, G. M., G. R. Dawson, L. O. Wilkinson, T. W. Robbins, and B. J. Everitt. 1995. "The Effects of AMPA-Induced Lesions of the Medial Septum and Vertical Limb Nucleus of the Diagonal Band of Broca on Spatial Delayed Non-Matching to Sample and Spatial Learning in the Water Maze." *The European Journal of Neuroscience* 7 (5): 1034–49.

McGaughy, J., B. J. Everitt, T. W. Robbins, and M. Sarter. 2000. "The Role of Cortical Cholinergic Afferent Projections in Cognition: Impact of New Selective Immunotoxins." *Behavioural Brain Research* 115 (2): 251–63.

McGaughy, Jill, Randal A. Koene, Howard Eichenbaum, and Michael E. Hasselmo. 2005. "Cholinergic Deafferentation of the Entorhinal Cortex in Rats Impairs Encoding of Novel but Not Familiar Stimuli in a Delayed Nonmatch-to-Sample Task." *The Journal of Neuroscience: The Official Journal of the Society for Neuroscience* 25 (44): 10273–81.

McGaughy, J., T. Kaiser, and M. Sarter. 1996. "Behavioral Vigilance Following Infusions of 192 IgG-Saporin into the Basal Forebrain: Selectivity of the Behavioral Impairment and Relation to Cortical AChE-Positive Fiber Density." *Behavioral Neuroscience* 110 (2): 247–65.

Mesulam, M-Marsel, and Changiz Geula. 1988. "Nucleus Basalis (Ch4) and Cortical Cholinergic Innervation in the Human Brain: Observations Based on the Distribution of Acetylcholinesterase and Choline Acetyltransferase." *The Journal of Comparative Neurology* 275 (2): 216–40.

Mesulam, M. M., E. J. Mufson, A. I. Levey, and B. H. Wainer. 1983. “Cholinergic Innervation of Cortex by the Basal Forebrain: Cytochemistry and Cortical Connections of the Septal Area, Diagonal Band Nuclei, Nucleus Basalis (substantia Innominata), and Hypothalamus in the Rhesus Monkey.” *The Journal of Comparative Neurology* 214 (2): 170–97.

Mesulam, M. M., E. J. Mufson, B. H. Wainer, and A. I. Levey. 1983. “Central Cholinergic Pathways in the Rat: An Overview Based on an Alternative Nomenclature (Ch1-Ch6).” *Neuroscience* 10 (4): 1185–1201.

Miller, Earl K., Mikael Lundqvist, and André M. Bastos. 2018. “Working Memory 2.0.” *Neuron* 100 (2): 463–75.

Mirenowicz, J., and W. Schultz. 1994. “Importance of Unpredictability for Reward Responses in Primate Dopamine Neurons.” *Journal of Neurophysiology* 72 (2): 1024–27.

Murray, John D., Alberto Bernacchia, Nicholas A. Roy, Christos Constantinidis, Ranulfo Romo, and Xiao-Jing Wang. 2017. “Stable Population Coding for Working Memory Coexists with Heterogeneous Neural Dynamics in Prefrontal Cortex.” *Proceedings of the National Academy of Sciences of the United States of America* 114 (2): 394–99.

O’Reilly, Randall C., and Michael J. Frank. 2006. “Making Working Memory Work: A Computational Model of Learning in the Prefrontal Cortex and Basal Ganglia.” *Neural Computation* 18 (2): 283–328.

Otto, T., and H. Eichenbaum. 1992. “Complementary Roles of the Orbital Prefrontal Cortex and the Perirhinal-Entorhinal Cortices in an Odor-Guided Delayed-Nonmatching-to-Sample Task.” *Behavioral Neuroscience* 106 (5): 762–75.

Parikh, Vinay, Rouba Kozak, Vicente Martinez, and Martin Sarter. 2007. “Prefrontal Acetylcholine Release Controls Cue Detection on Multiple Timescales.” *Neuron* 56 (1): 141–54.

Pastalkova, Eva, Vladimir Itskov, Asohan Amarasingham, and György Buzsáki. 2008. “Internally Generated Cell Assembly Sequences in the Rat Hippocampus.” *Science* 321 (5894): 1322–27.

Perry, E. K., B. E. Tomlinson, G. Blessed, K. Bergmann, P. H. Gibson, and R. H. Perry. 1978.

"Correlation of Cholinergic Abnormalities with Senile Plaques and Mental Test Scores in Senile Dementia." *British Medical Journal* 2 (6150): 1457–59.

Pinto, Lucas, Michael J. Goard, Daniel Estandian, Min Xu, Alex C. Kwan, Seung-Hee Lee, Thomas C. Harrison, Guoping Feng, and Yang Dan. 2013. "Fast Modulation of Visual Perception by Basal Forebrain Cholinergic Neurons." *Nature Neuroscience* 16 (12): 1857–63.

Reardon, Thomas R., Andrew J. Murray, Gergely F. Turi, Christoph Wirblich, Katherine R. Croce, Matthias J. Schnell, Thomas M. Jessell, and Attila Losonczy. 2016. "Rabies Virus CVS-N2c(ΔG) Strain Enhances Retrograde Synaptic Transfer and Neuronal Viability." *Neuron* 89 (4): 711–24.

Richardson, R. T., and M. R. DeLong. 1990. "Context-Dependent Responses of Primate Nucleus Basalis Neurons in a Go/no-Go Task." *The Journal of Neuroscience: The Official Journal of the Society for Neuroscience* 10 (8): 2528–40.

Robbins, T. W., B. J. Everitt, H. M. Marston, J. Wilkinson, G. H. Jones, and K. J. Page. 1989. "Comparative Effects of Ibotenic Acid- and Quisqualic Acid-Induced Lesions of the Substantia Innominata on Attentional Function in the Rat: Further Implications for the Role of the Cholinergic Neurons of the Nucleus Basalis in Cognitive Processes." *Behavioural Brain Research* 35 (3): 221–40.

Roesch, Matthew R., Donna J. Calu, and Geoffrey Schoenbaum. 2007. "Dopamine Neurons Encode the Better Option in Rats Deciding between Differently Delayed or Sized Rewards." *Nature Neuroscience* 10 (12): 1615–24.

Romo, R., C. D. Brody, A. Hernández, and L. Lemus. 1999. "Neuronal Correlates of Parametric Working Memory in the Prefrontal Cortex." *Nature* 399 (6735): 470–73.

Rye, D. B., B. H. Wainer, M-M Mesulam, E. J. Mufson, and C. B. Saper. 1984. "Cortical Projections Arising from the Basal Forebrain: A Study of Cholinergic and Noncholinergic Components Employing Combined Retrograde Tracing and Immunohistochemical Localization of Choline Acetyltransferase." *Neuroscience* 13 (3): 627–43.

Salamone, J. D., S. L. Channell, S. A. Welner, R. Gill, T. W. Robbins, and S. D. Iversen. 1987. “Nucleus Basalis Lesions and Anticholinergic Drugs Impair Spatial Memory and Visual Discrimination Performance in the Rat.” In *Cellular and Molecular Basis of Cholinergic Function*, 835–40. Ellis Horwood Chichester.

Saper, C. B. 1984. “Organization of Cerebral Cortical Afferent Systems in the Rat. II. Magnocellular Basal Nucleus.” *The Journal of Comparative Neurology* 222 (3): 313–42.

Sarter, Martin, and Vinay Parikh. 2005. “Choline Transporters, Cholinergic Transmission and Cognition.” *Nature Reviews. Neuroscience* 6 (1): 48–56.

Saunders, Benjamin T., Jocelyn M. Richard, Elyssa B. Margolis, and Patricia H. Janak. 2018. “Dopamine Neurons Create Pavlovian Conditioned Stimuli with Circuit-Defined Motivational Properties.” *Nature Neuroscience* 21 (8): 1072–83.

Sawaguchi, T., and P. S. Goldman-Rakic. 1991. “D1 Dopamine Receptors in Prefrontal Cortex: Involvement in Working Memory.” *Science* 251 (4996): 947–50.

Sawaguchi, T., M. Matsumura, and K. Kubota. 1990. “Effects of Dopamine Antagonists on Neuronal Activity Related to a Delayed Response Task in Monkey Prefrontal Cortex.” *Journal of Neurophysiology* 63 (6): 1401–12.

Schultz, W., P. Dayan, and P. R. Montague. 1997. “A Neural Substrate of Prediction and Reward.” *Science* 275 (5306): 1593–99.

Seamans, Jeremy K., and Charles R. Yang. 2004. “The Principal Features and Mechanisms of Dopamine Modulation in the Prefrontal Cortex.” *Progress in Neurobiology* 74 (1): 1–58.

Seidemann, E., I. Meilijson, M. Abeles, H. Bergman, and E. Vaadia. 1996. “Simultaneously Recorded Single Units in the Frontal Cortex Go through Sequences of Discrete and Stable States in Monkeys Performing a Delayed Localization Task.” *The Journal of Neuroscience: The Official Journal of the Society for Neuroscience* 16 (2): 752–68.

Shafi, M., Y. Zhou, J. Quintana, C. Chow, J. Fuster, and M. Bodner. 2007. “Variability in Neuronal Activity in Primate Cortex during Working Memory Tasks.” *Neuroscience* 146 (3): 1082–1108.

Shalinsky, Mark H., Jacopo Magistretti, Li Ma, and Angel A. Alonso. 2002. “Muscarinic Activation of a Cation Current and Associated Current Noise in Entorhinal-Cortex Layer-II Neurons.” *Journal of Neurophysiology* 88 (3): 1197–1211.

Silva, Joaquim Alves da, Fatuel Tecuapetla, Vitor Paixão, and Rui M. Costa. 2018. “Dopamine Neuron Activity before Action Initiation Gates and Invigorates Future Movements.” *Nature* 554 (7691): 244–48.

Simon, H., B. Scatton, and M. L. Moal. 1980. “Dopaminergic A10 Neurones Are Involved in Cognitive Functions.” *Nature* 286 (5769): 150–51.

Spaak, Eelke, Kei Watanabe, Shintaro Funahashi, and Mark G. Stokes. 2017. “Stable and Dynamic Coding for Working Memory in Primate Prefrontal Cortex.” *The Journal of Neuroscience: The Official Journal of the Society for Neuroscience* 37 (27): 6503–16.

Teles-Grilo Ruivo, Leonor M., Keeley L. Baker, Michael W. Conway, Peter J. Kinsley, Gary Gilmour, Keith G. Phillips, John T. R. Isaac, John P. Lowry, and Jack R. Mellor. 2017. “Coordinated Acetylcholine Release in Prefrontal Cortex and Hippocampus Is Associated with Arousal and Reward on Distinct Timescales.” *Cell Reports* 18 (4): 905–17.

Torres, E. M., T. A. Perry, A. Blockland, L. S. Wilkinson, R. G. Wiley, D. A. Lappi, and S. B. Dunnet. 1994. “Behavioural, Histochemical and Biochemical Consequences of Selective Immunolesions in Discrete Regions of the Basal Forebrain Cholinergic System.” *Neuroscience* 63 (1): 95–122.

Turner, J. J., H. Hodges, J. D. Sinden, and J. A. Gray. 1992. “Comparison of Radial Maze Performance of Rats after Ibotenate and Quisqualate Lesions of the Forebrain Cholinergic Projection System: Effects of Pharmacological Challenge and Changes in Training Regime.” *Behavioural Pharmacology*. https://psycnet.apa.org/record/1993-08985-001.

Vijayraghavan, Susheel, Min Wang, Shari G. Birnbaum, Graham V. Williams, and Amy F. T. Arnsten. 2007. “Inverted-U Dopamine D1 Receptor Actions on Prefrontal Neurons Engaged in Working Memory.” *Nature Neuroscience* 10 (3): 376–84.

Vuckovich, J. A. 2004. “Extensive Lesions of Cholinergic Basal Forebrain Neurons Do Not Impair

Spatial Working Memory." *Learning & Memory*. https://doi.org/10.1101/lm.63504.

Wang, Yun, Henry Markram, Philip H. Goodman, Thomas K. Berger, Junying Ma, and Patricia S. Goldman-Rakic. 2006. "Heterogeneity in the Pyramidal Network of the Medial Prefrontal Cortex." *Nature Neuroscience* 9 (4): 534–42.

Watanabe, Kei, and Shintaro Funahashi. 2014. "Neural Mechanisms of Dual-Task Interference and Cognitive Capacity Limitation in the Prefrontal Cortex." *Nature Neuroscience* 17 (4): 601–11.

Wickersham, Ian R., David C. Lyon, Richard J. O. Barnard, Takuma Mori, Stefan Finke, Karl-Klaus Conzelmann, John A. T. Young, and Edward M. Callaway. 2007. "Monosynaptic Restriction of Transsynaptic Tracing from Single, Genetically Targeted Neurons." *Neuron* 53 (5): 639–47.

Wiley, R. G., T. N. Oeltmann, and D. A. Lappi. 1991. "Immunolesioning: Selective Destruction of Neurons Using Immunotoxin to Rat NGF Receptor." *Brain Research* 562 (1): 149–53.

Williams, G. V., and P. S. Goldman-Rakic. 1995. "Modulation of Memory Fields by Dopamine D1 Receptors in Prefrontal Cortex." *Nature* 376 (6541): 572–75.

Wimmer, Klaus, Duane Q. Nykamp, Christos Constantinidis, and Albert Compte. 2014. "Bump Attractor Dynamics in Prefrontal Cortex Explains Behavioral Precision in Spatial Working Memory." *Nature Neuroscience* 17 (3): 431–39.

Zaborszky, Laszlo, Attila Csordas, Derek L. Buhl, Alvaro Duque, Jozsef Somogyi, and Zoltan Nadasdy. n.d. "Computational Anatomical Analysis of the Basal Forebrain Corticopetal System." In *Computational Neuroanatomy*, 171–98.

Zaborszky, Laszlo, Alvaro Duque, Matthew Gielow, Peter Gombkoto, Zoltan Nadasdy, and Jozsef Somogyi. 2015. "Organization of the Basal Forebrain Cholinergic Projection System." In *The Rat Nervous System*, 491–507.

Zaborszky, Laszlo, L. Hoemke, H. Mohlberg, A. Schleicher, K. Amunts, and K. Zilles. 2008. "Stereotaxic Probabilistic Maps of the Magnocellular Cell Groups in Human Basal Forebrain." *NeuroImage* 42 (3): 1127–41.

Zaborszky, Laszlo, Anthony van den Pol, and Erika Gyengesi. 2012. “The Basal Forebrain Cholinergic Projection System in Mice.” In *The Mouse Nervous System*, 684–718.

Zaborszky, L., A. Csordas, K. Mosca, and J. Kim. 2013. “Neurons in the Basal Forebrain Project to the Cortex in a Complex Topographic Organization That Reflects Corticocortical Connectivity Patterns: An Experimental Study ….” *Cerebral*. https://academic.oup.com/cercor/article-abstract/25/1/118/367269.

Zahrt, J., J. R. Taylor, R. G. Mathew, and A. F. Arnsten. 1997. “Supranormal Stimulation of D1 Dopamine Receptors in the Rodent Prefrontal Cortex Impairs Spatial Working Memory Performance.” *The Journal of Neuroscience: The Official Journal of the Society for Neuroscience* 17 (21): 8528–35.